The design, synthesis and evaluation of aminocaffeine derivatives as inhibitors of monoamine oxidase B

Christina Moraal

(B.Sc. Hons Biochemistry)

Dissertation submitted in the partial fulfillment of the requirements for the degree

MAGISTER SCIENTIAE

in the

Faculty of Health Sciences, School of Pharmacy (Pharmaceutical Chemistry)

at the

North-West University, Potchefstroom Campus

Supervisor: Dr. G. Terre'Blanche

Co-supervisor: Prof. J.P. Petzer

Assistant supervisor: Prof. J.J. Bergh

Potchefstroom

2011

Table of Contents

ACKNOWLEDGEMENTS

- Dr. G. Terre'blanche, thank you for your support and guidance. Your patience is greatly appreciated by us all.

- Prof. J.P. Petzer, thank you for sharing your knowledge and for the enthusiasm you have shown towards my study.

- Prof. J.J. Bergh, thank you for your valuable advice and guidance.

- My parents, whose love and support mean a lot to me. Thank you for the opportunities you have created and the sacrifices you have made for my benefit.

"Trust in the LORD with all your heart
and lean not on your own understanding;
in all your ways acknowledge him,
and he will make your paths straight."

Proverbs 3:5-6

ABBREVIATIONS

α-KGDC – α-Ketoglutarate decarboxylase

5-HT – 5-Hydroxytryptamine

6-OHDA – 6-Hydroxydopamine

Apaf-1 – Apoptosis activating factor 1

ATP – Adenosine triphosphate

COMT – Catechol-o-methyltransferase

Co-Q_{10} – Coenzyme Q_{10}

CSC – (E)-8-(3-Chlorostyryl)caffeine

DMSO – Dimethylsulfoxide

DNA – Deoxyribonucleic acid

DS – Discovery Studio

EIMS – Electron ionization mass spectrum

FAD – Flavin adenine dinucleotide

GBA – Glucocerebrosidase

HPLC – High performance liquid chromatography

HRMS – High resolution mass spectrum

L-AAD – L-amino acid decarboxylase

LB – Lewy body

LRRK2 – Leucine-rich repeat kinase 2

MAO – Monoamine oxidase

$MPDP^+$ - 1-Methyl-4-phenyl-2,3-dihydropyridinium

MPP^+ - 1-Methyl-4-phenylpyridinium

MPTP – 1-Methyl-4-phenyl-1,2,3,6-tetrahydropyridine

MS – Mass spectroscopy

NADH – Nicotinamide adenine dinucleotide

NADPH – Nicotinamide adenine dinucleotide phosphate

NMDA – N-methyl-D-aspartate

NMR – Nuclear magnetic resonance

PD – Parkinson's Disease

ROS – Reactive oxygen species

SET – Single electron transfer

SI – Selectivity index

SNpc – Substantia nigra pars compacta

SOD – Superoxide dismutase

TLC – Thin layer chromatography

ABSTRACT

Monoamine oxidase (MAO) is responsible for dopamine catabolism in the brain and therefore is especially important in the treatment of Parkinson's disease (PD). MAO-B inhibition provides symptomatic relief by indirectly elevating dopamine levels in the PD brain. PD is caused by the loss of dopaminergic neurons in the substantia nigra and the formation of proteinaceous structures in the brain. The cause of idiopathic PD is unknown, but one theory states that reactive oxygen species (ROS), partly derived from the catalytic cycle of MAO, may be to blame for damaging dopaminergic neurons. Since MAO inhibitors may reduce the MAO-catalyzed production of ROS, these compounds may protect dopaminergic neurons against degeneration in PD. It is commonly accepted that by the time PD symptoms manifest, about 80% of striatal dopamine has been lost.

MAO is present as two subtypes in the human brain, namely MAO-A and MAO-B. MAOs are found mainly attached to the mitochondrial membrane and is responsible for the oxidative deamination of various monoamines, including dopamine. MAO is a dimeric enzyme which operates in conjunction with a co-factor, flavin adenine dinucleotide (FAD), to which it is covalently bound. The flavin is in a bent conformation, which assists the catalytic activity of MAO. As mentioned above, the catalytic action of MAO also produces harmful substances such as hydrogen peroxide, ammonia, aldehydes and may also increase the levels of hydroxyl radicals. In the healthy brain, these substances are metabolized rapidly, but the PD brain may exhibit reduced clearance of these species. Thus the inhibition of MAOs may be beneficial to the PD sufferer as it indirectly increases dopamine levels in the brain and may also slow the formation of harmful substances.

MAO inhibitors, of the MAO-A type, were first used as anti-depressants. It was these drugs that first prompted researchers to explore MAO inhibitors as novel anti-parkinsonian drugs, as MAO-A inhibition slows the degradation of dopamine. Two types of inhibition modes exist, irreversible and reversible inhibition. Irreversible inhibitors do not allow for competition with the substrate and inactivate the enzyme permanently. Selegiline, a propargyl amine derivative, is an example of an irreversible MAO-B selective inhibitor. The major disadvantage of irreversible inhibitors is that after terminating treatment, recovery of the enzyme activity may require several weeks, since the turnover rate for the biosynthesis of MAO in the human brain may be as much as 40 days. Reversible inhibitors have better safety profiles since they allow for competition with the substrate. (E)-8-(3-Chlorostyryl)caffeine (CSC) is an example of a reversible inhibitor of MAO-B and is also an antagonist of the adenosine A_{2A} receptor. Since antagonism of A_{2A} receptors also produces

an antiparkinsonian effect, dual acting compounds such as CSC, which block both the A_{2A} receptors and MAO-B, may have an enhanced therapeutic potential in PD therapy.

Current PD therapy available only treats the symptoms of PD and do not halt or slow the progression of the neurodegenerative processes. There therefore exists the need for the development of antiparkinsonian drugs with neuroprotective effects. Since both MAO-B inhibitors and A_{2A} receptor antagonists are reported to possess protective effects in PD and PD animal models, dual acting drugs, that antagonize A_{2A} receptors and inhibit MAO-B, may be candidates for neuroprotection. Using the structure of CSC as lead, we investigate in the current study, the possibility that aminocaffeines may also possess potent MAO-B inhibitory properties. The structures of the aminocaffeine derivatives that were investigated bear close structural resemblance to CSC as well as to a series of alkyloxycaffeine analogues that was recently found to be potent MAO inhibitors. This study therefore further explores the structural requirements of caffeine derivatives to act as MAO inhibitors by examining the possibility that aminocaffeine derivatives may be MAO inhibitors. Such compounds may act as lead compounds for the development of improved PD therapy.

In this study, a series of 8-aminocaffeine derivatives were synthesized and evaluated as inhibitors of human MAO-A and –B. For this purpose, 8-chlorocaffeine was reacted with the appropriate amine at high temperatures to produce the desired 8-aminocaffeine derivatives. The inhibitory activities of the compounds were determined towards recombinant human MAO-A and –B and expressed as IC_{50} values.

The results showed that human MAO-B was most potently inhibited by 8-[methyl(4-phenylbutyl)amino]caffeine with an IC_{50} value of 2.97 µM. Human MAO-A was most potently inhibited by 8-[2-(3-chlorophenyl)-ethylamino]caffeine with an IC_{50} value of 5.78 µM. It was found that methylation of the amine group at C8 of the caffeine ring increases inhibition but also selectivity towards MAO-B inhibition. For example, 8-[4-(phenylbutylamino)]caffeine inhibits MAO-B with an IC_{50} value of 7.56 µM whereas 8-[methyl(4-phenylbutyl)amino]-caffeine has an increased inhibition potency of 2.97 µM. The selectivity for MAO-B inhibition also increases over MAO-A when the C8 amine is methylated. It was found that the aminocaffeine derivatives bind reversibly to both enzyme isoforms and the mode of inhibition is competitive for MAO-B. From these results it can be concluded that although the 8-aminocaffeine derivatives are only moderately potent MAO-B inhibitors, they may act as lead compounds for the design of more potent reversible MAO inhibitors.

Docking studies revealed that the 8-aminocaffeine and 8-[(methyl)amino]caffeine derivatives traverse both the entrance and substrate cavities of the MAO-B enzyme, with the caffeinyl moiety oriented towards the FAD co-factor while the amino-side chain protrudes into the entrance cavity.

Key words: Monoamine oxidase; Reversible inhibition; Caffeine; Aminocaffeine.

OPSOMMING

Monoamienoksidase (MAO) is verantwoordelik vir dopamienkatabolisme in die brein en is daarom veral belangrik in die behandeling van Parkinson se siekte (PD). Inhibisie van MAO-B verskaf simptomatiese verligting deur indirek dopamienvlakke in die Parkinson-brein te verhoog. Parkinson se siekte word veroorsaak deur die verlies van dopamien-geleidende neurone in die substantia nigra en die vorming van proteïenagtige strukture in die brein. Die oorsaak van idiopatiese PD is onbekend, maar een teorie stel dat reaktiewe suurstofspesies (ROS), wat gevorm word tydens die katalitiese werking van MAO, moontlik skade veroorsaak aan die dopamien-geleidende neurone. MAO-inhibeerders kan moontlik die MAO-gekataliseerde produksie van ROS verlaag en kan dus moontlik die dopamien-geleidende neurone teen verdere degenerasie beskerm. Dit word algemeen aanvaar dat PD-simptome eers manifesteer nadat omtrent 80% van striatale dopamien verlore is.

MAO bestaan as twee subtipes in die menslike brein, naamlik MAO-A en MAO-B. MAO is hoofsaaklik aan die mitochondriale membrane verbind en is verantwoordelik vir die oksidatiewe deaminasie van verskeie monoamiene, insluitend dopamien. MAO is 'n dimeriese ensiem wat flavienadeniendinukleotied (FAD) as 'n ko-faktor benut. Die MAO is deur middel van 'n kovalente binding aan FAD verbind. Soos bo genoem, veroorsaak die katalitiese aktiwiteit van MAO die vorming van skadelike stowwe soos waterstofperoksied, ammoniak en aldehied en dit mag ook die vlakke van hidroksielradikale verhoog. In die gesonde brein word die stowwe geredelik gemetaboliseer, maar by persone wat aan PD ly, word die stowwe meesal stadiger verwyder. Die inhibisie van MAO mag dus voordeling wees vir die PD-pasiënt omdat dit dopamienvlakke in die brein indirek verhoog en ook die vorming van gevaarlike stowwe vertraag.

MAO-A inhibeerders is aanvanklik as antidepressante gebruik. Dit was dié middels wat navorsers aangemoedig het om MAO-inhibeerders as nuwe anti-parkinsoniese middels te verken, aangesien MAO-A inhibisie dopamienkatabolisme vertraag. Twee tipes metodes van inhibisie bestaan, naamlik onomkeerbare en omkeerbare inhibisie. By onomkeerbare inhibeerders vind daar nie kompetisie vir die substraat plaas nie en word die ensiem permanent geïnaktiveer. Selegilien, 'n propargielamien-derivaat, is 'n voorbeeld van 'n onomkeerbare, MAO-B selektiewe inhibeerder. Die grootste nadeel van onomkeerbare inhibeerders is die lang tyd wat die ensiem nodig het om te herstel na die staking van behandeling. Die MAO-ensiem in die menslike brein benodig soveel as 40 dae om nuwe

ensiem te vorm. Omkeerbare inhibeerders het beter veiligheidsprofiele aangesien daar in hulle geval kompetisie vir die substraat kan plaasvind. (E)-8-(3-Chlorosteriel)kaffeïen (CSC) is 'n voorbeeld van 'n omkeerbare MAO-B inhibeerder en dit is ook 'n antagonis van die adenosien A_{2A}-reseptor. Aangesien antagonisme van A_{2A}-reseptore ook 'n anti-parkinsonistiese effek het, kan middels wat tweesydig optree, soos CSC, wat beide die A_{2A}-reseptore blokkeer en MAO-B inhibeer, 'n verhoogde terapeutiese voordeel inhou vir die behandeling van Parkinson se siekte.

Huidige behandeling van PD berus slegs op die behandeling van simptome en vertraag of stop nie die neurodegenerasie nie. Dus is daar 'n behoefte vir die ontwikkeling van anti-parkinsonistiese middels wat neurone kan beskerm. Aangesien aangetoon is dat beide die MAO-B-inhibeerders en A_{2A}-reseptorantagoniste in PD en PD-dier-modelle oor beskermende eienskappe beskik, kan middels wat tweeledig optree dus moontlik vir neurobeskerming gebruik word. Deur CSC as leidraadverbinding te gebruik het ons in hierdie studie nagevors of aminokaffeïenderivate as MAO-B inhibeerders kan optree. Die strukture van die aminokaffeïenderivate wat ondersoek is, stem grootliks ooreen met dié van CSC en 'n reeks alkieloksiekaffeïen analoë, wat onlangs as goeie MAO-inhibeerders aangetoon is. Hierdie studie het die strukturele vereistes van kaffeïenderivate, om as MAO-inhibeerders op te tree, verder uitgebrei, deur die moontlikheid van aminokaffeïenderivate as MAO-inhibeerders te ondersoek. Sulke verbindings kan moontlik as leidraadverbindings gebruik word vir die ontwikkeling van verbeterde PD-terapie.

In hierdie studie is 'n reeks 8-aminokaffeïenderivate gesintetiseer en geëvalueer as inhibeerders van menslike MAO-A en -B. 8-Chlorokaffeïen is by hoë temperature met die geskikte amien laat reageer om die gewenste 8-aminokaffeienderivaat te lewer. Die inhibisieaktiwiteite van die verbindings is vir rekombinante menslike MAO-A en -B bepaal en uitgedruk as IC_{50}-waardes.

Die resultate het getoon dat menslike MAO-B die meeste geïnhibeer is deur 8-[metiel(4-fenielbutiel)amino]kaffeïen, met 'n IC_{50}-waarde van 2.97 µM. Menslike MAO-A is die beste geïnhibeer deur 8-[2-(3-chlorofeniel)-etielamino]kaffeïen met 'n IC_{50}-waarde van 5.78 µM. Daar is gevind dat metilering van die amiengroep, in die C8-posisie van die kaffeïenring, inhibisie asook die selektiwiteit teenoor MAO-B-inhibisie verhoog. Byvoorbeeld, 8-[4-(fenielbutielamino)]kaffeïen inhibeer MAO-B met 'n IC_{50}-waarde van 7.56 µM, maar 8-[metiel(4-fenielbutiel)amino]kaffeïen toon 'n verhoogde inhibisiesterkte van 2.97 µM. Die selektiwiteit vir MAO-B-inhibisie verhoog bo dié vir MAO-A wanneer die C8 amien gemetileer is. Daar is gevind dat die aminokaffeïenderivate omkeerbaar aan beide ensiemisovorme

bind en dat die wyse van binding vir beide ensiemvorme kompeterend is. Uit dié resultate kan die gevolgtrekking gemaak word dat, alhoewel die 8-aminokaffeïenderivate slegs matige inhibeerders van MAO-B is, hulle tog as uitgangsverbindings gebruik kan word om meer potente MAO-inhibeerders te ontwerp.

Molekulêre modelleringstudies het getoon dat die 8-aminokaffeïen- en 8-[(metiel)amino]kaffeïenderivate in beide die ingangs- en substraatholtes van die MAO-B ensiem gesetel is, met die kaffeïenring na die FAD ko-faktor georiënteer, terwyl die aminosyketting tot in die ingangsholte strek.

Kernwoorde: Monoamienoksidase; Omkeerbare inhibisie; Kaffeïen; Aminokaffeïen.

CHAPTER 1

INTRODUCTION

1.1 BACKGROUND

Parkinson's disease (PD) is a neurodegenerative disorder that is caused by the death of dopaminergic neurons in the brain and the formation of protein aggregates, known as Lewy bodies. This result in the depletion of dopamine levels in the striatum, which leads to the characteristic movement disorders observed in PD patients. PD is an age-related disease and thus the incidence of PD increases in the elderly (Dauer & Prezdborski, 2003). Age therefore increases the risk of developing PD with 95% of the cases being sporadic. Only approximately 5% of PD cases are due to genetic factors (Dauer & Prezdborski, 2003). Neuronal loss is observed in different parts of the substantia nigra in PD patients compared to the pattern of neuronal loss observed with normal ageing. Normal ageing is typically associated with cell loss in the dorsomedial area whereas in PD neuronal death is concentrated in the ventral and caudal areas of the substantia nigra (Fearnley & Lees, 1991).

The monoamine oxidase (MAO) isozymes have long been linked to PD as they are responsible for the catabolism of neuronal dopamine. MAO-A and –B are mitochondrial bound enzymes that catalyze the oxidative deamination of a variety of neurotransmitters and biogenic amines. The MAO enzymes require a flavin adenine nucleotide (FAD) co-factor to perform its function. The enzyme is covalently bound to the 8α-carbon of the isoalloxazine ring via a thioether bond with a conserved cysteinyl residue (fig1.1) (Edmondson *et al*., 2004).

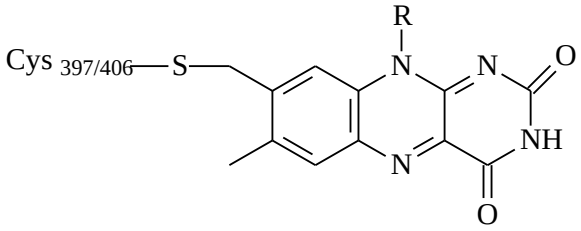

Figure 1.1 *Isoalloxazine ring of the FAD cofactor indicating the thioether bond to the cysteinyl residue. (Cys 397 for MAO-B and Cys 406 for MAO-A).*

MAO-B is a dimeric enzyme, with each monomer containing a membrane binding domain, a flavin binding domain and a substrate binding domain. The membrane binding domain has

an α-helix structure which is anchored to the outer mitochondrial membrane. Membrane binding is important for the optimal function of the MAO enzymes (Son *et al*., 2008). The flavin binding domain and substrate binding domain makes up the active site. The FAD is in a bent-planar conformation, which is necessary to accommodate substrate binding in the active site (Edmondson *et al*., 2004). Mutations of certain key amino acids, such as glycine 110 of the active site of MAO-A, greatly affects the catalytic efficiency of the enzyme (Son *et al*., 2008). It can thus be concluded that genetic and environmental factors influence MAO activity.

MAO-A and –B share approximately 70% sequence identity and are found on the X-chromosome (Shih *et al*., 1999). This might explain why men predominantly suffer from MAO-related defects. Deficiency of platelet MAO-B, for example, may be responsible for personality traits such as substance abuse, aggression and impulsiveness (Oreland *et al*., 2004; Fowler *et al*., 2003). Although MAO-A and –B are structurally similar, they have different but overlapping biological functions. The MAO enzymes are found in peripheral tissues such as the brain, intestines, liver, lungs, blood platelets and placenta. The amount, activity and ratio of MAO-A to MAO-B differ within these tissues. MAO-B is found mainly in blood platelets while MAO-A is the only isoform present in the placental tissue. Both isoforms of MAO are present in the brain, but MAO-B is present in higher concentrations (Kalaria & Harik, 1987). The levels of MAO-B increase with aging and elevated MAO-B activity is common in the PD brain (Mandel *et al*., 2005).

As mentioned above, the MAO enzymes are responsible for the oxidative deamination of a variety of monoamines, including neurotransmitters and dietary amines. MAO-A is responsible for the oxidation of serotonin while MAO-B degrades 2-phenylethylamine and benzylamine. Adrenaline, noradrenaline and dopamine are substrates for both isoforms (Youdim & Bakhle, 2006). The activity of MAO may protect tissues and neurons in the brain against the stimulatory effects of extraneous amines and by degrading endogenous neurotransmitters (Shih *et al*., 1999). The oxidative deamination reaction catalysed by the MAO enzymes also produces endogenous toxins. Hydrogen peroxides, aldehydes and ammonia are toxic by-products of MAO catalysis (fig 1.2). Hydrogen peroxide may in turn contribute to the production of hydroxyl radicals (Youdim & Bakhle, 2006). In the healthy brain, aldehyde dehydrogenase and glutathione peroxidase are responsible for the rapid detoxification of these endogenous toxins, but in the PD brain, the levels of these detoxifiers are greatly decreased (Youdim *et al*., 2006). This may cause additional damage to neurons, already strained by the decreased amount of functional neuronal activity in the PD brain.

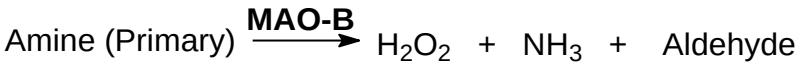

Figure 1.2 *The MAO-B catalysis of amines, which produces toxic substances.*

Both MAOs are capable of activating neurotoxins. This enables researchers to create PD symptoms in laboratory animals. An example of such a neurotoxin is 1-methyl-4-phenyl-1,2,3,6-tetrahydropyridine (MPTP), which is used to create animal models of PD. MPTP was first discovered as an impurity in a meperidine substitute synthesised by drug users. The drug users developed parkinsonian symptoms, dopamine depletion and neuronal degradation after self administration of MPTP (Langston *et al*., 1983). MPTP is however only a pro-neurotoxin and requires activation by the MAO enzymes in order to be neurotoxic. Oxidation of MPTP by MAO-A and -B produces the active neurotoxin, 1-methyl-4-phenylpyridinium (MPP^+) (fig 1.3). *In vivo*, only MAO-B produces significant amounts of MPP^+ since this neurotoxic species rapidly inactivates MAO-A. Inhibition of MAO-B therefore blocks the neurotoxic action of MPTP (Singer *et al*., 1988).

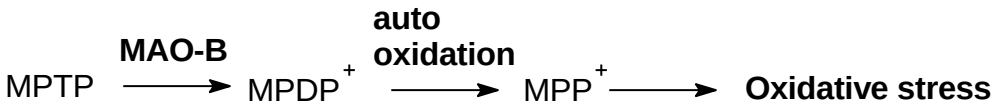

Figure 1.3 *Oxidation of MPTP by MAO-B.*

The role of the MAOs in the oxidative deamination of neurotransmitters makes these enzymes attractive targets for the development of centrally acting drugs and for the treatment of neurodegenerative diseases. For instance, as mentioned previously, the inhibition of MAO-B may slow the degradation of striatal dopamine and thus elevate the levels of this neurotransmitter. Inhibitors of MAO-B are frequently combined with levodopa, the mainstay in the treatment of PD (Chen & Swope, 2007). Levodopa is a dopamine precursor and leads to the replenishment of dopamine in the brain, which alleviates most PD symptoms. The long term use of levodopa however, causes involuntary dyskinesias which again impairs quality of life for PD patients. As an alternative, levodopa treatment is delayed as long as possible by the administration of drugs that inhibit the degradation of intraneuronal dopamine, such as MAO inhibitors (Youdim & Bakhle, 2006). Although this delays the need to start levodopa treatment, it does not replace levodopa therapy.

Reversible and irreversible MAO-A inhibitors have long been used to manage depression as it retards the degradation of serotonin as well as dopamine. Serotonin is known to have a

mood elevating and thus anti-depressant effect (Youdim *et al*., 2006). Since MAO-B is primarily responsible for dopamine catabolism in the brain, MAO-B inhibitors are used in PD therapy. Mixed MAO-A/B inhibitors may have enhanced value in the treatment of PD since PD patients frequently suffer from depression (Dauer & Prezdborski, 2003). The anti-depressant action of such drugs would be dependent upon the inhibition of MAO-A. It is however of importance that inhibitors of MAO-A are reversible as severe cardiovascular effects may occur with irreversible MAO-A inhibitors. This is due to dietary amines such as tyramine and indirectly acting sympathomimetic amines that enter the circulation. Under normal circumstances, MAO-A in the gut-wall rapidly metabolizes these amines, to prevent them from entering the circulation (Youdim & Bakhle, 2006).

1.2 RATIONALE

Based on above observations, the development of MAO-B inhibitors, that are reversible, may be of value in PD therapy. Selegiline is an example of a MAO-B inhibitor that has been shown to be effective in delaying the need to start levodopa therapy in PD patients. When used in combination with levodopa, selegiline reduces the amount of levodopa required to obtain a therapeutic effect (Riederer *et al*., 2004). Selegiline is however derived from propargylamine and is therefore an irreversible inhibitor of MAO-B. Irreversible MAO-B inhibitors have the disadvantage that the recovery of enzyme activity may require several weeks following drug withdrawal. From a drug safety point of view reversible inhibitors are considered more desirable since enzyme activity is regained relatively quickly after the drug has been cleared from the tissues (Youdim & Bakhle, 2006).

Previous studies have indicated that substitution at the C8 position of caffeine (**1**) (fig 1.4) yielded MAO-B inhibitors of various potencies. CSC (**2**) is an example of a caffeine derived MAO-B inhibitor and contains the 3-chlorostyryl substituent at the C8 position of caffeine. CSC is a potent MAO-B inhibitor with an enzyme-inhibitor dissociation constant (K_i value) of 70 nM (Chen *et al*., 2001). CSC is, however, not a MAO-A inhibitor (Chen *et al*., 2002).

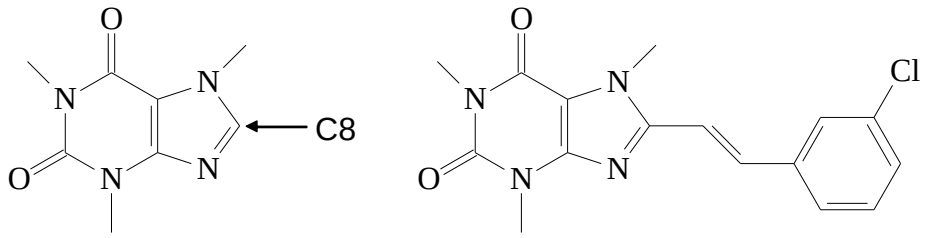

Figure 1.4 *The structure of caffeine (**1**) and CSC (**2**)*

In this study we will explore the possibility that substitution at C8 of caffeine, via an amino linkage, may also yield caffeine derivatives with potent MAO-B inhibition activities. It has been observed in previous studies, that oxy- and thioether linkages yielded derivatives with potent MAO-B inhibition activities. For example, 8-benzyloxycaffeine (**3**) and 8-benzylsulfanylcaffeine (**4**) inhibited MAO-B with IC_{50} values of 1.77 µM and 1.86 µM, respectively (fig 1.5) (Strydom *et al*., 2010). For this purpose, a variety of substituents with diverse physicochemical properties were selected and attached via an amino linkage at C8 of caffeine.

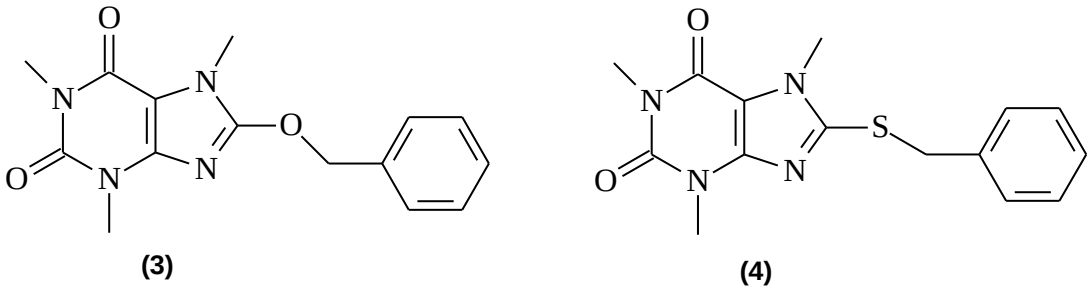

Figure 1.5 *The structures of 8-benzyloxycaffeine (**3**) and 8-benzylsulfanylcaffeine (**4**).*

This study is therefore an exploratory study to determine if 8-aminocaffeine derivatives may also act as MAO-B inhibitors. The 8-aminocaffeine derivatives (**5**, **6**) that were selected for this study are shown in Table 1.1 and 1.2.

Table 1.1 *The structures of the 8-aminocaffeine derivatives (**5a–h**) that were synthesized and investigated in this study.*

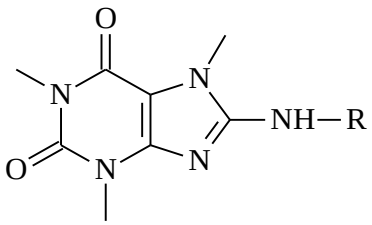

(5)

	-R		-R
5a	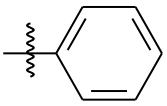	**5b**	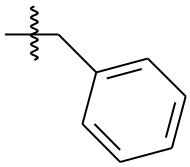
5c	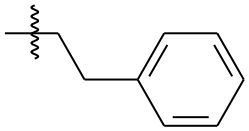	**5d**	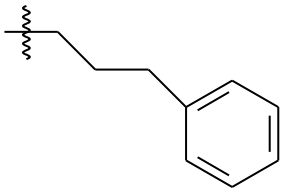
5e	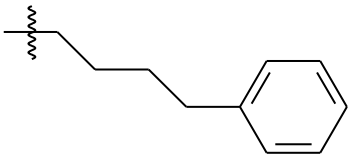	**5f**	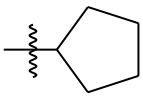
5g	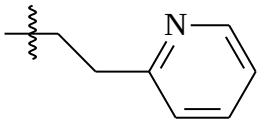	**5h**	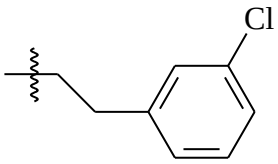

Table 1.2 *The structures of the 8-(methyl)aminocaffeine derivatives (**6a-b**) that were synthesized and investigated in this study.*

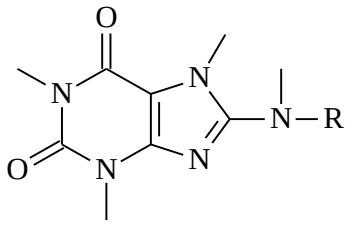

(6)

	-R		-R
6a	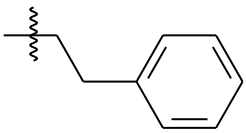	**6b**	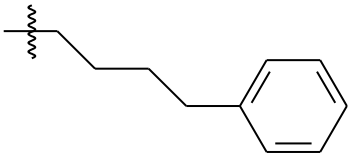

As shown in table 1.1, the C8 substituents that were selected are all substituted at C8 of caffeine, via an amino linkage and contain different carbon linker lengths between the caffeine and substituent aromatic ring. For example, the shortest substituent that was selected was the phenyl (**5a**), which is attached via an amino functional group at C8 of caffeine. 8-Aminocaffeine derivatives containing carbon linkers of length n = 1, 2, 3 and 4 were also examined, as exemplified by compounds **5b**, **5c**, **5d** and **5e**, respectively. Also included were 8-aminocaffeine derivatives containing a cyclopentyl (**5f**), pyridyl (**5g**) and 3-chlorophenyl ring (**5h**) in the C8 substituent. As shown in table 1.2, two derivatives, **6a** and **6b**, containing methylated tertiary aminyl linkages were also considered as potential MAO inhibitors.

1.3 OBJECTIVES OF THIS STUDY

The objectives of this study are summarized below:

- 8-Aminocaffeine derivatives **(5a–h)** and 8-(methyl)aminocaffeine derivatives **(6a**, **6b)** will be synthesized. 8-Chlorocaffeine and the appropriate substituted amine will be used as starting materials. All of the amines are commercially available, with exception of the secondary amines required for the synthesis of **6a** and **6b**. These will be prepared from the corresponding aminocaffeine derivative and methyliodide.

- The 8-aminocaffeine and 8-(methyl)aminocaffeine derivatives will be evaluated as MAO-A and –B inhibitors. Recombinant human MAO-A and –B are commercially available for this purpose. Inhibition potencies will be expressed as the IC_{50} values, which indicate the concentration of inhibitor that produces 50% inhibition. A fluorometric assay will be used to determine the inhibition activity. The enzyme activity measurements will be based on the amount of 4-hydroxyquinoline that is produced by the enzyme from the substrate, kynuramine. The concentration of 4-hydroxyquinoline may be determined by measuring the fluorescence of the samples at an excitation wavelength of 310 nm and an emission wavelength of 400 nm (Novaroli *et al*., 2005).

- The time-dependency of the inhibition for both MAO-A and –B will be evaluated for selected 8-aminocaffeine derivatives. This will be done to determine the reversibility or irreversibility of MAO inhibition by the test inhibitors. As discussed above, it is more desirable to have reversible inhibitors as therapeutic agents.

- Molecular modeling studies will be used to elucidate the type of interactions and binding modes of the inhibitors within the active sites of the MAO enzymes.

CHAPTER 2

LITERATURE OVERVIEW

2.1 PARKINSON'S DISEASE

2.1.1 Background

Parkinson's disease (PD) is a neurodegenerative disease, caused by the loss of dopaminergic neurons in the substantia nigra. This result in the loss of neuronal dopamine, which causes the classic motor dysfunctions observed in PD patients. PD is an age related disease, thus the incidence of PD is increased in older persons. 95% of PD cases are sporadic. Genetically linked cases are far less common (Dauer & Prezdborski, 2003). The disease is clinically characterized by movement disorders, termed dyskinesias. Tremors occur during rest, but voluntary movement decreases tremors so that the daily activities of these persons are not greatly impaired. Other more debilitating symptoms include slowness of movement (bradykinesia) and resistance to movement of the limbs, also known as "freezing" (Prezdborski, 2005). Slowness of speech, decreased size of handwriting, depression and dementia are common amongst PD patients.

Dementia is common in older patients suffering from PD and is caused by the degeneration of the hippocampal and cholinergic structures. Depression is noticed some months before the onset of PD symptoms due to the decreasing levels of dopamine. The diagnosis of PD is determined by the presence of both LBs and SNpc neuronal loss. LB formation is not exclusive to PD, as Alzheimer's disease patients also develop LBs. This is referred to as "dementia with LB disease" (Dauer & Prezdborski, 2003).

2.1.2 Pathology and mechanism

The main pathological features of PD are the loss of striatal dopamine and the formation of proteinaceous inclusions, termed "Lewy bodies" (LBs). The formation of proteinaceous structures may be partially responsible for the loss of neuronal function (Marsden, 1983). Proteins can misfold during faulty translation or the inability of natural "quality-control" centres within the ribosomes to recognize a protein of low quality. Normally these centres will degrade such proteins via a degradation system. This malfunction may be caused by environmental or genetic factors (Dauer & Predzborski, 2003).

PD caused by toxins:

The cause of sporadic PD is unknown, but environmental toxins might play a role. It is well known that certain neurotoxins are capable of inducing parkinsonism. The discovery that 1-methyl-4-phenyl-1,2,3,6-tetrahydropyridine (MPTP) induced parkinsonian symptoms in animals, supports this hypothesis. MPTP was first discovered when drug users injected themselves inadvertently with MPTP, which was a contaminant of the mepiridine heroin they were using and developed parkinsonian symptoms (Singer *et al*., 1988).

Several pesticides and herbicides have been implicated as neurotoxins. Chronic exposure to these compounds may cause the degeneration of dopaminergic neurons. Paraquat, a pesticide, has been implicated to cause neuron damage. Paraquat has a structure similar to the 1-methyl-4-pyridinium ion (MPP^+), which is the toxic metabolite of MPTP (fig 2.1). Experimental data indicates that paraquat is responsible for neuron damage in mouse models and is especially selective for dopaminergic neurons (McCormack *et al.*, 2002).

Rotenone is a mitochondrial poison and is commonly used to kill unwanted fish in lakes. Rotenone is unstable however, and degrades within a few days, but it is believed to induce parkinsonian symptoms (Tanner, 1992). Rotenone has been used in PD models. It interferes with normal mitochondrial actions, leading to ATP depletion.

Another possible cause of PD is that endogenous toxins cause a metabolic imbalance which creates toxic, oxidative species. The metabolism of dopamine by monoamine oxidase (MAO) produces reactive oxygen species (ROS) like hydrogen peroxide as well as aldehydes and ammonia. In healthy persons, the brain is capable of clearing these toxic substances, but the mechanisms responsible for this is impaired by PD. MAO levels increases during ageing but is present in even greater quantity in the brains of PD patients. Along with increased levels of the enzyme, aldehyde dehydrogenase and glutathione is decreased (Youdim *et al*., 2006). Low levels of aldehyde dehydrogenase and glutathione increase the levels of ROS and other toxic species.

PD is also referred to as a protein misfolding disease, because of the formation of LBs. Proteins can misfold and form mostly insoluble aggregates intra- or extracellularly. The aggregates might cause cell death by interfering with normal cell trafficking or by directly causing damage (Gibb & Lees, 1988). Protein aggregates are closely linked to neuronal damage and organ failure. Under normal circumstances a misfolded protein is recognized by so-called “quality-control checkpoints” and is degraded by the ubiquitin-protease system. Chaperons are also present during protein folding to ensure that the protein attains its

correct three-dimensional structure. Oxidative and thermal stresses, mutations and alterations during translation and transcription can all influence protein misfolding (Kopito, 2000). Inherited PD is caused primarily by mutations, although LBs are found in both sporadic and genetic cases of PD.

Since the discovery that MPTP inhibits the function of complex I of the oxidative phosphorylation pathway (Nicklas *et al.*, 1987), it has been suggested that mitochondrial dysfunction may play a part in PD pathogenesis. Experimental data have shown a marked decrease in complex I activity in the brains of patients who died of PD (Mizuno *et al.*, 1989). Defects of the mitochondria leave the cell susceptible to oxidative stress. Almost all molecular oxygen that enters the body is consumed by mitochondrial respiration. This produces harmful by-products, mostly oxidative species. Hydrogen peroxide and superoxide radicals are very common by-products of the respiratory chain reaction. The loss of complex I function increases the levels of ROS. These molecules cause damage to nucleic acids, lipids and proteins. Together with this increase of ROS, the natural anti-oxidant, glutathione is reduced in PD. Increased ROS levels create an increased production of misfolded proteins and a greater demand on the ubiquitin-protease system to degrade the misfolded proteins (Greenamyre *et al.*, 2001). Eventually the protease system is unable to degrade all the erroneous proteins and they become deposited. Degradation of the dopaminergic neurons in the substantia nigra is directly parallel to decreased complex I function. ROS has not been identified as the primary cause of the development of PD (Dauer & Prezdborski, 2003).

PD caused by genetics:

Parkinson's disease is sporadic for about 95% of cases, but in some cases it is hereditary. Several genes have been implicated in the cause of onset in PD.

The parkin gene is linked to an autosomal recessive form of juvenile parkinsonism. Mutations of the gene have been identified in a diverse group of families suffering from parkinsonism-like symptoms. The experimental data indicates that almost half of all inherited PD is from a parkin mutation. These patients typically develop PD from roughly 45 years of age. Patients with this mutation rarely develop LBs, but inclusions of tau-protein are frequently present. The parkin protein normally degrades improperly folded proteins, but due to a mutation in the parkin gene, it does not properly perform this function (Shimura *et al*., 2000).

Glucocerebrosidase (GBA) mutations have also been identified as a possible cause of PD. The inherited GBA mutation causes Gaucher disease. Patients later develop parkinsonism-like symptoms like bradykinesia, rigidity and tremors. Experimental data indicates the formation of LBs in about 60% of patients suffering from Gaucher disease (Tayebi *et al.*, 2003). Lwin *et al.* (2004) speculates that defective GBA function may be a risk factor in the development of parkinsonism. One possible cause is the loss of GBA function. This will cause an increase in glucocylceramide in the brain which upsets the osmotic balance, causing a cascade of events which leave neurons susceptible to damage (Lwin *et al.*, 2004). Another possible cause of parkinsonism due to a defective GBA gene may be that lysosomal activity decreases. This leads to a decreased degradation of misfolded α-synuclein, creating deposits in the brain. Aggregates of this type have been identified as typical in PD (Trojanowski *et al*., 1998).

Multiple mutations have been described for the leucine-rich repeat kinase 2 (LRRK2) genes in PD sufferers. The LRRK2 gene mutations are found in 1% of sporadic and 4% of familial PD cases. The LRR kinases are responsible for protein-protein interactions and disruption of these interactions may be causative of PD (Lesage *et al.*, 2006; Deng *et al.*, 2007). According to Zimprich *et al*. (2004) LRRK2 may be a crucial factor in the development of neurodegenerative disorders. Its kinase activity may hyperphosphorylate tau-protein and α-synuclein, causing the aggregation of these proteins (Zimprich *et al.*, 2004; Lees *et al.*, 2009).

α-Synuclein is a presynaptic nerve terminal protein involved in neuronal plasticity. It is a precursor non-amyloid component of Alzheimer's disease. α-Synuclein mutations are frequent in hereditary cases of PD, but sporadic cases cannot satisfactorily be linked to α-synuclein mutations (Polymeropoulos & Layedan, 1997). Evidence suggests that a mutation in the gene coding for α-synuclein may accelerate the formation of aggregates and cause early-onset PD. The formation of α-synuclein aggregates may increase LB production, as α-synuclein is a component of the LB structure (Conway *et al.*, 1998). The accumulation of α-synuclein aggregation appears to be very specific. It is found first in the olfactory lobe, which may explain the loss of smell commonly experienced in PD patients. Then it is found in the lower brainstem from where it ascends into the higher substantia nigra (Lees *et al.*, 2009).

2.1.2 Toxin-induced models of Parkinson's disease

The discovery of toxins that cause parkinsonian symptoms in animals has greatly attributed to the study of PD. This creates the opportunity for scientists to develop drugs that may treat PD. The most frequently used neurotoxins are MPTP, 6-hydroxydopamine (6-OHDA),

rotenone and paraquat. Of these, MPTP is the most frequently used and thus more attention will be given to the neurotoxicity induced by MPTP in humans and animals.

1-Methyl-4-phenyl-1,2,3,6-tetrahydropyridine (MPTP)

MPTP (fig 2.1) is a complex I inhibitor of the mitochondrial respiratory chain. It has been successfully used to imitate PD symptoms in a variety of mammalian species, from nonhuman primates to worms (Kitamura *et al.*, 1998). The murine-MPTP model is most commonly used, as the animals are small and easy to care for. Rats are not used as a MPTP model as their dopaminergic neurons are relatively resistant to the toxic effects of MPTP. Nonhuman primates do however give the most accurate PD model of any animal and when treated with MPTP, give symptoms very similar to those exhibited by PD patients (Decamp & Schneider, 2004). MPTP models do not show the formation of LBs, probably due to the acuteness of the toxin. The proteins do not have time to aggregate because the toxin is so fast acting. Both humans and monkeys intoxicated with MPTP respond well to treatment with levodopa/carbidopa. Monkeys even develop the dyskinesias common with the long term treatment of levodopa, making them the gold standard for studying PD and the parkinsonian symptoms that develop with treatment (Kostic *et al.*, 1991). It has been shown that by protecting the striatal terminals against MPTP, damage decreased neuron death may be obtained (Wu *et al.*, 2003), This evidence suggests that dopaminergic terminals are the primary target in MPTP induced parkinsonism (Herkenham *et al.*, 1991).

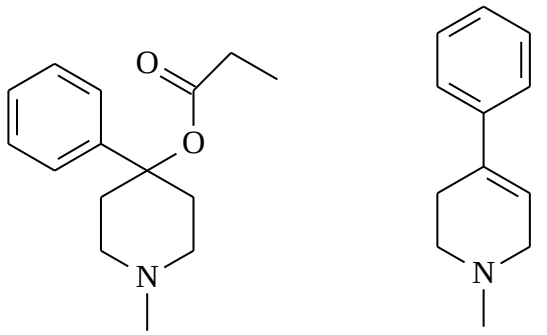

MPPP **MPTP**

Figure 2.1 *Structure of MPPP and MPTP.*

The toxicity of MPTP is due to its oxidation by MAO-B in the glial cells and astrocytes in the brain to firstly yield 1-methyl-4-phenyl-2,3-dihydropyridinium ($MPDP^+$) and then the ultimate neurotoxin 1-methyl-4-phenylpyridinium (MPP^+). The latter conversion occurs by an unknown mechanism. MPP^+ is then concentrated in the mitochondria where it combines with NADH dehydrogenase, inhibiting oxidative phosphorylation. This will eventually lead to ATP

depletion and cell death. The inhibition of MPP^+ is reversible, but the damage to the neurons is permanent and once the ATP supply has been cut off the cells die. Neuronal cells are unable to recover from injury (Singer *et al.*, 1988).

6-Hydroxydopamine (6-OHDA)

This neurotoxin also destroys catecholaminergic structures along with dopaminergic structures and it is an older model of PD than the MPTP-models. 6-OHDA destroys neurons by the combined effect of ROS production and the production of quinones (fig 2.2). This causes mitochondrial damage and impaired ATP production, leading to cell death. This model is used on a variety of animals, but mostly on small mammals because they handle easier. 6-OHDA needs to be injected directly into the brain because it does not cross the blood-brain barrier very well. Injections are usually done unilaterally. This causes a circling behaviour in rodent models. Effectiveness of treatments can easily be assessed by the reduction or the unchanged circling behaviour of the animal (Ungerstedt & Arbuthnott, 1970). No LB formation has been satisfactorily demonstrated in the brains of 6-OHDA treated rats (Bové *et al.*, 2005).

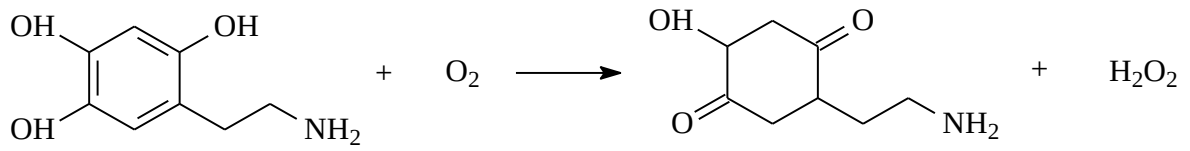

6-OHDA **_para_-quinone**

Figure 2.2 *Oxidation of 6-OHDA. The production of hydrogen peroxide can cause oxidative stress and may damage neurons.*

Rotenone

Rotenone (fig 2.3) is most commonly used to kill unwanted fish in lakes. It is an inhibitor of mitochondrial complex I. It breaks down rapidly when exposed to sunshine, leading some researchers to believe that it is not a viable cause of PD. Rotenone is not easily absorbed by the intestines, thus it has to be injected intravenously. The high lipophilicity of rotenone enables it to easily gain access to organs (Bové *et al.*, 2005). The degree of dopaminergic neuron damage in rats treated with rotenone is highly variable, making the model less than ideal. Proteinaceous inclusions have been found in the brains of rotenone treated rats

(Betarbet *et al.*, 2000) which may make the rotenone model ideal to study the protein aggregation pathology of PD.

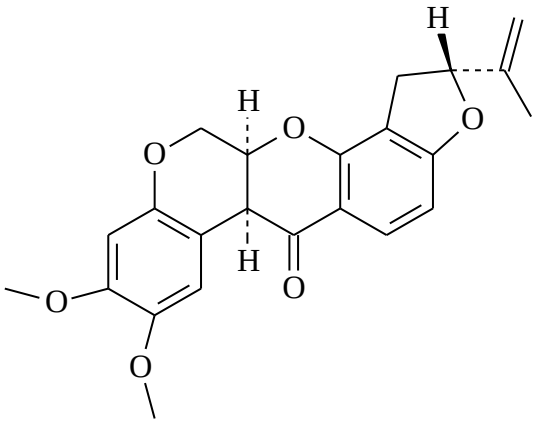

Figure 2.3 *Structure of rotenone.*

Paraquat

Paraquat is used as a herbicide. Its toxicity is mediated by a redox cycling action, producing harmful superoxide radicals (fig 2.4). Every cycle produces more radicals and eventually the natural anti-oxidants are unable to keep up with detoxification processes. Paraquat is similar in structure to MPP^+ and despite the fact that paraquat does not easily cross the blood-brain barrier, it has been reported that L-neutral amino acids may transport it into the brain (McCormack & Di Monte, 2003). Increased levels of α-synuclein have been found in the brains of paraquat treated mice (Manning-Bog *et al.*, 2002). This model may therefore be used to study the aggregation of proteins. The main mechanism of neurodegeneration as caused by paraquat however, remains the production of ROS (Bové *et al.*, 2005).

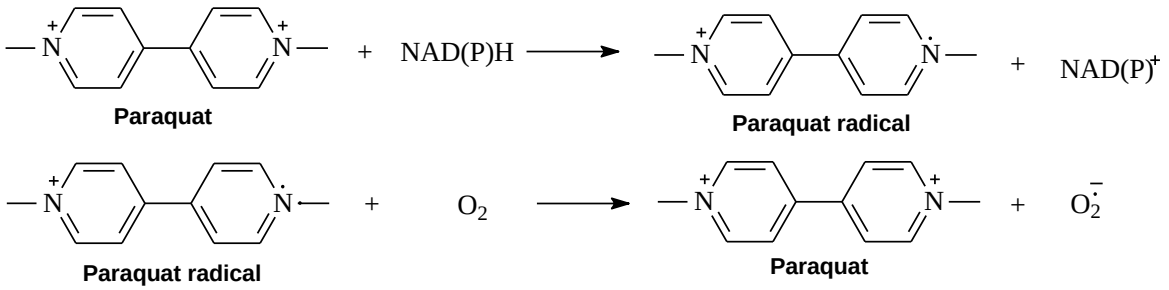

Figure 2.4 *The reduction-oxidation cycling reaction of paraquat, producing superoxide radicals. The cycle is able to continue almost infinitely, thus one molecule of paraquat can produce multiple molecules of superoxide radicals.*

2.1.3 Drugs for neuroprotection and symptomatic treatment

Current pharmacotherapies for PD are aimed at treating the symptoms of PD. No compound has yet been found to provide neuroprotection in PD. Various therapies for PD exist, according to the patient's unique needs, but all of them will eventually include levodopa in conjugation with other symptomatic drugs. Treatment is usually aimed at improving motor and non-motor symptoms of the PD patient. The age of the patient also determines which drugs to use, as the metabolism of older persons does not have the same effectiveness as younger persons. The extent of the disease also ultimately decides which therapy will work best in prolonging the quality of life for a PD sufferer.

Levodopa

Levodopa is the most effective drug to treat the symptoms displayed by PD patients, especially bradykinesia and rigidity. It is a dopamine precursor which is metabolized to dopamine by L-amino acid decarboxylase (L-AAD) in the SNpc. Dopamine itself is unable to pass the blood-brain barrier. Dopamine is stored in the presynaptic neurons until stimulated and then released into the synaptic clefts (Chen & Swope, 2007).

After some time of levodopa treatment, patients may develop side effects, such as nausea, due to the peripheral conversion of levodopa to dopamine (Mayasaki *et al.*, 2002), (fig 2.6). Consequently, levodopa is given in combination with an L-AAD inhibitor to reduce the peripheral conversion of levodopa to dopamine. L-AAD inhibitors that are frequently used are carbidopa and benserazide. Patients may also develop dyskinesias and motor fluctuations due to long term levodopa therapy. L-AAD inhibitors are however ineffective in reducing the severity of these dyskinesias (Chen & Swope, 2007).

PD is a progressive disease and in early stages different treatments may be given to stave off the use of levodopa. Eventually all PD patients will require treatment with levodopa as it is still the best anti-symptomatic drug available.

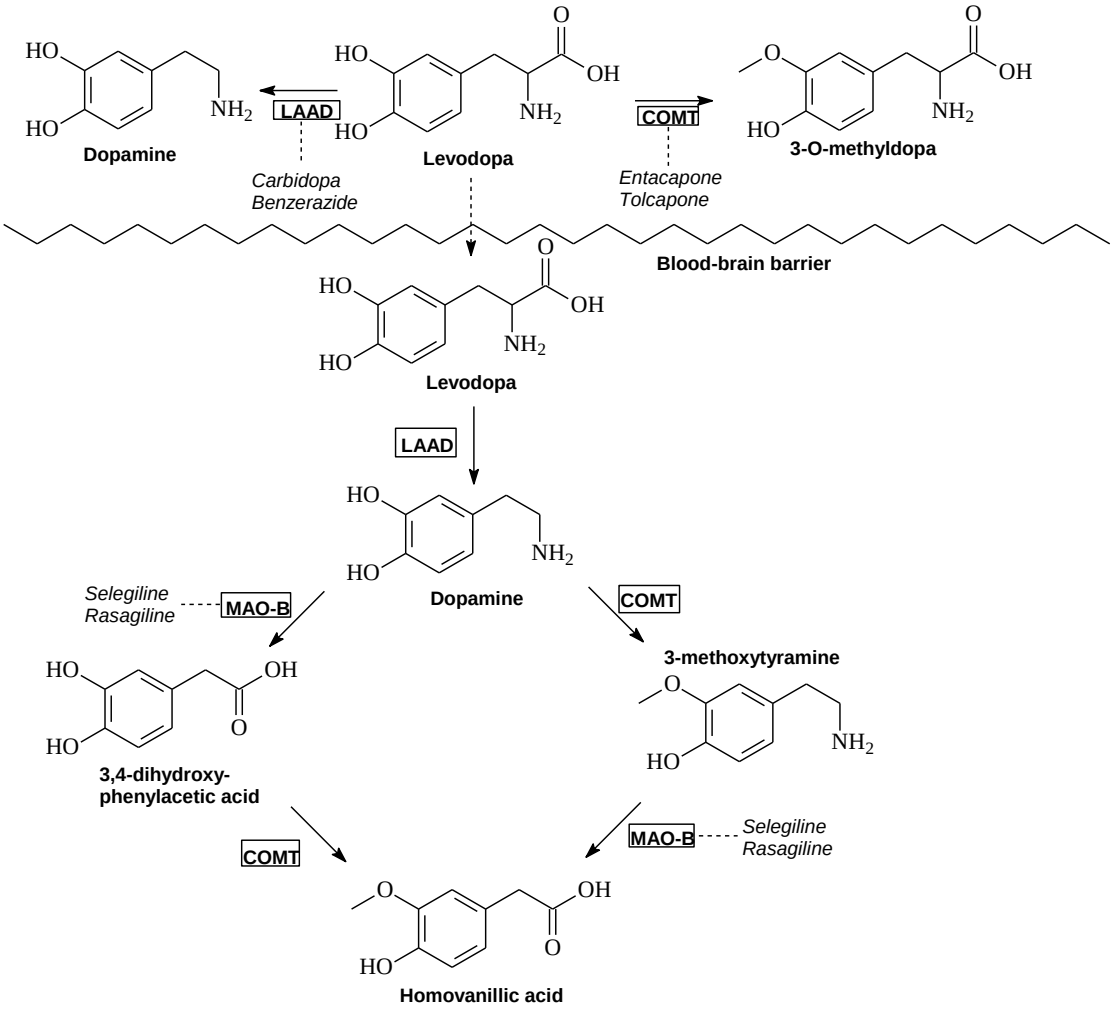

Figure 2.6 *The metabolism of levodopa and dopamine, showing the action sites of different inhibitory drugs used in combination with levodopa. Peripheral conversion of levodopa is inhibited by carbidopa, benserazide, entacapone and tolcapone.*

Dopamine agonists

Dopamine agonists work by acting on the dopamine receptors and mimicking dopamine function, thereby inhibiting dopamine release and reducing oxidative stress. Dopamine agonists are used in both monotherapy, in mild-to-moderate cases of PD, and as adjuncts to levodopa treatment. The metabolism of the dopamine agonist does not produce harmful reactive species and it suppresses the release of endogenous dopamine, thereby protecting neuron terminals (Brooks, 2000).

Dopamine agonists display dopaminergic side-effects such as nausea, delusions, vasospasm and skin inflammation. In a study in 1999, patients were treated with ropinirole and pramipexole. Interestingly, some of these patients later reported incidents of “sleep

attacks" during which the person suddenly fell asleep and only realized this after awakening. Some of these patients had sleep attacks while driving a vehicle and one even fell asleep in mid-sentence of a conversation (Frucht *et al.*, 2000). It could not be confirmed nor denied that the drugs were responsible for the sleep attack, but the patients stopped the therapy and the sleep attacks did not return.

Catechol-*O*-methyltransferase inhibitors

Levodopa is peripherally metabolized by L-AAD to dopamine and secondarily by catechol-*o*-methyltransferase (COMT) to 3-*o*-methyldopa. To prevent the peripheral metabolism of levodopa, an L-AAD inhibitor is administered with the levodopa. When the L-AAD inhibitor is present, most levodopa is metabolized via the methylation pathway and very little levodopa reaches the brain unchanged (fig 2.6). A COMT-inhibitor administered alone does not have any effect on PD symptoms. It is usually administered as a combination of levodopa-carbidopa-entacapone, which requires the patient to take fewer pills during the day (Chen & Swope, 2007).

Monoamine oxidase (MAO)-B inhibitors

MAO-B inhibitors, such as selegiline and rasagiline, display neuroprotective effects as they inhibit the deamination of dopamine (fig 2.6). Deamination produces hydrogen peroxide which, in turn, leads to free radical production. Free radicals are unstable molecules that react with molecules present in cells and cause damage to the neurons. The catabolism of dopamine by MAO-B produces toxic by products. MAO-B inhibitors reduce the formation of these radicals and also prolong the effect of dopamine by reducing the degradation of dopamine. MAO-B inhibitors may therefore be useful in the treatment of PD (Chen & Swope, 2007; Lewitt & Taylor, 2008).

Anticholinergic drugs

Dopamine naturally inhibits acetylcholine neurons in the brain. The depletion of dopamine in PD causes the activation of these neurons and it is believed that increased acetylcholine levels contribute to the tremors seen in PD. Anticholinergic drugs, such as atropine and dicyclomine, are used to treat the tremors in PD. The use of anticholinergics is limited because it has severe side-effects such as confusion, constipation, dry mouth, blurred vision, impaired memory and sedation (Mayasaki *et al*., 2002).

Adenosine A_{2A} receptor antagonists

Adenosine A_{2A} receptor antagonists block the A_{2A} receptors, thereby increasing dopamine transmission in the PD brain. This occurs because stimulation of the A_{2A} receptor in the brain opposes the function of dopamine. A_{2A} antagonists pared with a decreased dose of levodopa provide the same symptomatic relief of a normal dose of levodopa with a decrease of dyskinesias (Bara-Jimenez *et al*., 2003). A_{2A} antagonists may also exhibit neuroprotective functions by reducing the mitochondrial toxic effects that occur in the dopaminergic neurons. They may also reduce the formation of protein aggregates (Dall'Inga *et al*., 2003). A well known A_{2A} antagonist is KW-6002 or istradefylline, which has entered the clinical phases of drug development.

Mitochondrial energy enhancement drugs: Coenzyme Q_{10} and antioxidant therapy

The loss of function of complex I in the respiratory chain has long been associated with PD. Coenzyme Q_{10} (Co-Q_{10}) is a co-factor for complex I where it serves as an electron acceptor and an antioxidant. This creates the possibility that treatment with Co-Q_{10} may alleviate symptoms associated with PD. In a clinical trial, patients were treated with increased amounts of Co-Q_{10}. These patients showed an increase in the ease of performing normal daily activity (Schultz *et al*., 2002).

The use of antioxidants as a possible therapy for PD has been studied but with inconclusive results. It appears that the antioxidants administered do not have a marked effect on slowing neuronal damage (Lewitt & Taylor, 2008).

Anti-apoptotic drugs

Evidence has pointed out that apoptosis may play a role in the loss of neuronal cells and neurodegeneration. This creates a niche for anti-apoptotic drugs that may slow the loss of functional neurons. Despite the evidence there is no consensus that apoptosis is a primary mechanism for neurodegeneration in PD and even if it is, some researchers feel that by the time apoptosis sets in, the neurons are terminal and not much can be done to save them.

Minocycline has been shown to improve the survival of dopaminergic neurons in rodent models. It inhibits activation of the microglia, which is prominent in PD and it reduces the factors that cause apoptosis (Du *et al*., 2001).

2.1.4 Mechanisms of neurodegeneration

Two hypotheses exist as to the mechanism of neurodegeneration in PD pathogenesis. One states that the misfolding and aggregation of proteins damage dopaminergic neurons and the other states that mitochondrial damage due to oxidative stress may be the primary cause of PD. The pathogenic factors are not exclusive and both may be present in a PD case.

Oxidative stress and mitochondrial dysfunction

Evidence suggests that a dysfunction of complex I of the mitochondria, whether genetic or sporadic, contribute to the cause of PD. The function of complex I is reduced in the brain and platelets of PD patients. Mitochondria are the primary mediators of cell death when levels of Ca^{2+} increase (fig 2.7) as is the case with excitotoxicity. The mechanisms of cell death include oxidative stress and apoptosis. Mild injury to the mitochondria allows ATP levels to be maintained, causing cell death via oxidative stress, but during more extensive injury, ATP levels are not maintained and Ca^{2+} levels increase. This is responsible for necrosis of the neuronal cells in PD (Fiskum *et al.*, 2003).

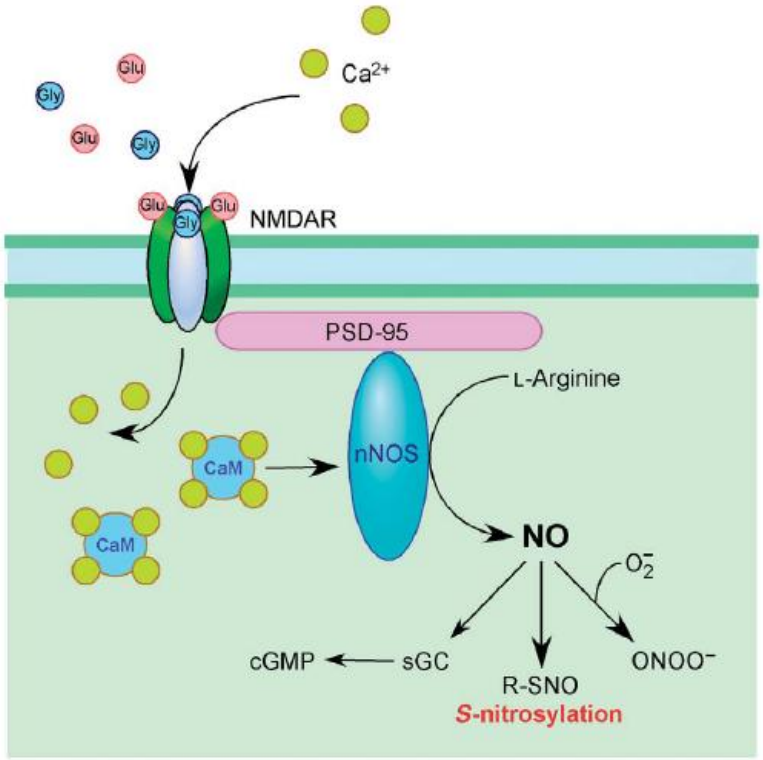

Figure 2.7 *The schematic illustrates one way that ROS is formed due to increased influx of Ca^{2+}. The N-methyl-D-aspartate (NMDA) receptor is activated by glutamate and glycine. Activation of NMDA receptors causes an influx of Ca^{2+}. This in turn activates neuronal NO synthase and the generation of ROS. (Schematic from Lipton et al., 2007)*

The endogenous metabolism of dopamine also produces hydrogen peroxide, which can cause oxidative stress if it is not removed by the anti-oxidant glutathione, for example. Increased iron in the brain may also lead to the production hydroxyl radicals via the Fenton reaction (fig 2.13). Oxidative stress thus occurs when ROS are produced and the ROS buffering systems are dysfunctional. These dysfunctions may occur due to sporadic, environmental or genetic causes.

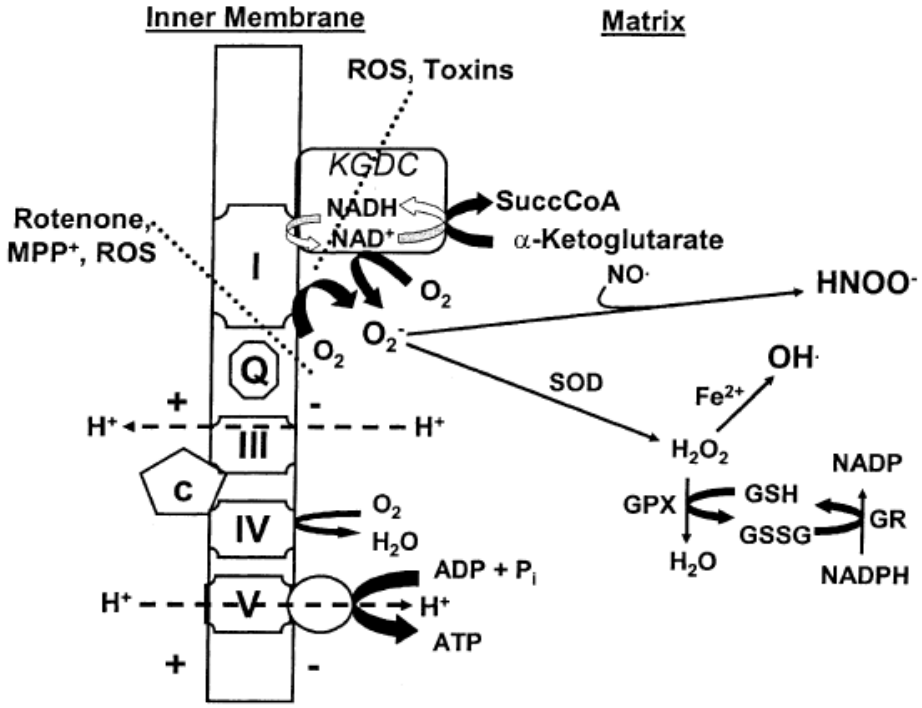

Figure 2.8 *The production and detoxification of ROS. Complex I is the site most implicated for ROS production in PD. The neurotoxins rotenone and MPP^+ are capable of inhibiting complex I in vivo and can also stimulate production of ROS in vitro (Lenaz, 1998). These compounds lead to the overall inhibition of α-ketoglutarate decarboxylase (αKGDC) activity. This complex catalyzes the formation of superoxide and consequently hydrogen peroxide (H_2O_2) production. Hydroxyl ($OH^{\bullet}$) radicals and peroxynitrite ($HNOO^-$) cause oxidative damage and inhibition of complex I. This causes metabolic failure as ATP cannot be produced. Superoxide dismutase (SOD) activity is reduced in PD and the detoxification of the harmful radicals does not occur naturally. (Fiskum et al., 2003).*

There exist a great body of evidence that oxidative stress contributes to the neurodegenerative features of PD. Autopsies of PD patients revealed oxidative damage to lipids, DNA and protein and decreased levels of the natural antioxidant, glutathione. This oxidative stress may contribute to the misfolding of proteins in PD (Sherer *et al.*, 2002).

Certain factors are responsible for the activation of cell death. Elevated Ca^{2+}, ceramide, ROS and apoptotic proteins are all capable of releasing proapoptotic proteins from the mitochondria (fig 2.9). Evidence from both human and animal models has shown that the mitochondrial pathway of apoptosis and cell death are present in dopaminergic neurons in PD (Dawson & Dawson, 2002). Activation of apoptotic mechanisms represents end-stage PD, at which stage therapeutic intervention is usually too late.

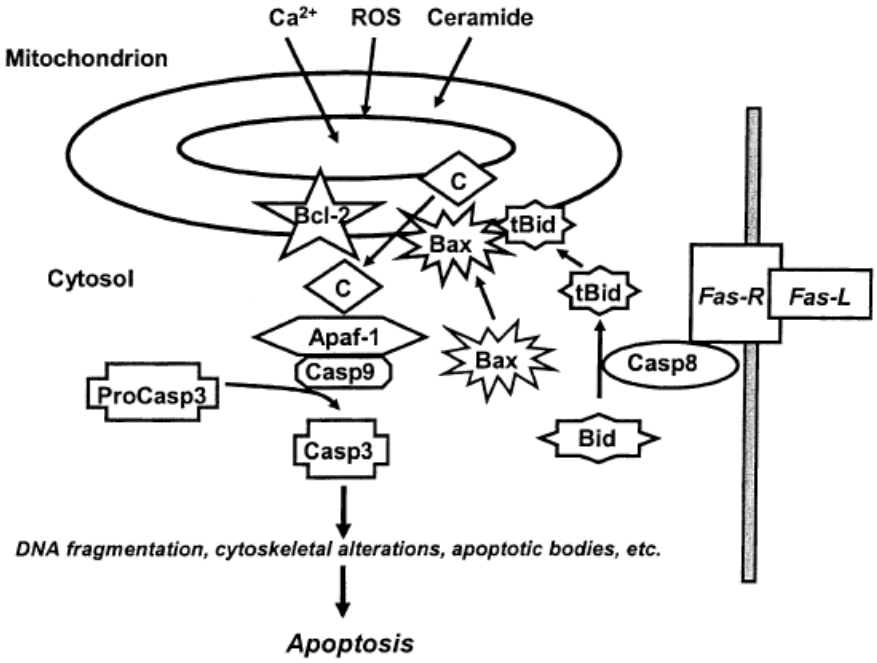

Figure 2.9 *The mitochondrial pathway of apoptosis. Ca^{2+}, ROS and ceramide and proapoptotic factors, Bax and tBid, stimulate the release of other proapoptotic factors such as cytochrome c (C). Cytochrome c and procaspase 9 form a complex with apoptosis activating factor 1 (Apaf-1) to activate caspase 9. Cleavage of procaspase 3 by caspase 9 gives caspase 3. This caspase together with others, degrade proteins responsible for apoptosis. The antiapoptotic protein, Bcl-2, can inhibit the release of cytochrome c (Fiskum et al., 2003).*

Protein aggregation and misfolding

Protein aggregation occurs when a protein undergoes partial unfolding or misfolding caused by oxidative or thermal stress, by alterations of the DNA and during RNA transcription and translation faults. Protein aggregates are generally insoluble and stable in the physiological environment. Certain systems exist that recognize misfolded proteins and degrade them.

Examples are the ubiquitin system and the parkin protein. If these degradation systems malfunction, protein aggregates may also be deposited (Dobson, 2003).

Aggregated proteins may cause damage to the neurons in PD by directly interfering with the cell systems of the neurons. Another theory states that aggregated proteins may serve a protective function by sequestering the important proteins in a damaged neuron and thereby keeping the proteins safe. This is an unlikely mechanism as the sequestered proteins are unable to function optimally (Saudou *et al*., 1998).

Oxidative stress may also be a trigger for the incorrect folding of proteins. In PD, oxidatively modified α-synuclein is the principal protein found in LBs. The amount of neurons damaged by oxidative stress increases with age, and as neurons are post mitotic, they are unable to renew and repair damage (Dauer & Przedborski, 2003).

Inflammation may be caused as a result of the deposition of protein aggregates. Aggregation of α-synuclein may trigger the release of cytokines. The complement system is also activated, as complement proteins have been found in LBs in the PD brain (Yamada *et al*., 1992).

Inflammation also occurs when microglia start to cluster around the damaged dopaminergic neurons. The mechanism by which the microglia is activated is not certain. In neurodegenerative diseases, the microglia are instructed to remove cellular debris that is formed when neurons die, thus implicating that the immune system might play an important role in the pathology of PD. Inflammation is the start to a cascade of mechanisms that eventually leads to apoptosis and necrosis (Cicchetti *et al*., 2002). Inflammation is one of the first lines of defence against neuronal injury, but under the conditions observed in PD it causes more damage than protection. Under these conditions it is preferable to save the neurons even if damaged. Non-steroidal, anti-inflammatory drugs are most commonly administered (McGeer *et al*., 1987).

2.2 MONOAMINE OXIDASE

2.2.1 Background

Two isoforms of monoamine oxidase (MAO) exist, MAO-A and MAO-B. These enzymes are found mainly in the mitochondrial membrane, although a small proportion of the enzymes is also found in the cytoplasm. MAO is found in almost all mammalian tissue, but the distribution of MAO-A and MAO-B differs from organ to organ and also between species.

MAO-A is found exclusively in the placenta with MAO-B mainly present in blood-platelets. Both isoforms are present in the brain, liver, lungs and gastro-intestinal tract (Kalaria & Harik, 1987).

MAO is responsible for the oxidative deamination of different monoamines. MAO-A mainly catalyses the deamination of 5-hydroxytryptamine (serotonin), whilst MAO-B is the predominant form responsible for the deamination of 2-phenylethylamine and benzylamine. Dopamine, adrenaline and noradrenalin are substrates for both isoforms, although MAO-B is the preferred enzyme for dopamine catalysis (Youdim & Bakhle, 2006). MAO-B is found in higher concentrations in the brain than MAO-A (Mandel *et al*., 2005). MAO seems to play a protective role in the peripheral tissues by oxidizing amines in the blood or by preventing entry into circulation. Both MAO-A and MAO-B may protect the neurons from exogenous amines. MAO-A in serotonergic neurons degrade the neurotransmitter serotonin. Inhibitors of MAO-A have been shown to have anti-depressant activity by increasing serotonin levels in the brain. MAO-B in serotonergic neurons may degrade foreign amines and inhibit their access to the synaptic vessels (Youdim *et al*., 2006).

2.2.2 Genetics

MAO-A and MAO-B are approximately 70% identical and consists of 527 and 520 amino acids, respectively. cDNA cloning was used to elucidate the amino acid sequences of MAO-A and –B. Differences in the promoter regions may account for the differences in biological function between the two enzymes. (Nagatsu, 2004; Shih *et al*., 1999).

The genes that encode for the MAOs are located on the X chromosome. This may indicate that men are at higher risk for developing Parkinson's disease than women (Wooten *et al*., 2004; Van den Eeden *et al*., 2003). Both isoforms consist of 15 exons with identical exon-intron organization. The FAD binding site is encoded by exon 12 and it shares 93.9% similarity between the isoforms. This is indicative of MAO-A and –B sharing a common ancestral gene (Nagatsu, 2004; Shih *et al*., 1999).

MAO activity is not essential for survival, but it is important during development. MAO-A knockout mice have elevated serotonin, noradrenalin and dopamine levels in the brain and in MAO-B knockout mice only 2-phenylethylamine is increased. MAO knockout animals have shown increased stress levels (Youdim *et al*., 2006).

MAO-A deficiency has been shown to result in compulsive aggressive behaviour in humans (Brunner *et al*., 1993). Deficiency of platelet MAO-B may result in behaviour that includes

impulsiveness and sensation seeking. These traits have been linked to substance abuse such as smoking, gambling and alcoholism. Since cigarette smoke contains MAO-B inhibitors, it is unclear whether people smoke because of lowered MAO-B activity or whether smoking causes low MAO-B activity (Fowler *et al*., 2003; Oreland, 2004).

2.2.3 The three-dimensional structure of MAO

Both forms of MAO are mitochondrial enzymes containing covalently bound flavin adenine dinucleotide (FAD) as a cofactor. The covalent attachment to the enzyme is via a thioether bond between a cysteinyl residue and the 8α-methylene of the isoalloxazine ring of the FAD (Kearney *et al*., 1971) (fig 2.10). The flavin is in a bent, non-planar conformation, which is expected to facilitate the catalytic activity of MAO.

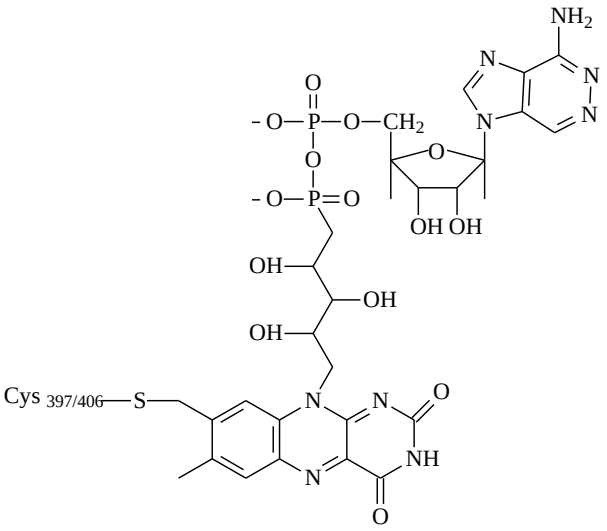

Figure 2.10 *Structure of the covalent-bound FAD in MAO-B showing the interaction with the Cys397 and the 8α of the isoalloxazine rings. In MAO-A the linkage is to the Cys406 residue.*

MAO-B crystallizes as a dimer with each monomeric unit containing a flavin-binding region, a membrane binding region and a substrate binding region. The membrane binding region or the carboxyl terminal region is from residues 461 to 520. A 27 residue α-helix is predicted to be inserted into the membrane as it has an apolar surface, which will facilitate its insertion into the membrane (fig 2.11). This proposal is supported by C-terminal truncation studies and sequence analysis predictions (Edmondson *et al*., 2004; Son *et al*., 2008). Additional membrane interactions are formed between hydrophobic residues Trp157, Pro109, Ile110 and possibly residues 481-488. This may also explain why C-terminal truncated MAO-B retains some affinity for membranes, although not as strong as the non-truncated enzyme

(Edmondson *et al*., 2004). Son *et al*. (2008) proved that the catalytic activity of MAO-A greatly decreases when the c-terminal is truncated, thus concluding that membrane anchoring is important in the functioning of the MAOs (Son *et al*., 2008). MAO-A forms interactions with the membrane at hydrophobic residues Arg129, His148, Lys151, Lys163, Arg493, Lys503, Lys520 and Lys522.

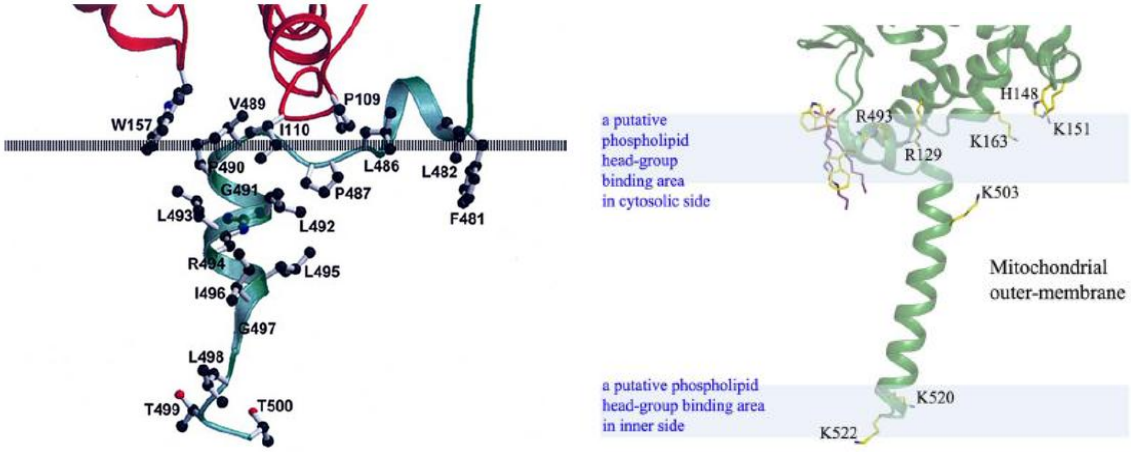

Figure 2.11 *Left: The membrane binding domain of human MAO-B. Additional interaction sites may be Trp157, Pro109 and Ile110. Right: The membrane binding domain of MAO-A. Interactions between the membrane and residues Arg129, His148, Lys151, Lys163, Arg493, Lys503, Lys520 and Lys522 are shown.*

The active site structure of MAO-B consists of two cavities lined with hydrophobic residues that connect the opening of the active site to the flavin-binding domain. This is the “entrance cavity”. The entry point for the substrate is close to the membrane surface. A flexible loop (99-112) must move for the substrate to enter, this is referred to as a “gating switch”. The membrane surface is negatively charged and this will attract the positively charged amine substrates to MAO-B (fig 2.12). The amine must be deprotonated for binding and catalysis. The side chain of Ile199 serves as a gate between the two cavities and can exist in the “open” or “closed” conformation. The residue is in the “closed” conformation when small substrates bind and in the “open” conformation when large molecules bind to the active site. This residue, Ile199, plays an important role in determining the selectivity of MAO-B (Edmondson *et al*., 2004).

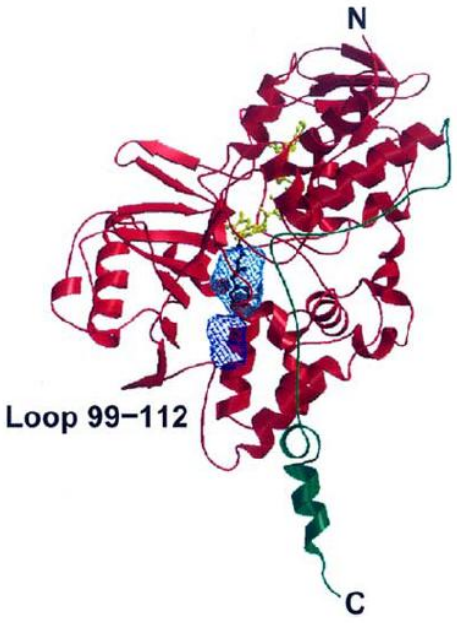

Figure 2.12 *Structure of monomeric human MAO-B. The substrate enters from below to the flavin in the MAO-B. Loop 99-112 indicates the position of the gating switch. The FAD is shown in the ball-and-stick conformation and the substrate is shaded with the membrane binding C-terminal shown in green.*

Flexibility may also play a role in selectivity. Son *et al*. (2008) has shown that a mutation at Gly110 to an alanine residue of human MAO-A decreases catalytic activity. This is because alanine is slightly more rigid than glycine. Further substitution of Gly110 with a proline showed even greater decrease in the catalytic activity of MAO-A. It may thus be concluded that the amount of conformational change the enzyme can undergo influences substrate specificities (Son *et al*., 2008).

2.2.4 Catalytic cycle of amine oxidation

The catalytic activity of MAO produces toxic-by products such as aldehyde, hydrogen peroxide and ammonia (fig 1.2). In healthy brains aldehyde dehydrogenase deals with detoxification of aldehydes and prevents the accumulation of aldehydes in the brain. In PD the levels of aldehyde dehydrogenase in the substantia nigra are reduced, which may cause the accumulation of aldehydes. This may play a role in the degenerative processes in PD (Lamensdorf *et al*., 2000).

Normally hydrogen peroxide is inactivated by glutathione peroxidase with glutathione as co-factor. In PD, levels of glutathione is reduced which may lead to the accumulation of hydrogen peroxide. On its own, hydrogen peroxide causes oxidative damage, but the high

levels of hydrogen peroxide in the PD brain may make it available for the Fenton reaction (fig 2.13). During the Fenton reaction a form of iron molecule, in this case the ferrous ion Fe^{2+}, produces a hydroxyl radical when it reacts with hydrogen peroxide. Hydroxyl radicals deplete the anti-oxidants in the brain, increase oxidative stress and react with DNA, lipids and proteins to cause damage (Youdim & Bakhle, 2006).

Interestingly, smokers have a reduced risk of developing PD. This may be because nicotine is a MAO inhibitor and it increases striatal dopamine release (Lees *et al.*, 2009). Iron may also influence the activity of MAO. Iron deficiency in rats has caused abnormal behaviour and influenced the normal activity of monoamine neurotransmitters (Youdim & Green, 1975) and is known to accumulate at sites of neuronal death.

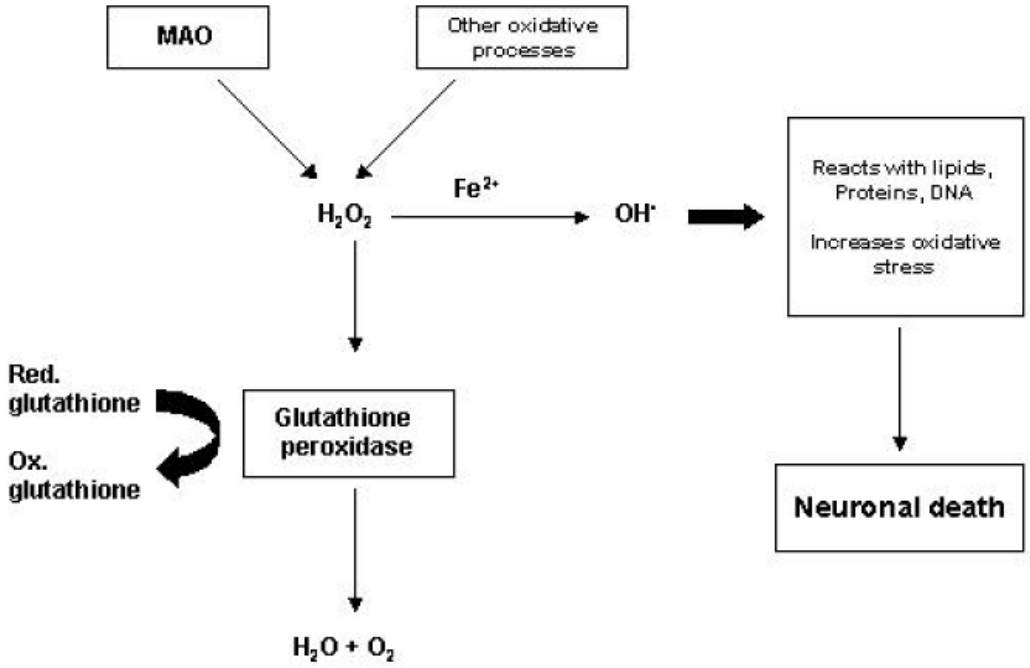

Figure 2.13 *The Fenton reaction. When glutathione (GSH) levels are low as in PD, excess hydrogen peroxide (H_2O_2) accumulates and is available to react with a ferrous ion (Fe^{2+}) to produce hydroxyl radicals ($OH^{\cdot}$). The radicals cause damage to DNA, lipids and proteins and eventually lead to neuronal death.*

The reaction catalyzed by MAO is the oxidative deamination of primary, secondary and tertiary amines. The pathway of MAO catalysis depends on the nature of the substrate. For example, benzylamine and analogues thereof follow the lower pathway of figure 2.14. Phenethylamine follows the top pathway of fig 2.14. The imine products dissociate from the reduced enzyme and the free reduced enzyme then react with O_2. MAO catalysis occurs via

the lower loop of fig 2.14. The major difference between MAO-A and MAO-B catalysis is in their K_m (O_2) values. MAO-A exhibits a value of ~6 µM while MAO-B has a value of ~250 µM, which is approximately the concentration of O_2 in air-saturated aqueous solutions. Thus at saturating concentrations, MAO-A is working at maximal velocity while MOA-B is only working at half maximal velocity (Edmondson *et al.*, 2004).

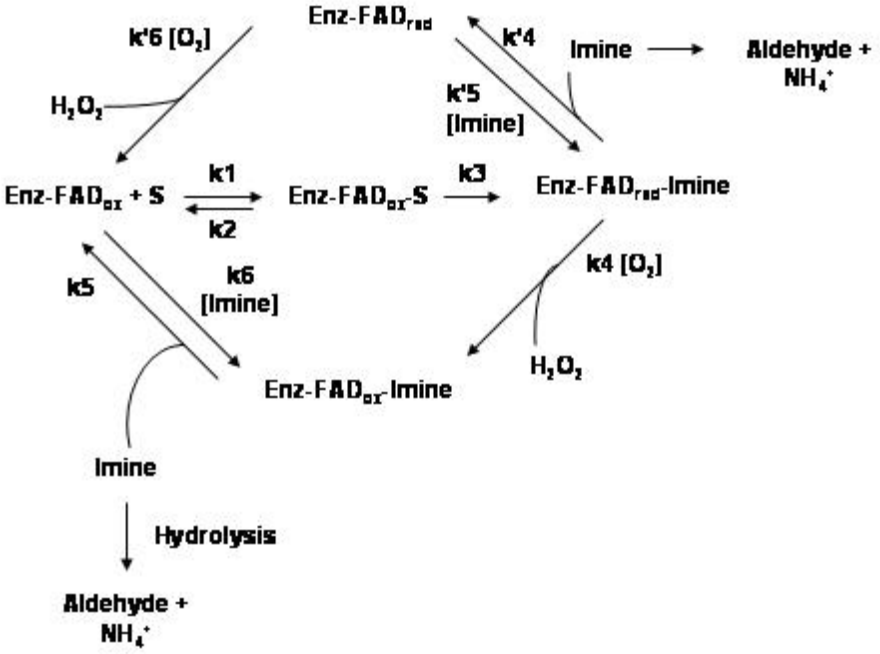

Figure 2.14 *Reaction pathway for MAO catalysis.*

Two proposals have been suggested for the mechanism of electron transfer which is essential for amine oxidation: the single electron transfer (SET) mechanism (fig 2.15) or the polar nucleophilic mechanism (fig 2.16).

Single electron transfer mechanism

The first step is the one-electron oxidation of the lone-pair on the amine nitrogen. An aminium cation radical and flavin radical are formed. The aminium cation results in a lowered pKa value for the α-carbon hydrogen. This is thought to allow for the removal of the α-carbon H^+ by an active site base in the catalytic site. MAO-B has no amino acid residues in the catalytic site which can perform this action. Further studies have also revealed that the equilibrium constant is 10^{15} – 10^{25} in the favour of the reactants. The formation of an aminium cation is also expected to interact with the aromatic cage in a π-cation interaction,

making the intermediate very stable. This makes the SET mechanism kinetically and thermodynamically improbable (Edmondson *et al*., 2004).

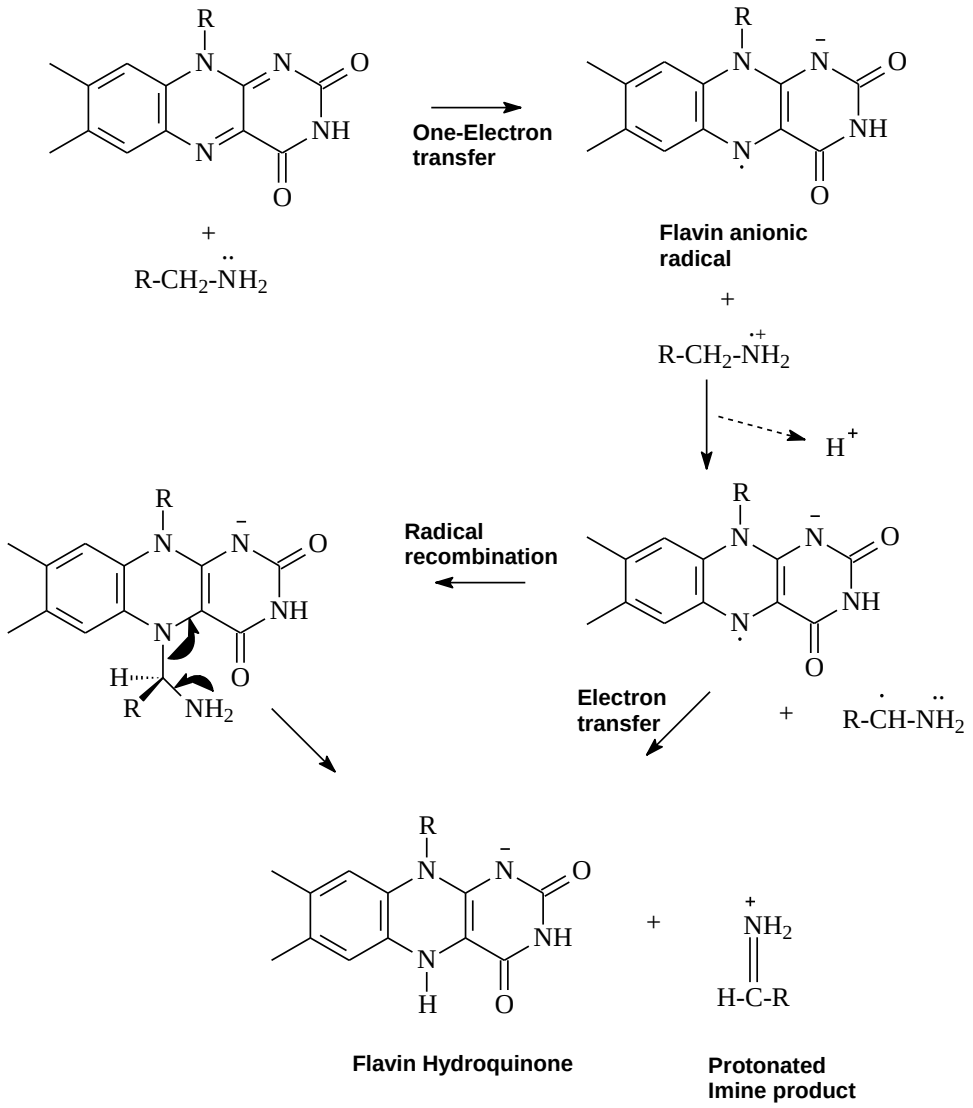

Figure 2.15 *The single electron transfer (SET) mechanism.*

Polar nucleophilic mechanism

The polar nucleophilic mechanism gives an explanation of how a benzyl proton with a pKa value between 26 – 28 can be deprotonated by a base in the catalytic site. The deprotonated amine nucleophilically attacks the flavin at the C(4a) position. This allows the N(5) position of the flavin to become basic with a pKa between 25 – 27, which makes it strong enough to abstract the α-H from the substrate. This mechanism is consistent with the existing structural data of MAO-B and this is a more probable mechanism for MAO catalysis (Edmondson *et al*., 2004).

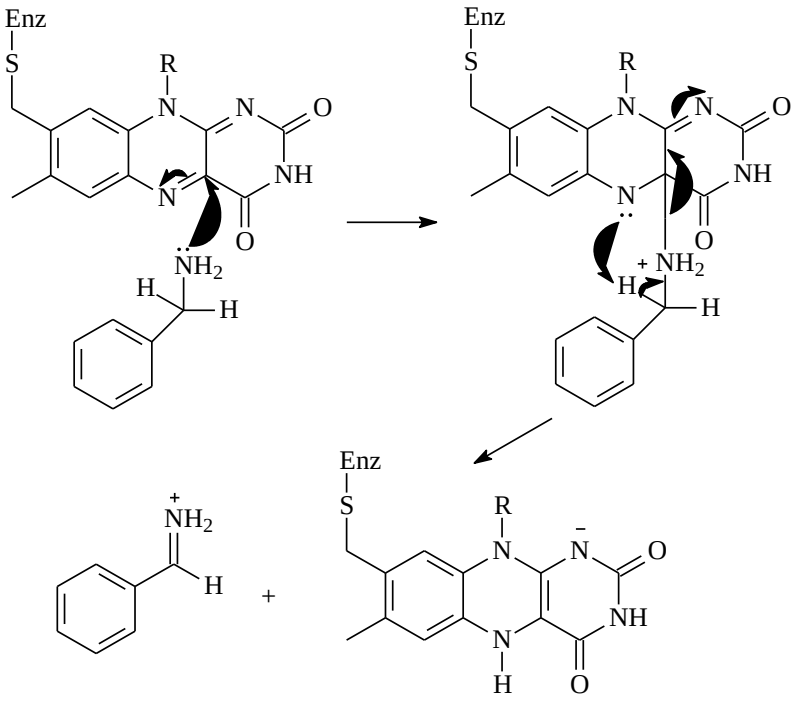

Figure 2.16 *The polar nucleophilic mechanism.*

2.2.5 The role of MAO in Parkinson's disease

Dopamine is synthesized from tyrosine in the brain, where it is metabolized by both MAO-A and MAO-B in the glial cells and astrocytes. MAO-B is present in higher concentrations in the brain and is the preferred enzyme for dopamine catabolism (Youdim *et al*., 2006).

As mentioned earlier, MAO catalysis produces harmful substances such as hydrogen peroxide, aldehydes and ammonia. In healthy brains this is not a problem, as aldehyde dehydrogenase and glutathione peroxidase rapidly detoxifies these substances. The PD brain presents low levels of the above mentioned enzymes and added to that, the amount of MAO is increased in PD brains. Thus more hydrogen peroxide is available for the formation of hydroxyl radicals (Mandel *et al*., 2005).

MAO-B also plays a role in the activation of neurotoxins, as is shown by the oxidation of MPTP to MPP^+, which causes severe parkinsonian symptoms (Langston *et al*., 1983). This suggests that MAO-B activity can contribute to the onset of PD.

It is clear that MAO-B plays an important part in the progression and possibly the onset of PD. This creates the rationale to investigate MAO-B inhibitors for the treatment of PD.

Several such inhibitors are already in use for the symptomatic relief of PD. Selegiline inhibits the action of MAO-B and may have added neuroprotective properties. Rasagiline activates the release of dopamine in addition to inhibiting the degradation of dopamine (Fernandez & Chen, 2007).

2.2.6 Inhibitors of MAO

Inhibitors of MAO were first used as a treatment for depression. MAO metabolizes dopamine, thus inhibiting the action of MAO results in an enhanced availability of dopamine in the brain. Later, selective inhibitors for MAO-A and MAO-B were developed. MAO-B inhibitors show particular promise as anti-parkinsonian drugs (Riederer *et al*., 2004).

Irreversible inhibitors of MAO-B

Selegiline is a propargyl amphetamine derivative that produces methamphetamine and amphetamine when metabolized by the liver. Amphetamine is neurotoxic and may produce adverse cardiovascular and psychiatric effects. Selegiline prevents neurodegeneration by competing with dopamine for binding to MAO-B. Metabolism of dopamine by MAO-B produces reactive species and inhibition of MAO-B is associated with reduced oxidative stress. Selegiline can also prevent apoptosis by altering pro- and anti-apoptotic proteins due to their propargylamine structure and it may have a neuroprotective action, as it slows the rate of neurodegeneration (Fernandez & Chen, 2007; Youdim & Bakhle, 2006).

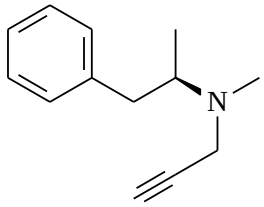

Figure 2.17 *The structure of selegiline.*

Rasagiline is another example of a propargylamine containing selective MAO-B inhibitor. Rasagiline also causes the release of dopamine and the retardation of dopamine catabolism by MAO-B. Rasagiline is given as an adjunctive to levodopa treatment to prolong the effect of dopamine derived from levodopa. The neuroprotective properties of rasagiline stems from its anti-apoptotic and anti-oxidant capacity. Rasagiline has been shown to preserve mitochondrial membrane integrity (Fernandez & Chen, 2007; Youdim & Bakhle, 2006).

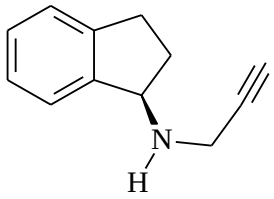

Figure 2.18 *The structure of rasagiline.*

Ladostigil is structurally related to rasagiline, but it is not a selective inhibitor for MAO-B since it also inhibits MAO-A. Ladostigil has been shown to display cognitive improvement in animal models and it seems to be tissue-specific, inhibiting only MAO in the brain and not in the gut, making it devoid of the cheese reaction (Mandel *et al.*, 2005; Sagi *et al.*, 2005). Ladostigil increases levels of 5-HT, noradrenalin and dopamine in the brain and also has an anti-depressant activity in animal models (Sagi *et al.*, 2005). It prevents neurodegeneration in the MPTP mouse model of PD and it has anti-apoptotic activity similar to that of rasagiline (Mandel *et al.*, 2005). It is also an inhibitor of cholinesterases and is thus able to improve cognition.

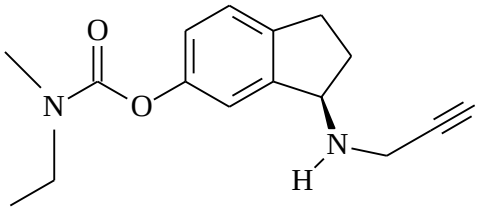

Figure 2.19 *The structure of ladostigil.*

Reversible inhibitors of MAO-B

Reversible inhibitors of MAO-B are inhibitors that can compete with the substrate for the binding site of MAO-B. This means that enzyme recovery is almost immediate and thus prevents toxic reactions like the cheese reaction.

Safinamide is an α-amino amide derivative. It is a sodium and calcium channel blocker and also a MAO-B inhibitor. Safinamide has excellent anti-parkinsonian and anti-convulsant properties and has been shown to have promising neuroprotective properties in animal models. Safinamide improves cognitive function and may be co-administered with levodopa. It is considered to be exceptionally safe for use as a drug (Marzo *et al.*, 2004).

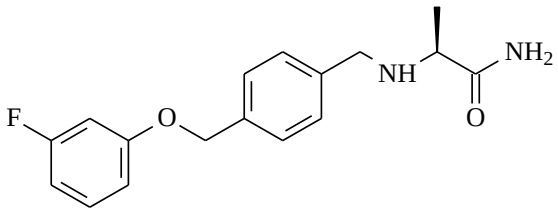

Figure 2.20 *The structure of safinamide.*

Lazabemide is a selective and reversible inhibitor of MAO, but it has a significantly higher selectivity towards MAO-B than MAO-A. Clinical studies have shown that lazabemide may have potential as a treatment strategy in PD (Dingemanse *et al*., 1997). The metabolism of lazabemide produces an inactive acidic metabolite, which makes it more tolerable, unlike the amphetamine-like derivatives derived from selegiline metabolism (Dingemanse *et al.*, 1997). Monotherapy with lazabemide delays the requirement for the initiation of dopaminergic treatment.

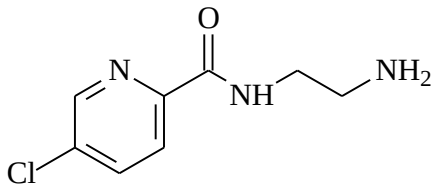

Figure 2.21 *The structure of lazabemide.*

(E)-8-(3-Chlorostyryl)caffeine (CSC) is a dual acting compound which inhibits MAO-B and antagonises the adenosine A_{2A} receptor. Studies have shown that caffeine is an inhibitor of the adenosine A_{2A} receptor and that it reduces the risk of developing PD (Ross *et al.*, 2000; Ascherio *et al.,* 2001). Based on this protective effect of caffeine, CSC has also been found to exert neuroprotective properties by blocking the A_{2A} receptor in animal models (Chen *et al.*, 2002). CSC may therefore have a dual function in the treatment of PD. By inhibiting MAO-B it may conserve dopamine supply in the brain, and by blocking A_{2A} receptors CSC may protect against further neurodegeneration (Chen *et al*., 2002).

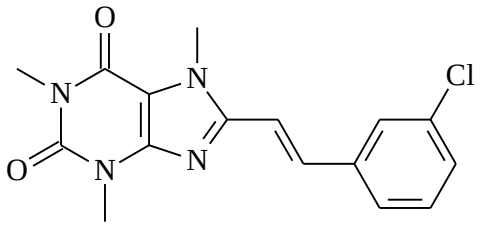

Figure 2.22 *The structure of (E)-8-(3-chlorostyryl)caffeine.*

1,4-Diphenyl-2-butene is a MAO-B inhibitor that was discovered by chance when MAO-B was crystallized using polystyrene containing vessels. Crystallization revealed that MAO-B appeared inhibited by some compound not initially added to the crystallization process. Thin Layer chromatography later revealed the compound as 1,4-diphenyl-2-butene (Hubalek *et al.*, 2003).

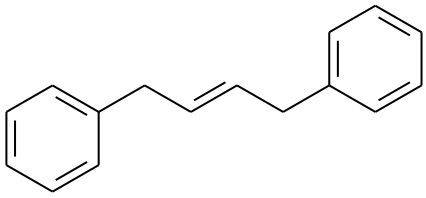

Figure 2.23 *The structure of 1,4-diphenyl-2-butene.*

Trans, trans-farnesol is a component of tobacco smoke. It is a reversible inhibitor specific for MAO-B in humans. It has also been shown to inhibit horse, rat and mouse MAO-B, but it is ineffective on bovine or sheep MAO (Hubalek *et al*., 2005).

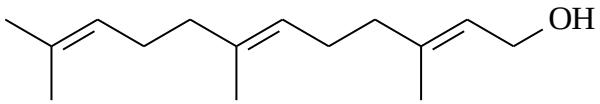

Figure 2.24 *The structure of trans, trans-farnesol.*

Inhibitors of MAO-A

MAO-A inhibitors were first used as antidepressants, but irreversible MAO-A inhibitors induced toxic effects known as the cheese reaction (fig 2.25). The cheese reaction is induced by tyramine, which is a naturally occurring compound in most cheeses (hence the name). Under normal circumstances, dietary amines (such as tyramine), are metabolized in the gut wall by MAO. This prevents them from entering circulation. When a MAO inhibitor is present, the tyramine is not metabolized and it enters circulation. Tyramine can then induce

the release of large amounts of noradrenalin, which causes a severe, sometimes fatal, hypertensive reaction. Irreversible MAO-A inhibitors allow large amounts of active tyramine to enter the circulation, which stimulates the release of noradrenalin. Reversible MAO-A inhibitors are displaced from the enzyme by the substrate, tyramine, thus unmetabolized tyramine does not enter the circulation (Youdim & Bakhle, 2006; Youdim *et al.*, 2006).

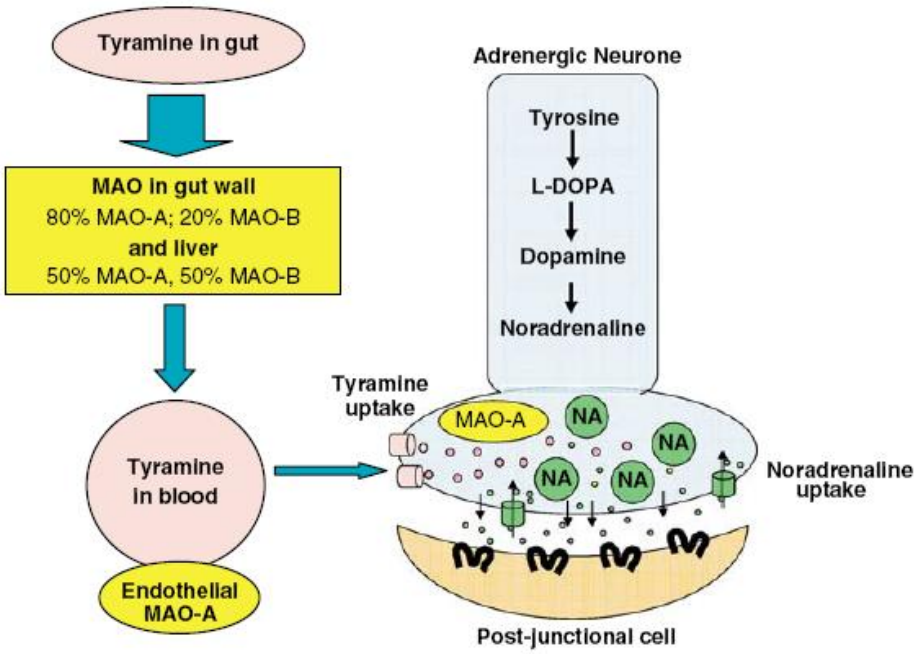

Figure 2.25 *The cheese reaction. Normally tyramine is metabolized in the gut by MAO which deactivates it. The tyramine not metabolized in the gut is inactivated by MAO in endothelial cells. Tyramine uptake by the adrenergic neurons stimulates the release of noradrenalin causing hypertensive reactions (Youdim & Bakhle, 2006).*

Iproniazid was the first MAO inhibitor used for depressive illness. It was discovered when patients treated for tuberculosis with a related compound, isoniazid, displayed antidepressive traits. Iproniazid itself is hepatotoxic due to its hydrazine structure. Later, non-hydrazine irreversible inhibitors were found to be safer in this regard (Youdim & Bakhle, 2006).

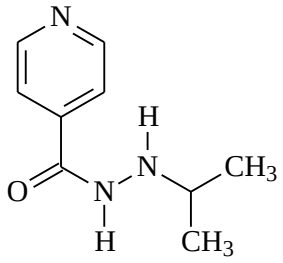

Figure 2.26 *The structure of iproniazid.*

Moclobemide and brofaromine are reversible MAO-A inhibitors that do not provoke the cheese reaction. The reversibility of these inhibitors allows for the competition of dietary amines to displace the inhibitor from the enzyme and is thus metabolized in the normal way. Free tyramine in the circulation is therefore limited and thus preventing the cheese reaction (Youdim & Bakhle, 2006).

Moclobemide increases dopamine, serotonin and noradrenaline in the brain, thus making it an effective antidepressant (Haefely *et al.*, 1992). In PD, the antidepressant effect is considered useful, since PD patients eventually suffer from depression. Moclobemide also shows a mild improvement of motor functions in PD.

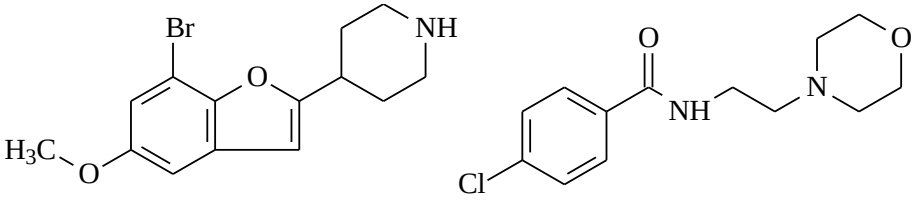

Figure 2.27 *The structures of brofaromine (left) and moclobemide (right).*

Clorgyline and tranylcypromine are selective irreversible MAO-A inhibitors that increase levels of noradrenaline and 5-HT in the brain and therefore exhibit anti-depressant activity. The consistent development of the cheese reaction forced the abandonment of further development of these inhibitors (Youdim & Bakhle, 2006).

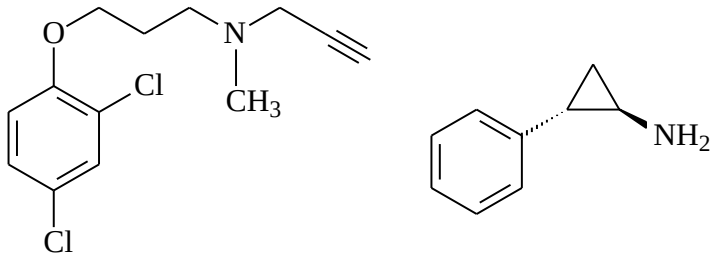

Figure 2.28 *The structures of clorgyline (left) and tranylcypromine (right).*

2.3 ENZYME KINETICS

2.3.1 Introduction

Enzymes function as biological catalysts in all living cells. They accelerate reactions by lowering the activation energy of the rate-determining step of a reaction. Enzymes frequently utilize other small molecules, such as metallic ions or small organic molecules, as co-enzymes. This helps the natural function of the enzyme.

Enzymes (E) have a catalytic site where the substrate (S) binds at the active site to form an enzyme-substrate complex (ES). The enzyme-substrate complex is transformed to a product (P) via subsequent steps and at the end of the reaction, the enzyme is released from the product and is free to catalyse a new reaction (Palmer & Bonner, 2007).

$$E + S \underset{k_{-1}}{\overset{k_1}{\rightleftharpoons}} ES \underset{k_{-2}}{\overset{k_2}{\rightleftharpoons}} E + P$$

Figure 2.29 *Enzyme-catalysed reaction*

Enzyme kinetics are used to describe enzyme-catalysed reactions both *in vivo* and *in vitro*. When an inhibitor is added to an enzyme-catalysed reaction, the rate of the reaction is decreased. Enzyme kinetics are used to measure the potency by which an inhibitor interacts with a specific enzyme

2.3.2 V_{max} and K_m determination

A first order reaction takes place when the concentration of the substrate is directly proportional to the rate of the reaction. During enzyme-catalysed reactions, the rate of the reaction increases as the substrate concentration is increased. The reaction then achieves a steady state where the rate of the reaction is no longer influenced by the amount of

substrate and the reaction rate is dependent on the concentration of the enzyme-substrate complex. Steady state kinetics analysis describes the steady state as the point where ES becomes constant and remains so for a period of time. The velocity of the enzyme is indicated by V. V_0 is the initial velocity at which the enzyme has consumed very little substrate so as to be negligible. If the concentration of substrate [S] increases, the initial velocity [V_0] will increase until the maximum velocity [V_{max}] is reached where all enzyme available is saturated. Further addition of substrate will not affect V_0 or V_{max}. The substrate concentration where the substrate produces half maximal velocity of the enzyme reaction ($V_{max}/2$), is termed K_m or the Michaelis constant. K_m can be determined by graphically plotting V_0 vs. [S] (fig 2.30) (Palmer & Bonner, 2007). All these parameters are described by the Michaelis-Menten equation:

$$V = \frac{V_{max} \times [S]}{K_m + [S]}$$

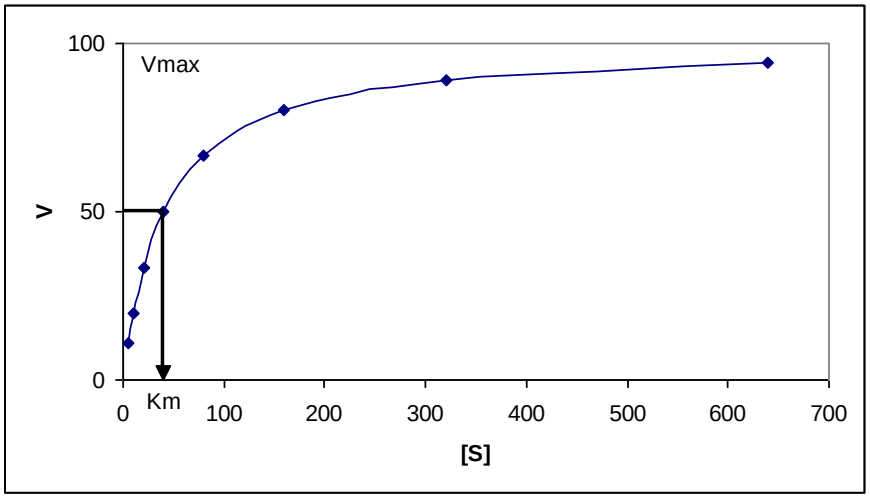

Figure 2.30 *Graphical representation of the Michaelis-Menten equation.*

The Michaelis-Menten graphical representation is not suitable to permit the accurate determination of V_{max} and K_m for certain enzymes. The inversion of the Michaelis-Menten equation gives the Lineweaver-Burk equation (fig 2.31). When the inverse of initial velocity [$1/V_0$] and the inverse of the substrate concentration [1/S] are graphically plotted, a straight line is obtained (fig 2.31). The K_m and V_{max} values are obtained from this plot as the y-axis intercept is equal to $1/V_{max}$ and the slope is K_m/V_{max}. The x-axis intercept is equal to $-1/K_m$ (Palmer & Bonner, 2007).

Lineweaver-Burk equation:

$$\frac{1}{V} = \left(\frac{K_m}{V_{max}}\right)\left(\frac{1}{[S]}\right) + \frac{1}{V_{max}}$$

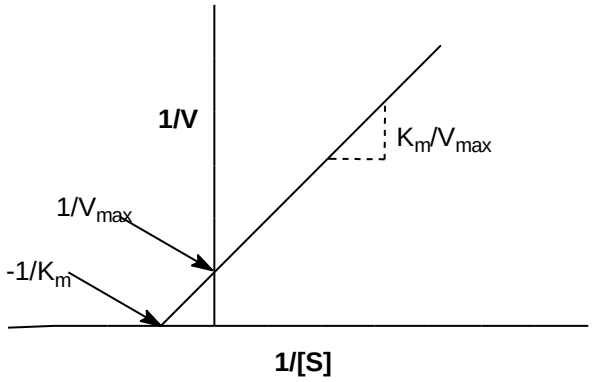

Figure 2.31 *Graphical representation of the Lineweaver-Burk equation.*

Enzyme inhibitors are molecules that are similar to an enzyme's normal substrate. When an inhibitor binds to the enzyme active site, the enzyme is incapable of performing its natural action. Inhibitors can be classified in the way that it binds to the enzyme. Irreversible inhibitors bind in a covalent way, thereby rendering the enzyme useless for any further reactions. Reversible inhibitors bind in a noncovalent way and can easily be displaced by the substrate, thus the enzyme function remains intact (fig 2.32). Reversible inhibitors can further be classified as non-competitive or competitive inhibitors. Competitive inhibitors are the most favourable kind when developing a drug as it competes for the binding site with the substrate (fig 2.33). A sufficient amount of substrate can thus eliminate the effect of the inhibitor.

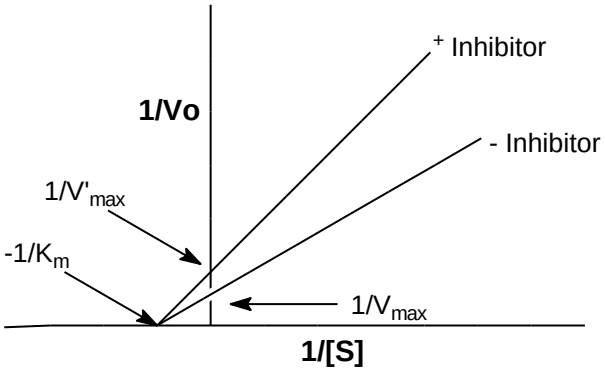

Figure 2.32 *Graphical representation of Lineweaver-Burk plots for non-competitive inhibition*

Non-competitive inhibition however, gives constant K_m values while the V_{max} tends to decrease (Palmer & Bonner, 2007).

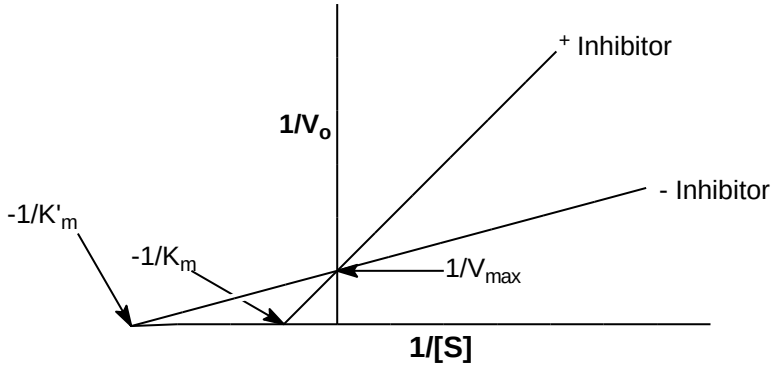

Figure 2.33 *Graphical representation of Lineweaver-Burk plots for competitive inhibition*

Competitive inhibition increases the slope of the straight line while the y-axis intercept stays the same. A competitive inhibitor raises the K_m values while V_{max} remains unchanged. The Michaelis-Menten equation describing competitive inhibition is shown in figure 2.34. The inverse of this equation describes the double reciprocal plot in the presence of a competitive inhibitor (fig 2.34).

Equation describing competitive inhibition:

$$V_i = \left(\frac{V_{max} \times \frac{[S]}{K_m}}{1 + \frac{[S]}{K_m} + \frac{[I]}{K_i}} \right)$$

Equation describing double reciprocal plot:

$$\frac{1}{V_i} = \frac{K_m}{V_{max}} \left(1 + \frac{[I]}{K_i}\right) \times \frac{1}{[S]} + \frac{1}{V_{max}}$$

The K_i (enzyme inhibitor dissociation constant) describes the degree of inhibition. The lower the K_i value the greater the inhibition is at a fixed concentration of inhibitor [I]. K_i may be determined from creating a secondary plot in which the slope of each reciprocal plot is graphed against the inhibitor concentration. The x-axis value is equal to $-K_i$ (fig 2.34). The K_i value can be calculated

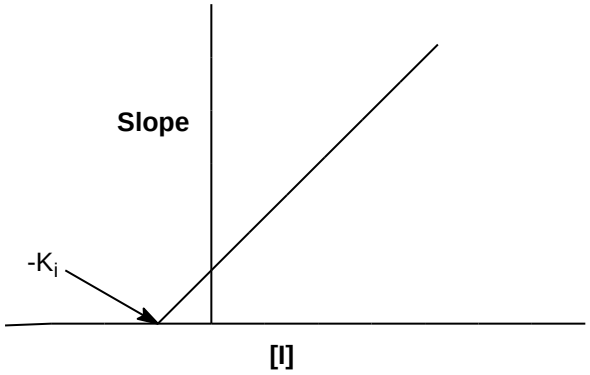

Figure 2.34 *Graph of the slopes from the double reciprocal plot versus inhibitor concentration.*

2.3.3 K_i and IC_{50} determination

The affinity of a competitive inhibitor for the active site of the enzyme is described by the K_i value, the enzyme-inhibitor dissociation constant. The lower the K_i value of an inhibitor the greater it's inhibition at a fixed concentration of the inhibitor [I] (Palmer & Bonner 2007).

IC_{50} is a term that describes the point at which a concentration of inhibitor produces 50% inhibition. This value will be used in this study to describe inhibitor potencies. The

relationship between K_i and IC_{50} of a competitive inhibitor of a monosubstrate reaction is described by the Cheng-Prusoff equation (Cheng & Prusoff, 1973).

Cheng-Prusoff equation:

$$K_i = \frac{IC_{50}}{\left(1 + \frac{[S]}{K_m}\right)}$$

CHAPTER 3

SYNTHESIS

3.1 INTRODUCTION

As mentioned in the introduction, the current study aimed to synthesize 8-aminocaffeine (**5a-h**) derivatives and 8-(methyl)aminocaffeine derivatives (**6a, 6b**) and evaluate them as inhibitors of MAO-B. Substitution of the caffeine ring at the C8 position has been shown to increase the inhibition potency of MAO-B compared to unsubstituted caffeine. This is examplified by the following observations. The substitution of caffeine at C8 with an (E)-(3-chlorostyryl) substituent yields CSC, an inhibitor with a K_i value of 70 nM for inhibition of MAO-B (Vlok *et al*., 2006). Substitution at the C8 position of caffeine with a benzyloxy side chain also yields potent inhibitors of both MAO-A and –B (Strydom *et al*., 2010). The aim of this study was thus to determine how the inhibition potencies of 8-aminocaffeine derivatives and 8-(methyl)aminocaffeine derivatives compare to the corresponding 8-benzyloxycaffeines. The 8-aminocaffeine derivatives that were prepared and evaluated as MAO-A and -B inhibitors are illustrated in table 3.1. Two 8-aminocaffeines were selected for methylation at the C8 amino group. The structures of these derivatives are given in table 3.2.

Table 3.1 *The aminocaffeine derivatives that were synthesized in this study*

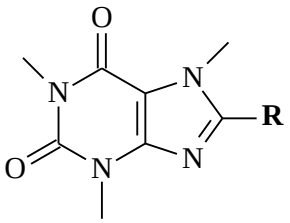

	R
5a	-NH-C_6H_5
5b	-NH-CH_2-C_6H_5
5c	-NH-$(CH_2)_2$-C_6H_5
5d	-NH-$(CH_2)_3$-C_6H_5
5e	-NH-$(CH_2)_4$-C_6H_5
5f	-NH-C_5H_6
5g	-NH-$(CH_2)_2$-(pyridin-2-yl)
5h	-NH-$(CH_2)_2$-(3-ClC_6H_4)

Table 3.2 *The methylaminocaffeine derivatives that were synthesized in this study*

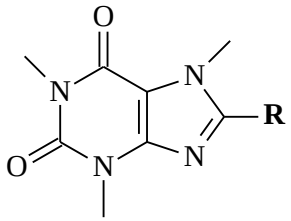

	R
6a	-(NCH_3)-(CH_2)$_2$-C_6H_5
6b	-(NCH_3)-(CH_2)$_4$-C_6H_5

3.2 GENERAL SYNTHETIC APPROACHES

3.2.1 Approach for the synthesis of the 8-aminocaffeine derivatives

A convenient synthetic route to 8-aminocaffeine derivatives has previously been reported (Cramer, 1894). This method involves the reaction between 8-chlorocaffeine (**7**) and aniline (**8**) to yield 8-(phenylamino)caffeine (**5a**) (fig 3.1). In the current study, this method was used to prepare the target 8-aminocaffeine derivatives **5a–h**, using the appropriate amine and 8-chlorocaffeine as reagents.

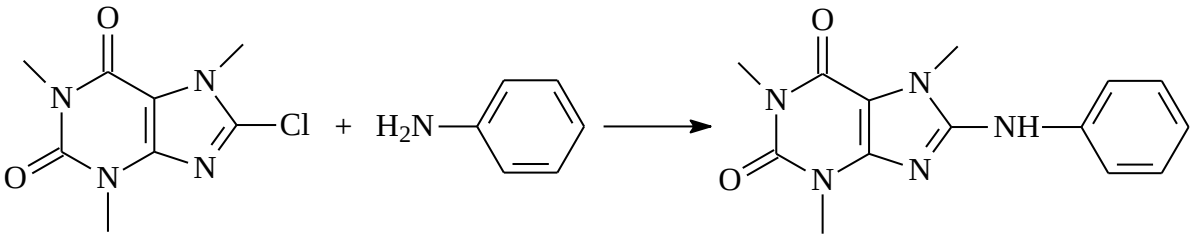

(7) **(8)** **(5a)**

Figure 3.1 *Reaction scheme for the formation of 8-(phenylamino)caffeine (**5a**) from 8-chlorocaffeine (**7**) and aniline (**8**).*

3.2.2 Approach for the synthesis of the 8-(methyl)aminocaffeine derivatives

The synthesis of 8-(methyl)aminocaffeine derivatives were carried out using iodomethane (**9**) as alkylating reagent (Avila-Zarraga & Martinez, 2001). In the current study the alkylation of 8-aminocaffeine derivatives **5c** and **5e** yielded 8-(methyl)aminocaffeine derivatives **6a** and **6b**, respectively. These reactions were carried out in dimethylsulfoxide (DMSO) as solvent and potassium hydroxide as base.

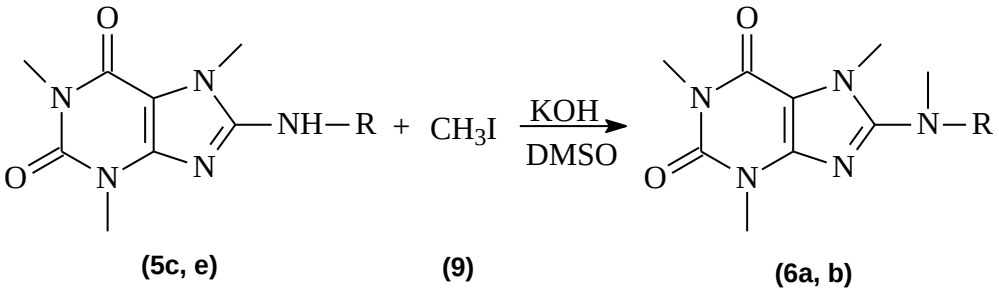

Figure 3.2 *Reaction scheme for the formation of the 8-(methyl)aminocaffeine (**6a** and **6b**) derivatives from the 8-aminocaffeines (**5c** and **5e**) and the alkylation agent iodomethane (**9**).*

3.2.3 Approach for the synthesis of 8-chlorocaffeine

Since 8-chlorocaffeine, the starting material required for the synthesis of the 8-aminocaffeine derivatives, is not commercially available, it was synthesized according to the protocol given by Fischer & Reese (1883). Caffeine (**10**) was reacted with chlorine gas (**11**). Chlorine gas was prepared by reacting hydrochloric acid and potassium permanganate. The resulting chlorine gas was passed through a solution of caffeine and chloroform to give 8-chlorocaffeine (**7**).

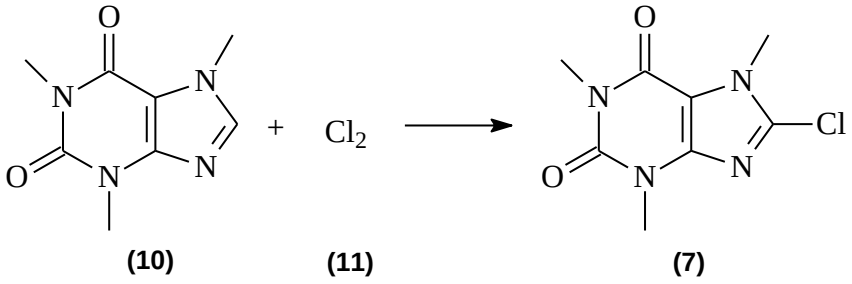

Figure 3.3 *Reaction scheme for the formation of 8-chlorocaffeine (**7**) from caffeine (**10**) and chlorine gas (**11**).*

3.3 MATERIALS AND INSTRUMENTATION

All chemical compounds were obtained from Sigma-Aldrich®.

Thin layer chromatography (TLC):

TLC was used to determine if the reactions were complete. TLC was carried out using silica gel 60 (Merck®) with UV_{254} fluorescent indicator. The mobile phase consisted of 30% petroleum ether and 70% ethyl acetate. All compounds were dissolved in ethyl acetate. A UV-lamp, at a wavelength of 254 nm, was used to observe the thin layer plates.

Melting points:

The melting points for all the compounds were recorded and compared to literature values where available. All melting points are uncorrected. For this purpose, a Stuart® SMP10 melting point apparatus was used.

Mass spectra (MS):

Direct insertion electron impact ionization (EIMS) and high resolution mass spectra (HRMS) were obtained on a DFS high resolution magnetic sector mass spectrometer (Thermo Electron® Corporation) in electron ionization (EI) mode.

Nuclear magnetic resonance (NMR):

Proton (^{1}H) and carbon (^{13}C) NMR spectra were recorded on a Bruker® Avance III 600 spectrometer at frequencies of 600 MHz and 150 MHz, respectively. All NMR measurements were conducted in DMSO-d_6 and the chemical shifts are reported in parts per million (δ) downfield from the signal of tetramethylsilane added to the deuterated solvent. Spin multiplicities are given as s (singlet), brs (broad singlet), d (doublet), dd (doublet of doublets), t (triplet), q (quartet), qn (quintet) or m (multiplet).

HPLC analysis:

The purity of the synthesized compounds were determined via HPLC analyses, which were conducted with an Agilent® 1100 HPLC system equipped with a quaternary pump and an Agilent® 1100 series diode array detector. HPLC grade acetonitrile (Merck®) and Milli-Q water (Millipore®) were used for the chromatography. A Venusil® XBP C18 column (4.60 × 150 mm, 5 µm) was used and the mobile phase consisted initially of 30% acetonitrile and 70% MilliQ water at a flow rate of 1 ml/min. At the start of each HPLC run a solvent gradient

program was initiated by linearly increasing the composition of the acetonitrile in the mobile phase to 85% acetonitrile over a period of 5 min. Each HPLC run lasted 15 min and a time period of 5 min was allowed for equilibration between runs. A volume of 20 µl of solutions of the test compounds in acetonitrile (1 mM) was injected into the HPLC system and the eluent was monitored at wavelengths of 210, 254 and 300 nm.

3.4 DETAILED SYNTHETIC PROCEDURES

3.4.1 Synthesis of the 8-aminocaffeine derivatives

A mixture of 8-chlorocaffeine (2 mmol) and the appropriate amine (10 mmol) was heated under reflux (175–180 ºC) for 3 hours. The reaction was cooled to room temperature and treated with 50 ml acetic acid (5%). The resulting suspension was stirred for 15 min at room temperature and the precipitate was collected by filtration. The product was dried at 60 ºC and recrystallised twice from ethanol (30 ml) at 0 ºC (Cramer, 1894).

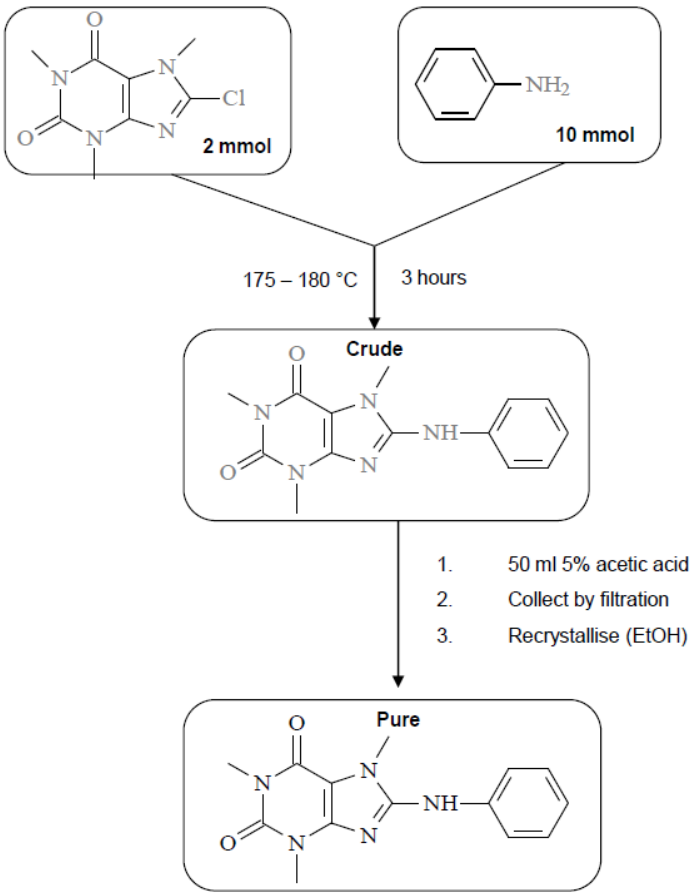

Figure 3.4 *Diagrammatic representation of the synthesis of 8-aminocaffeine derivatives*

3.4.2 Synthesis of 8-(methyl)aminocaffeine derivatives

Potassium hydroxide (0.05 g) was powderised and suspended in 5 ml DMSO. The resulting mixture was stirred for 30 min at room temperature and the appropriate aminocaffeine analogue (3 mmol) dissolved in DMSO (5 ml) was added. The reaction was heated to 40 ºC (in order for the aminocaffeine analogue to remain in solution) and iodomethane (0.8 mmol) was added. Stirring of the reaction was continued and another portion of iodomethane (0.8 mmol) was added every 20 min until silica gel TLC (petroleum ether/ ethyl acetate 30:70) indicated completion of the reaction. The pH of the reaction was also continually measured with pH paper, and when acidic, additional portions of potassium hydroxide (0.05 g) and iodomethane (0.8 mmol) were added. Upon completion, the reaction was cooled to room temperature and water (250 ml) was added. The resulting solution was incubated for several days at 4 ºC and the formed crystals were collected by filtration (Avila-Zárraga & Martinez, 2001).

3.4.3 Synthesis of 8-chlorocaffeine

8-Chlorocaffeine was prepared according to the method of Fischer & Reese (1883). An amount of 2.5 g dry caffeine was added to 20 ml chloroform and heated under reflux until all the caffeine had dissolved. Chlorine gas was firstly passed through sulphuric acid in order to dry the gas and subsequently passed through the caffeine solution. A precipitate formed, the HCl salt of caffeine, but as the reaction continued, the precipitate redissolved. When all of the precipitate had been redissolved, the chloroform was removed by distillation, using a rotary evaporator and white 8-chlorocaffeine crystals were obtained in high yield (95–100%). The chlorine gas was prepared by the reaction between HCl and potassium permanganate.

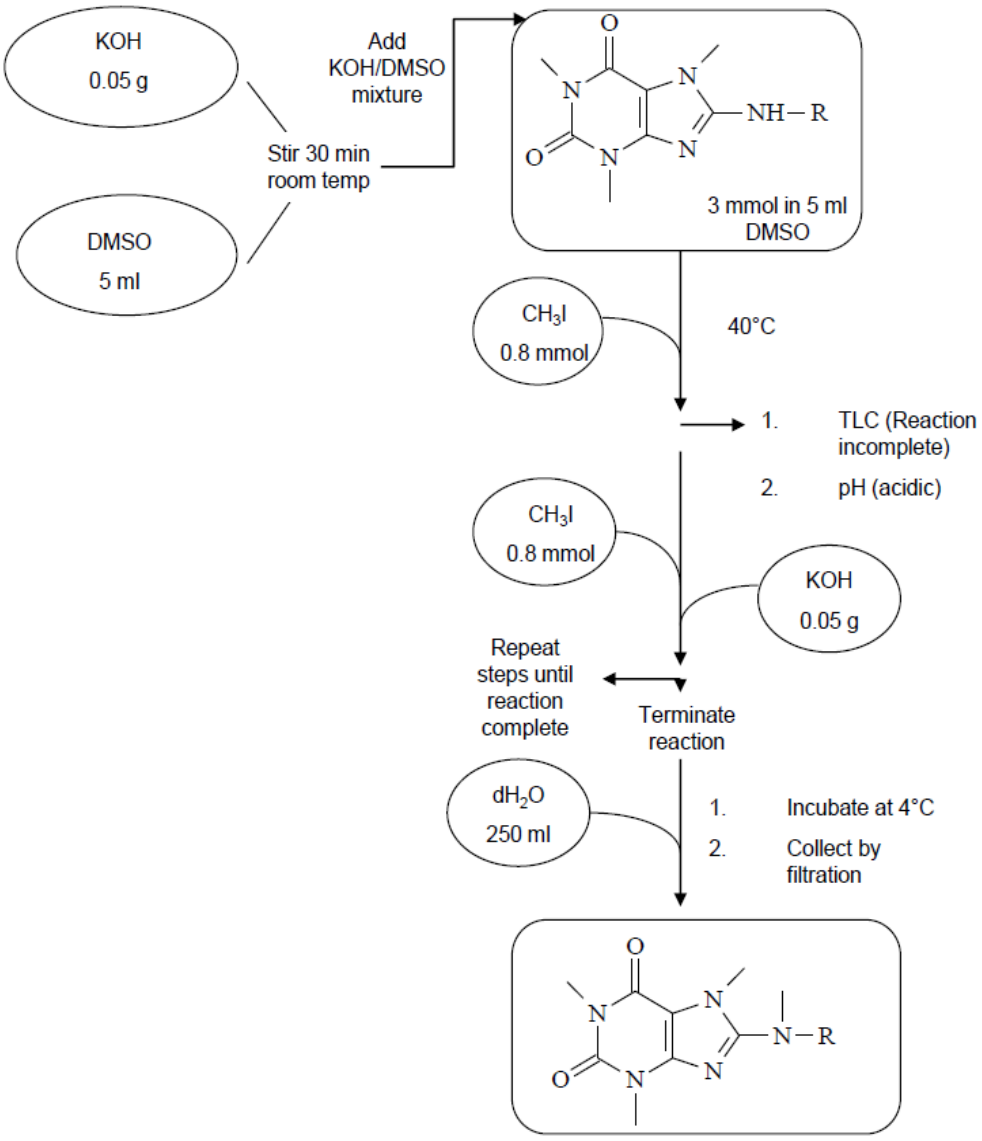

Figure 3.5 *Diagrammatic representation of the synthesis of 8-(methyl)aminocaffeine derivatives.*

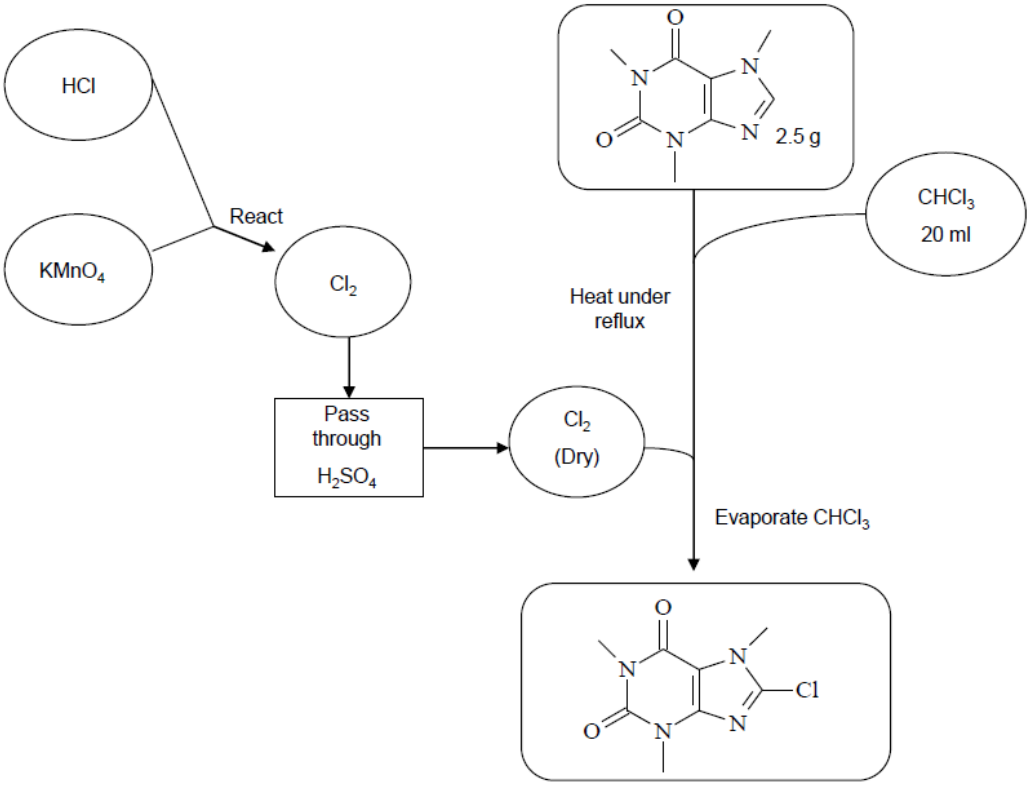

Figure 3.6 *Diagrammatic representation of the synthesis of 8-chlorocaffeine.*

3.5 PHYSICAL CHARACTERIZATION

3.5.1 Physical data for the C8-substituted aminocaffeine analogues (5a-h)

*8-(Phenylamino)caffeine (**5a**)*

The title compound was prepared from aniline and 8-chlorocaffeine in a yield of 24.2%: mp 164–265 °C (ethanol). ^{1}H NMR (Bruker Avance III 600, DMSO-d_6) δ 3.15 (s, 3H), 3.35 (s, 3H), 3.74 (s, 3H), 6.96 (t, 1H, J = 7.5 Hz), 7.29 (t, 2H, J = 7.5 Hz), 7.67 (d, 2H, J = 8.3 Hz), 9.07 (s, 1H); ^{13}C NMR (Bruker Avance III 600, DMSO-d_6) δ 27.3, 29.4, 30.5, 102.0, 118.1, 121.7, 128.7, 140.0, 147.2, 149.3, 150.9, 153.3; ESI-HRMS *m/z*: calcd for $C_{14}H_{15}N_5O_2$, 285.1226, found 285.1230; Purity (HPLC): 98%.

*8-(Benzylamino)caffeine (**5b**)*

The title compound was prepared from benzylamine and 8-chlorocaffeine in a yield of 74.0%: mp 230 °C (ethanol). ^{1}H NMR (Bruker Avance III 600, DMSO-d_6) δ 3.14 (s, 3H), 3.35 (s, 3H), 3.58 (s, 3H), 4.53 (d, 2H, J =5.6 Hz); 7.23 (t, 1H, J = 7.5 Hz), 7.32 (t, 2H, J = 7.5 Hz),

7.36 (m, 2H), 7.56 (t, 1H, J = 5.6 Hz); ^{13}C NMR (Bruker Avance III 600, DMSO-d_6) δ 27.1, 29.2, 29.8, 45.7, 102.0, 126.9, 127.4, 128.3, 139.6, 148.2, 150.9, 152.9, 154.0; ESI-HRMS *m*/*z*: calcd for $C_{15}H_{17}N_5O_2$, 300.1460, found 300.1459; Purity (HPLC): 99%.

*8-[(2-Phenylethyl)amino]caffeine (**5c**)*

The title compound was prepared from 2-phenylethylamine and 8-chlorocaffeine in a yield of 68.3%: mp 221 °C (ethanol). ^{1}H NMR (Bruker Avance III 600, DMSO-d_6) δ 2.88 (t, 2H, J = 7.5 Hz) 3.14 (s, 3H), 3.35 (s, 3H), 3.51 (s, 3H), 7.11 (t, 1H, J = 5.3 Hz), 7.19 (t, 1H, J = 7.2 Hz), 7.22 (d, 2H, J = 7.5 Hz), 7.29 (t, 2H, J = 7.5 Hz); ^{13}C NMR (Bruker Avance III 600, DMSO-d_6) δ 27.1, 29.2, 29.7, 35.3, 44.1, 101.8, 126.1, 128.3, 128.7, 139.4, 148.3, 150.9, 152.9, 153.9; ESI-HRMS *m*/*z*: calcd for $C_{16}H_{19}N_5O_2$, 314.1617, found 314.1621; Purity (HPLC): 99%.

*8-(3-Phenyl-1-propylamino)caffeine (**5d**)*

The title compound was prepared from 3-phenyl-1-propylamine and 8-chlorocaffeine in a yield of 76.8%: mp 204 – 205 °C (ethanol). ^{1}H NMR (Bruker Avance III 600, DMSO-d_6) δ 1.88 (q, 2H, J = 7.5 Hz), 2.64 (t, 2H, J = 7.5 Hz), 3.13 (s, 3H), 3.30 (s, 3H), 3.31 (m, 2H), 3.52 (s, 3H), 6.98 (t, 1H, J = 5.3 Hz), 7.16 (t, 1H, J = 7.2 Hz), 7.22 (d, 2H, J = 7.5), 7.26 (t, 2H, J = 7.5 Hz); ^{13}C NMR (Bruker Avance III 600, DMSO-d_6) δ 27.1, 29.2, 29.7, 30.8, 32.3, 42.0, 101.8, 125.7, 128.2, 141.7, 148.3, 150.9, 152.8, 154.1; ESI-HRMS *m*/*z*: calcd for $C_{17}H_{21}N_5O_2$ 328.1773, found 328.1774; Purity (HPLC): 99%.

*8-[4-(Phenylbutylamino)]caffeine (**5e**)*

The title compound was prepared from 4-phenylbutylamine and 8-chlorocaffeine in a yield of 63.0%: mp 179 – 180 °C (ethanol). ^{1}H NMR (Bruker Avance III 600, DMSO-d_6) δ 1.59 (m, 4H,), 2.60 (t, 2H, J = 7.2 Hz), 3.13 (s, 3H), 3.30 (s, 3H), 3.32 (m, 2H), 3.51 (s, 3H), 6.94 (t, 1H, J = 5.6 Hz), 7.14 (t, 1H, J = 7.2 Hz), 7.18 (d, 2H, J = 7.2 Hz), 7.25 (t, 2H, J = 7.2 Hz); ^{13}C NMR (Bruker Avance III 600, DMSO-d_6) δ 27.1, 28.2, 28.8, 29.2, 29.7, 34.8, 42.2, 101.7, 125.6, 128.3, 142.1, 148.3, 150.9, 152.8, 154.1; ESI-HRMS *m*/*z*: calcd for $C_{18}H_{23}N_5O_2$ 342.1930, found 342.1929; Purity (HPLC): 99%.

*8-(Cyclopentyl)aminocaffeine (**5f**)*

The title compound was prepared from cyclopentylamine and 8-chlorocaffeine in a yield of 38.6%: mp 217 – 218 °C (ethanol). ^{1}H NMR (Bruker Avance III 600, DMSO-d_6) δ 1.52 (s, 4H), 1.68 (s, 2H), 1.93 (m, 2H), 3.13 (s, 3H), 3.31 (s, 3H), 3.53 (s, 3H), 4.10 (m, 1H), 6.76 (d,

1H, J = 7.2 Hz); ^{13}C NMR (Bruker Avance III 600, DMSO-d_6) δ 23.4, 27.1, 29.2, 29.8, 32.4, 54.2, 101.7, 148.3, 150.9, 152.8, 153.8; ESI-HRMS *m*/*z*: calcd for $C_{13}H_{20}N_5O_2$, 278.1617, found 278.1612; Purity (HPLC): 98%.

*8-[2-(2-Pyridyl)-ethylamino]caffeine (**5g**)*

The title compound was prepared from 2-(2-pyridyl)-ethylamine and 8-chlorocaffeine in a yield of 20.4%: mp 196 - 197°C (ethanol). ^{1}H NMR (Bruker Avance III 600, DMSO-d_6) δ 3.03 (t, 2H, J = 7.2 Hz), 3.13 (s, 3H), 3.31 (s, 3H), 3.50 (s, 3H), 3.65 (q, 2H, J = 6.7 Hz), 7.10 (t, 1H, J = 5.6 Hz), 7.20 (t, 1H, J = 5.6 Hz), 7.26 (d, 1H, J = 7.5 Hz), 7.69 (t, 1H, J = 7.5 Hz), 8.49 (d, 1H, J = 4.1 Hz); ^{13}C NMR (Bruker Avance III 600, DMSO-d_6) δ 27.1, 29.2, 29.7, 37.5, 42.4, 101.8, 121.5, 123.2, 136.4, 148.3, 149.0, 150.9, 152.8, 153.9, 159.1; ESI-HRMS *m*/*z*: calcd for $C_{15}H_{19}N_6O_2$, 315.1569, found 315.1570; Purity (HPLC): 98%.

*8-[2-(3-Chlorophenyl)-ethylamino]caffeine (**5h**)*

The title compound was prepared from 2-(3-chlorophenyl)-ethylamine and 8-chlorocaffeine in a yield of 48.5%: mp 210° C (ethanol). ^{1}H NMR (Bruker Avance III 600, DMSO-d_6) δ 2.88 (t, 2H, J = 7.2 Hz), 3.13 (s, 3H), 3.32 (s, 3H), 3.50 (s, 4H), 7.10 (t, 1H, J = 5.27, 5.65 Hz), 7.18 (d, 1H, J = 7.53 Hz), 7.23 (d, 1H, J = 7.15 Hz), 7.23 (t, 2H, J = 7.53, 8.28 Hz); ^{13}C NMR (Bruker Avance III 600, DMSO-d_6) δ 27.1, 29.2, 29.7, 34.8, 43.7, 101.8, 126.1, 127.5, 128.6, 130.1, 132.9, 142.0, 148.3, 150.9, 152.8, 153.8; ESI-HRMS *m*/*z*: calcd for $C_{16}H_{19}N_5O_2Cl$, 348.1227, found 348.1225; Purity (HPLC): 96%.

3.5.2 Physical data of the methylated C8-substituted aminocaffeine analogues (6a, 6b)

*8-[Methyl(2-phenylethyl)amino]caffeine (**6a**)*

The title compound was prepared from 8-[(2-phenylethyl)amino]caffeine (**5c**) and iodomethane in a yield of 57.7%: mp 103 °C (ethanol). ^{1}H NMR (Bruker Avance III 600, DMSO-d_6) δ 2.88 (t, 2H, J = 7.5 Hz), 2.98 (s, 3H), 3.16 (s, 3H), 3.33 (s, 3H), 3.47 (t, 2H, J = 7.5 Hz), 3.59 (s, 3H), 7.18 (m, 1H), 7.25 (m, 4H); ^{13}C NMR (Bruker Avance III 600, DMSO-d_6) δ 27.3, 29.3, 32.5, 33.0, 38.6, 54.5, 103.8, 126.1, 128.3, 128.8, 139.0, 147.1, 150.9, 153.5, 156.6; ESI-HRMS *m*/*z*: calcd for $C_{17}H_{22}N_5O_2$, 328.1773, found 328.1734; Purity (HPLC): 99%.

*8-[Methyl(4-phenylbutyl)amino]caffeine (**6b**)*

The title compound was prepared from 8-[(4-phenylbutyl)amino]caffeine (**5e**) and iodomethane in a yield of 49.95%: mp 114 °C (ethanol). ^{1}H NMR (Bruker Avance III 600, DMSO-d_6) δ 1.57 (m, 4H), 2.57 (t, 2H, J = 7.15 Hz), 2.90 (s, 3H), 3.16 (s, 3H), 3.26 (t, 2H, J = 7.15 Hz), 3.32 (s, 3H), 3.65 (s, 3H), 7.15 (m, 3H), 7.24 (t, 2H, J = 7.91 Hz); ^{13}C NMR (Bruker Avance III 600, DMSO-d_6) δ 26.3, 27.3, 27.9, 29.3, 32.6, 34.7, 38.4, 52.5, 103.8, 125.7, 128.2, 128.2, 142.0, 147.1, 150.9, 153.5, 156.9; ESI-HRMS *m*/*z*: calcd for $C_{19}H_{26}N_5O_2$, 356.2087, found 356.2088; Purity (HPLC): 98%.

3.5.3 Interpretation of the NMR spectra

In Table 3.3 the structures of the aminocaffeine and methylaminocaffeine derivatives are given and correlated with the ^{1}H NMR data. As shown in the table, all of the appropriate signals were observed for each compound **5a**–**h** and **6a**–**b**. These include the 3 singlets for the caffeine methyl groups, the signal of the NH attached to C8 of the caffeine, the signals of the aliphatic protons present in the C-8 side chain and the signals for the aromatic protons present on the ring systems of the C-8 side chains. The singlet of the NCH_3 groups of compounds **6a**–**b** is also observed. The appropriate integration values and chemical shifts were also observed for all signals. In addition, the ^{13}C NMR data (not tabulated) also corresponded to each of the target structures in terms of the number of ^{13}C signals and their expected chemical shifts.

Table 3.3 *Correlation of the ^{1}H NMR data with the structures of the 8-aminocaffeine and 8-(methyl)aminocaffeine derivatives.*

	Structure	**^{1}H NMR signal assignment**
5a	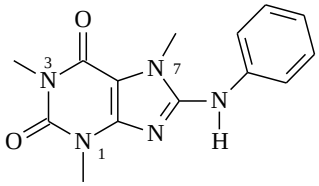	**a**. Methyl groups at N-1, N-3 and N-7 – singlets at 3.15 (3H), 3.35 (3H) and 3.74 (3H) ppm. **b**. NH – singlet at 9.07 (1H) ppm **c**. Aromatic protons – signals at 6.96 (1H), 7.29 (2H), 7.67 (2H) ppm.

	Structure	^{1}H NMR signal assignment
5b	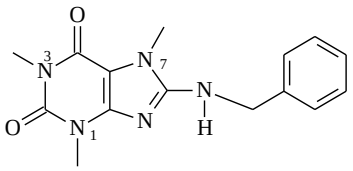	**a.** Methyl groups at N-1, N-3 and N-7 – singlets at 3.14 (3H), 3.35 (3H) and 3.58 (3H) ppm. **b.** CH_2 – doublet at 4.53 (2H) ppm. **c.** Aromatic protons – signals at 7.23 (1H), 7.32 (2H), 7.36 (2H), 7.56 (1H) ppm.
5c	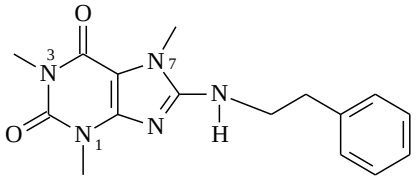	**a.** Methyl groups at N-1, N-3 and N-7 – singlets at 3.14 (3H), 3.35 (3H) and 3.51 (3H) ppm. **b.** C_2H_4 – triplet at 2.87 (2H) ppm. **c.** Aromatic protons – signals at 7.1 (1H), 7.19 (1H), 7.23 (2H), 7.29 (2H) ppm.
5d	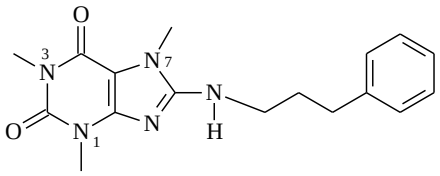	**a.** Methyl groups at N-1, N-3 and N-7 – singlets at 3.13 (3H), 3.3 (3H), 3.52 (3H) ppm. **b.** C_3H_6 – quartet at 1.88 (2H) and triplet at 2.64 (2H) ppm. **c.** Aromatic protons – signals at 6.98 (1H), 7.16 (1H), 7.2 (2H), 7.26 (2H) ppm.

	Structure	^{1}H NMR signal assignment
5e	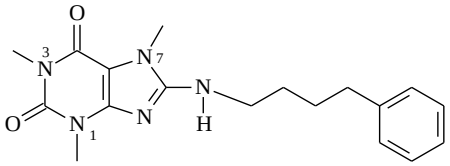	**a.** Methyl groups at N-1, N-3 and N-7 – singlets at 3.13 (3H), 3.3 (3H), 3.51 (3H) ppm. **b.** C_4H_8 – multiplet at 1.59 (4H), triplet at 2.6 (2H) and doublet at 5.18 (2H) ppm. **c.** Aromatic protons – signals at 6.94 (1H), 7.14 (1H), 7.25 (2H) ppm.
5f	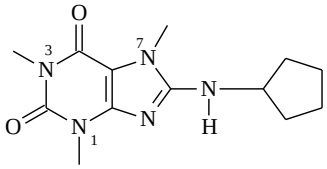	**a.** Methyl groups at N-1, N-3 and N-7 – singlets at 3.13 (3H), 3.31 (3H), 3.56 (3H) ppm. **b.** Cyclopentyl – singlets at 1.52 (4H), 1.68 (2H), multiplets at 1.93 (2H), 4.1 (1H), doublet at 6.76 (1H).
5g	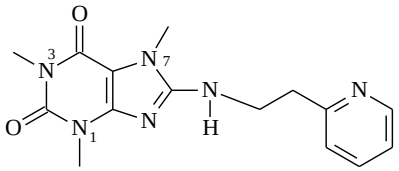	**a.** Methyl groups at N-1, N-3 and N-7 – singlets at 3.13 (3H), 3.31 (3H), 3.5 (3H) ppm. **b.** C_2H_4 – triplet at 3.03 (2H) and quartet at 3.65 (2H) ppm. Pyridyl – doublet at 8.49 (1H) ppm. **c.** Aromatic protons – signals at 7.1 (1H), 7.2 (1H), 7.26 (1H), 7.69 (1H) ppm.

	Structure	^{1}H NMR signal assignment
5h	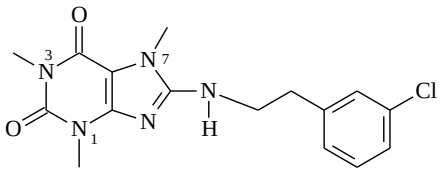	**a.** Methyl groups at N-1, N-3 and N-7 – singlets at 3.13 (3H), 3.32 (3H), 3.5 (3H) ppm. **b.** C_2H_4 – triplet at 2.88 (2H) ppm. **c.** Aromatic protons – signals at 7.1 (1H), 7.18 (1H), 7.23 (1H), 7.23 (2H) ppm.
6a	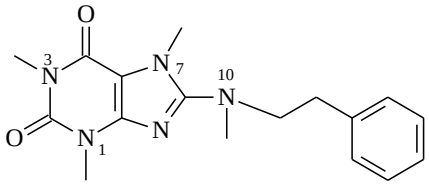	**a.** Methyl groups at N-1, N-3, N-7 and N-10 – singlets at 3.16 (3H), 3.33 (3H), 3.59 (3H) and 2.98 (3H) ppm. **b.** C_2H_4 – triplet at 2.88 (2H) ppm and 3.47 (2H) ppm **c.** Aromatic protons – signals at 7.18 (1H), 7.25 (4H) ppm.
6b	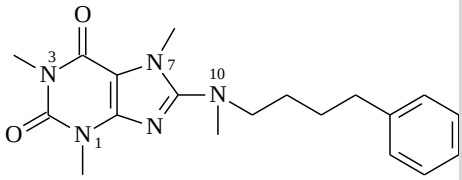	**a.** Methyl groups at N-1, N-3, N-7 and N-10 – singlets at 3.16 (3H), 3.32 (3H), 3.65 (3H) and 2.9 (3H) ppm. **b.** C_4H_8 - multiplet at 1.57 (4H), triplets at 2.57 (2H), 3.26 (2H). **c.** Aromatic protons – signals at 7.15 (3H), 7.24 (2H) ppm.

3.5.4 Interpretation of the mass spectra

As shown in table 3.4, the high resolution masses that were obtained for each of the 8-aminocaffeine and 8-(methyl)aminocaffeine derivatives very closely corresponded to the calculated values. This is further confirmation of the structures of these compounds.

Table 3.4 *Correlation of the calculated exact masses with the experimentally obtained masses of the 8-aminocaffeine and 8-(methyl)aminocaffeine derivatives.*

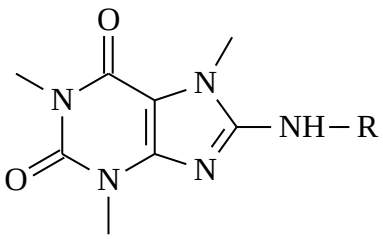

(5)

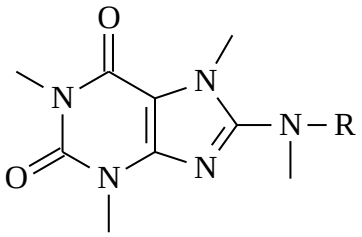

(6)

			Mass Spectrometry		
	-R	**Formula**	**Calcd.**	**Found**	**ppm**
		M + 1			
5a	$-C_6H_5$	$C_{14}H_{15}N_5O_2$	285.1226	285.1230	-1.4
5b	$-CH_2-C_6H_5$	$C_{15}H_{18}N_5O_2$	300.1460	300.1459	-0.3
5c	$-(CH_2)_2-C_6H_5$	$C_{16}H_{20}N_5O_2$	314.1617	314.1621	1.3
5d	$-(CH_2)_3-C_6H_5$	$C_{17}H_{22}N_5O_2$	328.1773	328.1774	0.3
5e	$-(CH_2)_4-C_6H_5$	$C_{18}H_{24}N_5O_2$	342.1930	342.1929	-0.3
5f	$-C_5H_9$	$C_{13}H_{20}N_5O_2$	278.1617	278.1612	-1.8
5g	$-(CH_2)_2$-(pyridin-2-yl)	$C_{15}H_{19}N_6O_2$	315.1569	315.1570	0.3
5h	$-(CH_2)_2$-(3-ClC_6H_4)	$C_{16}H_{19}N_5O_2Cl$	348.1227	348.1225	-0.6
6a	$-(CH_2)_2-C_6H_5$	$C_{17}H_{22}N_5O_2$	328.1773	328.1734	-11.9
6b	$-(CH_2)_4-C_6H_5$	$C_{19}H_{26}N_5O_2$	356.2087	356.2088	0.3

Ppm = (found – calcd.)/calcd. x 1 000 000. In general a ppm difference smaller than 5 is considered to be in good agreement.

3.6 CONCLUSION

This chapter described the successful synthesis of the target 8-aminocaffeine and 8-(methyl)aminocaffeine derivatives. All the structures were confirmed by NMR and MS and the purities by HPLC analysis. Both the ^{1}H NMR and ^{13}C NMR spectra corresponded with the proposed structures and the expected exact masses were also recorded for each compound. In addition, HPLC analysis revealed a single peak for each compound analysed.

CHAPTER 4

ENZYMOLOGY

4.1 MEASUREMENT OF MAO CATALYTIC ACTIVITY *IN VITRO*

Various methods exist for the *in vitro* measurement of catalytic activity of MAO. These measurements are based on the disappearance or formation of reagents and products, respectively. Measurements of MAO catalytic activity may be continuous or discontinuous and include spectrophotometric, radiometric, polarographic, luminometric or ammonia detection techniques.

- **Spectrophotometric:** This method is applied widely. It usually measures the amount of light absorbed at a specific wavelength by the product formed. A frequently used procedure of this technique/method is the spectrophotometric measurement of benzaldehyde at a wavelength of 250 nm after its MAO-B catalyzed formation from the substrate, benzylamine (Holt *et al*., 1997; Nicotra & Parvez, 1999).

- **Radiometric:** This is a discontinuous method that relies on the formation of a radiolabelled aldehyde product during incubation of MAO with the corresponding labelled amine. For example, the rate of oxidation of ^{3}H-tyramine by MAO may be measured after selectively extracting the labelled deaminated metabolite into an organic solvent (Holt *et al*., 1997; Tipton & Singer, 1993).

- **Ammonia detection:** The measurement of ammonia production from the oxidative deamination of primary amines by MAO can also be used to measure the enzyme catalytic rate. The disadvantage of this method is that the oxidation rate of only primary amine substrates can be measured, since secondary and tertiary amines do not yield ammonia upon oxidation by the MAO enzymes. (Holt *et al*., 1997).

- **Polarographic:** The consumption of oxygen is measured as an indication of the extent of oxidation. This assay is accurate but not suitable for a large amount of samples (Holt *et al*., 1997; Krueger & Singer, 1993).

- **Luminometric:** This assay measures the amount of hydrogen peroxide produced in the MAO catalytic cycle. When luminal reacts with hydrogen peroxide, light is

produced, which may be measured luminometrically. The amount of light produced is proportional to the amount of hydrogen peroxide formed by MAO. This assay is sensitive and has the advantage that it may be used for substrates, which do not yield readily measurable products (O' Brien *et al*., 1978).

- **Fluorometric:** When the MAO enzymes oxidize a substrate to yield a product that is fluorescent, fluorescence spectrophotometry may be used to measure the enzyme catalytic rate. An example is the oxidation of kynuramine, a non-fluorescent substrate, to the fluorescent metabolite 4-hydroxyquinoline. This method will be discussed in more detail below, since it was employed in this study to measure MAO activities.

4.1.1 MAO activity measurements using kynuramine

As mentioned in the description of the fluorometric assay, certain products formed by MAO-B oxidation may have fluorescent properties. In this study the MAO-A/B mixed substrate, kynuramine was used to measure the catalytic rates of these enzymes. Kynuramine is oxidized to 4-hydroxyquinoline, a fluorescent metabolite (Figure 4.1). The amount of the hydroxyquinoline produced may be measured with a fluorescence spectrophotometer at an excitation wavelength of 310 nm and an emission wavelength of 400 nm (Nicotra & Parvez, 1999). In this study the inhibitor potencies will be expressed as IC_{50} values. This is the concentration at which 50% of the enzyme is inhibited. Fluorometric assays are generally more sensitive than spectrophotometric assays (Matsumoto *et al*., 1985; Zhou *et al*., 1996).

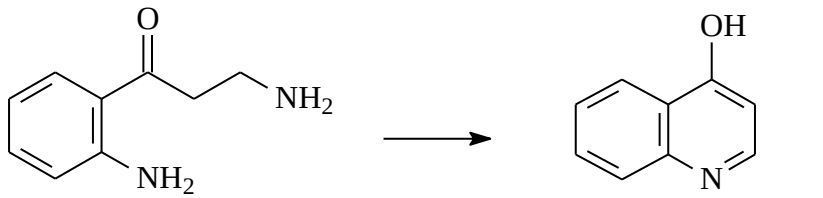

Kynuramine **4-Hydroxyquinoline**

Figure 4.1 *The oxidation of kynuramine to 4-hydroxyquinoline by MAO.*

4.1.2 Method

Recombinant human MAO-A and -B (5 mg/ml) were obtained from Sigma-Aldrich®, pre-aliquoted and stored at -80 ºC. For MAO-A activity measurements, the enzyme was diluted to 0.075 mg/ml while MAO-B was diluted to 0.15 mg/ml. Both these stock solutions of the enzymes were prepared in potassium phosphate buffer (100 mM, pH 7.4).

The reactions were prepared in potassium phosphate buffer (100 mM, pH 7.4) to which was added various concentrations of the test inhibitor, kynuramine (substrate) and the MAO enzyme. The concentrations of the inhibitor were 0, 0.003, 0.01, 0.1, 1, 10, and 100 µM. The kynuramine was added to the incubations to yield final concentrations of 30 µM for MAO-B and 45 µM for MAO-A. Stock solutions of the inhibitors were prepared to contain 4% (v/v) DMSO in the final incubation volume of 500 µl. The final enzyme concentration in each incubation was 0.0075 mg/ml for MAO-A and 0.015 mg/ml for MAO-B.

The reactions were subsequently incubated at 37 ºC for 20 minutes and subsequently terminated by the addition of 400 µl NaOH (2 N). Distilled water (1000 µl) was added to each incubation to yield a final volume of 1900 µl after which the reactions were centrifuged for 10 minutes at 16 000 g. The fluorescence intensities of the supernatant fractions were measured at an excitation wavelength of 310 nm and an emission wavelength of 400 nm to determine the concentration of 4-hydroxyquinoline. A Varian® Cary Eclipse fluorescence spectrophotometer was used for this purpose. The PMT voltage was set to low for MAO-A with an excitation slit width of 10 nm and an emission slit width of 20 nm while the PMT voltage was set to medium for MAO-B with an excitation slit width of 5 nm and an emission slit width of 10 nm.

To quantify the amounts of 4-hydroxyquinoline formed in the reactions, a calibration curve was prepared by measuring the fluorescence of increasing concentrations of 4-hydroxyquilonline (0.0469, 0.09375, 0.1875, 0.375, 0.75, 1.5 µM). Each of these calibration standards contained 4% (v/v) DMSO and potassium phosphate buffer to a final volume of 500 µl. To each calibration standard were added 400 µl of NaOH and 1000 µl of distilled water. An example of the calibration curves routinely obtained is given below.

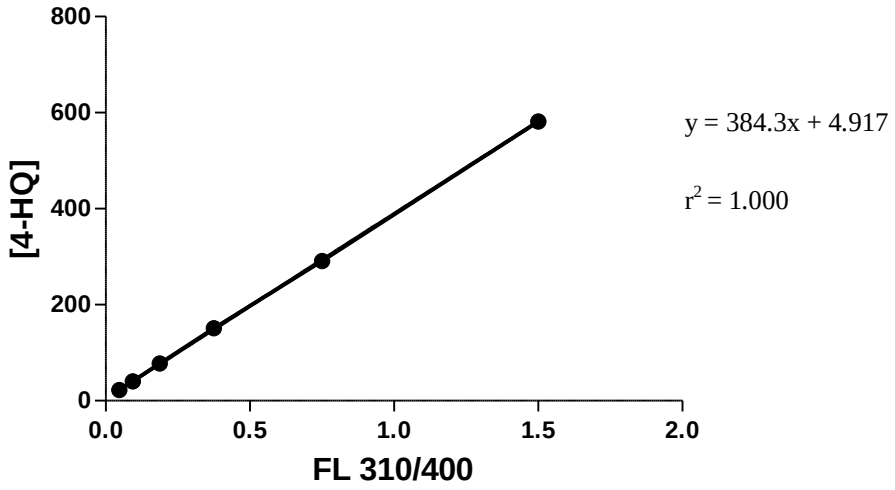

Figure 4.2 *An example of the calibration curves routinely obtained in this study.*

A sigmoidal dose-response curve was constructed to determine IC_{50} values. For this purpose the initial rate of oxidation versus the logarithm of the inhibitor concentration was plotted. The data obtained were fitted to a one-site competition model using the Prism® 5 software package (GraphPad®). The IC_{50} values were determined in triplicate and are expressed as mean ± standard deviation (SD).

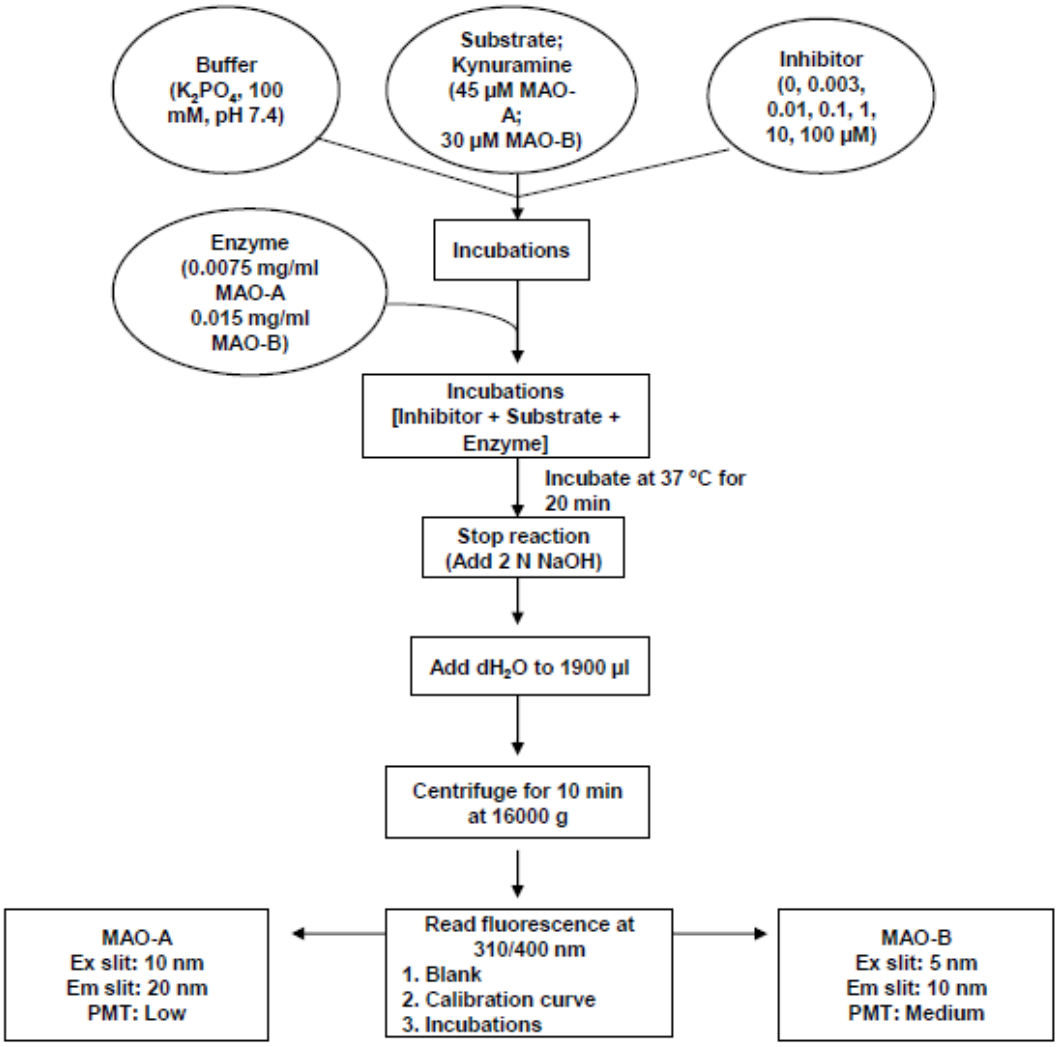

Figure 4.2 *Summary of the procedure used for the determination of IC_{50} values.*

4.1.3 Results

The IC_{50} values for the test compounds were determined by plotting the rate of the MAO catalyzed oxidation of kynuramine versus the logarithm of the concentrations of the inhibitor. The concentration of the inhibitor that reduces the rate to half of the maximal value is the IC_{50}. As an example, the sigmoidal curve for the determination of the IC_{50} value of 8-(3-bromobenzyloxy)caffeine (Strydom *et al*., 2010) towards human MAO-B is given in figure 4.3. Figure 4.4 gives a similar sigmoidal curve for the determination of the IC_{50} value towards MAO-B of 8-[methyl(4-phenylbutyl)amino]caffeine (**6b**) in this study.

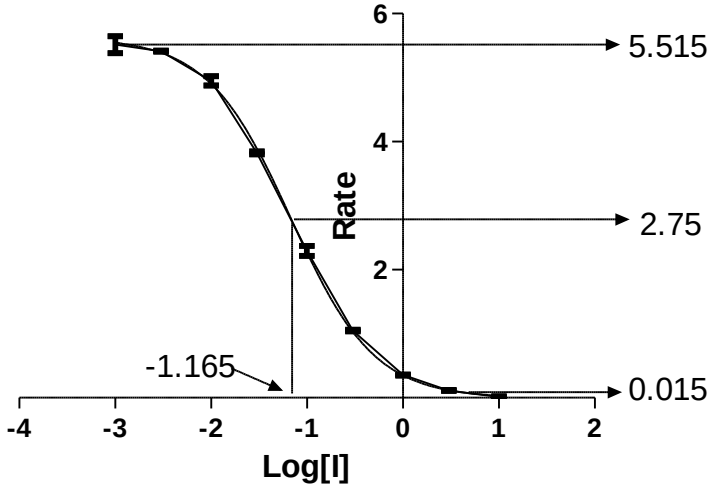

Figure 4.3 *The sigmoidal dose-response curve of the initial rates of kynuramine oxidation by recombinant human MAO-B vs. the logarithm of the concentration of the inhibitor, 8-(3-bromobenzyloxy)caffeine, expressed in nM. The logIC_{50} equals -1.165 µM which corresponds to an IC_{50} value of 0.068 µM.*

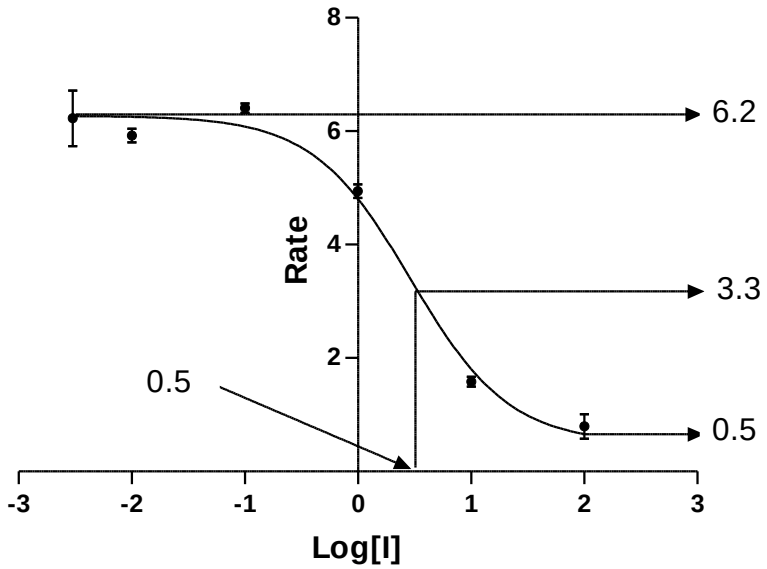

Figure 4.4 *The sigmoidal dose-response curve of the initial rates of kynuramine oxidation by recombinant human MAO-B vs. the logarithm of the concentration of the inhibitor, 8-[methyl(4-phenylbutyl)amino]caffeine (**6b**) expressed in µM. The logIC_{50} equals 0.5 µM which corresponds to an IC_{50} value of 2.97 µM.*

The IC_{50} values determined for the inhibition of recombinant human MAO-A and –B by the aminocaffeine derivatives are presented in table 4.1. The IC_{50} values given are expressed in

µM. A lower IC_{50} value indicates a stronger binding affinity of the inhibitor to the enzyme. Also listed is the selectivity index of each inhibitor. The selectivity index (SI) represents the selectivity for the MAO-B isoform and is the ratio of the IC_{50} value for the inhibition of MAO-A versus the IC_{50} value for the inhibition of MAO-B. The higher the SI, the more selective the inhibitor is toward the MAO-B isoform.

Table 4.1 *The IC_{50} values for the inhibition of recombinant human MAO-A and –B by compounds **5a-h** and **6a,b**.*

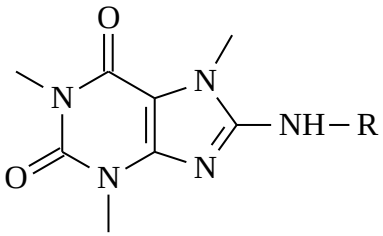

(5)

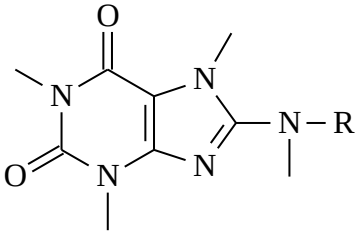

(6)

		IC_{50} (µM)		
	R	MAO-A[a]	MAO-B[a]	SI[b]
5a	$-C_6H_5$	–[c]	–[c]	–
5b	$-CH_2-C_6H_5$	–[c]	–[c]	–
5c	$-(CH_2)_2-C_6H_5$	46.78 ± 13.87	15.84 ± 2.89	2.95
5d	$-(CH_2)_3-C_6H_5$	–[c]	17.00 ± 4.60	–
5e	$-(CH_2)_4-C_6H_5$	25.51 ± 10.28	7.56 ± 0.54	3.37
5f	$-C_5H_9$	–[c]	–[c]	–
5g	$-(CH_2)_2$-(pyridin-2-yl)	–[c]	21.61 ± 13.88	–
5h	$-(CH_2)_2-(3\text{-}ClC_6H_4)$	***5.78 ± 0.41***	4.91 ± 3.45	0.7
6a	$-(CH_2)_2-C_6H_5$	101.47 ± 9.30	16.84 ± 6.83	3.7
6b	$-(CH_2)_4-C_6H_5$	37.7 ± 6.4	***2.97 ± 0.54***	***7.8***

[a] *All values are expressed as the mean ± SD of triplicate determinations.*

[b] *The selectivity index is the selectivity for the MAO-B isoform and is given as the ratio of IC_{50}(MAO-A)/IC_{50}(MAO-B).*

[c] *No inhibition observed at a maximal tested concentration of 100 µM.*

The following general observations may be made from the results presented in table 4.1:

- Compound **5h** was found to be the most potent MAO-A inhibitor with an IC_{50} value of 5.78 µM. This compound has a low degree of isoform selectivity with an SI value of 0.7.

- Compound **6b** was found to be the most potent MAO-B inhibitor with an IC_{50} value of 2.97 µM. Of all compounds that interacted with both MAO isoforms, **6b** is most selective for MAO-B with an SI value of 7.8.

- Methylation of the amine of compound **5e**, yields compound **6b**, which exhibits enhanced inhibition towards MAO-B and also a higher degree of selectivity for the MAO-B isoform. As shown in table 4.2, compound **6b** was found to be 2.54 fold more potent as a MAO-B inhibitor than **5e**. Compound **6b** (IC_{50} = 37.7 µM) was found to be slightly weaker as a MAO-A inhibitor than **5e** (IC_{50} = 25.5 µM).

Table 4.2 *A comparison of the IC_{50} values of compounds **5e** and **6b** for the inhibition of MAO-B*

Compound	IC_{50} value (µM)	Ratio 5e/5b[a]	SI
5e	7.56	-	3.7
6b	2.97	2.54	7.8

[a]The ratio of IC_{50}(**5e**)/IC_{50}(**6b**)

- Increasing the chain length of the C8 substituent seems to enhance the MAO-B inhibition potency. For example, while the compounds containing relatively short C8 side chains (**5e** and **5b**) are not MAO-B inhibitors, increasing the chain length, as exemplified by compounds **5c**, **5d**, and **5e**, yields structures that possess MAO-B inhibition properties. As shown in table 4.1, the structure with the longest C8 side chain, compound **5e**, is also the most potent MAO-B inhibitor among the homologues in this table.

- Chlorine substitution on the phenyl ring of the C8 substituent enhances both the MAO-A and -B inhibition potencies of the aminocaffeine derivatives. As shown in table 4.3, the chlorine substituted compound **5h** was found to be 3 fold more potent as a MAO-B inhibitor than the unsubstituted homologue, **5c**. Also compound **5h** was found to be 8 fold more potent as a MAO-A inhibitor than **5c** (table 4.4).

Table 4.3 *A comparison of the IC_{50} values of compounds **5c** and **5h** for the inhibition of MAO-B*

Compound	IC_{50} value (μM)	Ratio 5c/5h[a]
5c	15.84	-
5h	4.91	3.23

[a]The ratio of IC_{50}(**5c**)/IC_{50}(**5h**)

Table 4.4 *A comparison of the IC_{50} values of compounds **5c** and **5h** for the inhibition of MAO-A*

Compound	IC_{50} value (μM)	Ratio 5c/5h[a]
5c	46.78	-
5h	5.78	8.09

[a]The ratio of IC_{50}(**5c**)/IC_{50}(**5h**)

- Replacement of the phenyl ring of the C8 substituent with a pyridyl ring was accompanied by a slight reduction in MAO-B inhibition activity. For example, the pyridyl containing compound, **5g** (IC_{50} = 21.61 μM), was found to be slightly weaker as a MAO-B inhibitor than the phenyl containing homologue, **5c** (IC_{50} = 15.84 μM). Interestingly, substitution with a pyridyl ring abolished the MAO-A inhibition properties of **5c**.

Table 4.5 *A comparison of the IC_{50} values of compounds **5c** and **5g** for the inhibition of MAO-B*

Compound	IC_{50} value (μM)	Ratio 5c/5g[a]
5c	15.84	-
5g	21.61	0.73

[a]The ratio of IC_{50}(**5e**)/IC_{50}(**5g**)

- Compound **5f**, which contains a saturated ring system at the C8 amine did not interact with either MAO-A or –B. This finding is similar to that observed for **5a** and may be attributed to the proposal that aminocaffeine derivatives with relatively short C8 side chains are not inhibitors of MAO-A and –B.

As mentioned previously, one of the aims of this study was to compare the MAO inhibition potencies of the aminocaffeine derivatives to those obtained previously for a series of 8-bezyloxycaffeine analogues (Strydom *et al.*, 2010). The IC_{50} values of the 8-

benzyloxycaffeine analogues for the inhibition of recombinant human MAO-A and –B are given in table 4.6.

Table 4.6 *The IC_{50} values for the inhibition of recombinant human MAO-A and –B by 8-benzyloxycaffeine analogues (Strydom et al., 2010).*

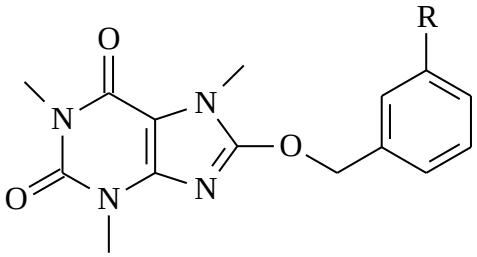

		IC_{50} (µM)		
Compound ID	**R**	MAO-A	MAO-B	SI[c]
3a	-H	1.24	1.77	0.7
3b	-Cl	0.666	0.107	6.2
3c	-Br	0.941	0.068	13.8
3d	-F	1.07	0.542	1.98
3e	$-CF_3$	3.72	0.152	24.8
3f	$-CH_3$	0.397	0.546	0.73
3g	$-OCH_3$	3.15	1.01	3.12

Compared to the IC_{50} values of the aminocaffeine derivatives (**5a-h, 6a, 6b**) it is clear that 8-benzyloxycaffeine analogues (**3**) are superior inhibitors of both human MAO-A and –B. The weakest MAO-B inhibitor among the benzyloxycaffeines, compound **3a** (IC_{50} = 1.77 µM), is a more potent inhibitor that the most potent MAO-B inhibitor, compound **6b** (IC_{50} = 2.97 µM), among the aminocaffeine derivatives. Likewise, the weakest MAO-A inhibitor among the benzyloxycaffeines, compound **3e** (IC_{50} = 3.72 µM), is a more potent inhibitor that the most potent MAO-A inhibitor, compound **5h** (IC_{50} = 5.78 µM), among the aminocaffeine derivatives. This clearly indicates that benzyloxycaffeine derivatives are better suited for interaction with MAO-A and –B than aminocaffeine derivatives.

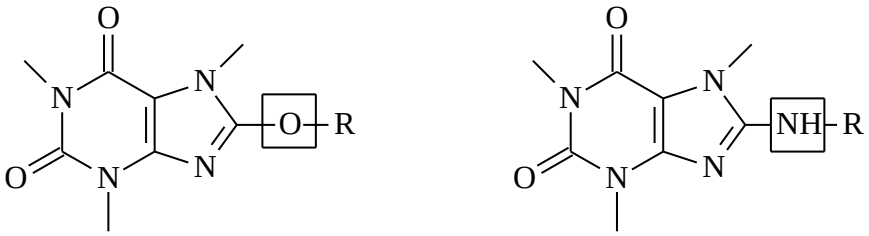

Figure 4.5. *A comparison of the structures of the C8-substituted oxycaffeines (**3**) and C8-substututed aminocaffeines (**5**).*

An explanation for the observation that benzyloxycaffeine derivatives are superior inhibitors of MAO-A and –B than aminocaffeine derivatives is not readily apparent. Differing ionization states of the benzyloxycaffeine and aminocaffeine analogues do not explain the difference in binding affinities to the MAO enzymes, since both the sulfanylcaffeine and aminocaffeine analogues are expected to be uncharged in the buffer used for the inhibition studies (pH 7.4). For example, the pKa values of the most acidic functional group of benzyloxycaffeines (-3.45) and benzylaminocaffeines (0.31), which is the N9 nitrogen of the caffeine ring, are well below 7.4, which indicate that these structures are uncharged at physiological pH as well as in the pH used for the inhibition studies.

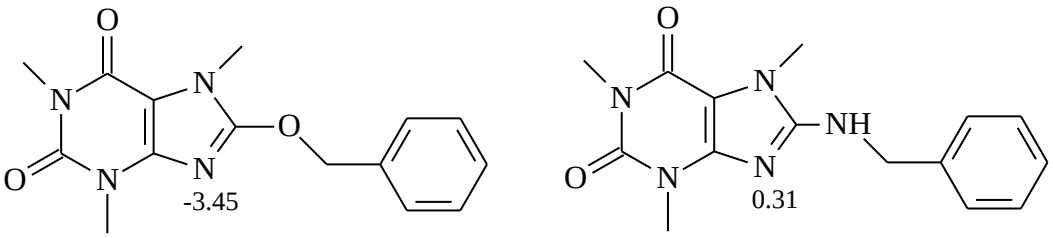

Figure 4.6 *Structures of benzyloxycaffeine and benzylaminocaffeine with pKa values of the N9 nitrogen.*

4.2 REVERSIBILITY STUDIES

4.2.1 Introduction

Also known as time-dependent studies, reversibility studies determine whether an inhibitor binds reversibly (non-covalently) or irreversibly (covalently) to an enzyme. It is preferable for an inhibitor to bind reversibly, as to allow substrate competition in an *in vivo* environment. In this study two inhibitors were selected for the examination of the reversibility of binding of the aminocaffeine derivatives to the MAO enzymes. 8-[2-(3-Chlorophenyl)-ethylamino]caffeine **(5h)** was selected as representative inhibitor for human MAO-A and 8-[methyl(4-

phenylbutyl)amino]caffeine **(6b)** was chosen as representative inhibitor for human MAO-B. In this study, the selected inhibitor was pre-incubated with the enzyme for various periods of time. The substrate was subsequently added to the reactions and the rate of substrate oxidation was measured fluorometrically. The rate of substrate oxidation versus the pre-incubation times was subsequently plotted on a bar graph. A constant oxidation rate for all incubation times is an indication of reversibility. Irreversible inhibitors will show a decrease in the rate of enzyme catalysis over time.

4.2.2 Method

Microsomes (5 mg/mL) from baculovirus infected insect cells, expressing recombinant human MAO-A or –B, were obtained from Sigma-Aldrich and were pre-aliquoted (33 µl) and stored at –70 °C. All enzymatic reactions were carried out to a volume of 250 µl in potassium phosphate buffer (100 mM, pH 7.4) and contained the following:

- MAO-A or MAO-B at concentrations of 0.03 mg/ml.
- **5h** at a concentration of 11.56 µM or **6b** at a concentration of 5.94 µM. These concentrations are approximately double the IC_{50} values for the inhibition of MAO-A and –B, respectively, by these inhibitors.

The MAO enzymes were pre-incubated with **5h** and **6b** for periods of 0, 15, 30 and 60 minutes at 37 ºC. The MAO-A/B mixed substrate, kynuramine, was subsequently added to the reactions to yield final concentrations of 45 µM and 30 µM where MAO-A and –B, respectively, were used as enzymes. The final volumes of the reaction were 500 µl. The reactions were incubated for a further 15 min. After the incubation time was completed, the reactions were terminated by adding 400 µl NaOH (2N). 1000 µl distilled water was added to each incubation before being centrifuged for 10 minutes at 16 000 g.

The fluorescence intensities of the supernatant fractions were measured at an excitation wavelength of 310 nm and an emission wavelength of 400 nm to determine the concentration of 4-hydroxyquinoline. A Varian® Cary Eclipse fluorescence spectrophotometer was used for this purpose. The PMT voltage was set to medium for both enzyme isoforms. The excitation and emission slit width was set to 5 nm for MAO-A. For MAO-B the excitation slit width was set to 5 nm and the emission slit width was set to 10 nm. To quantify the amounts of 4-hydroxyquinoline formed in the reactions, a calibration curve was prepared by measuring the fluorescence of increasing concentrations of 4-hydroxyquinoline (0.0469, 0.09375, 0.1875, 0.375, 0.75, 1.5 µM). Each of these calibration

standards contained 4% (v/v) DMSO and potassium phosphate buffer to a final volume of 500 µl. To each calibration standard were added 400 µl of NaOH and 1000 µl of distilled water.

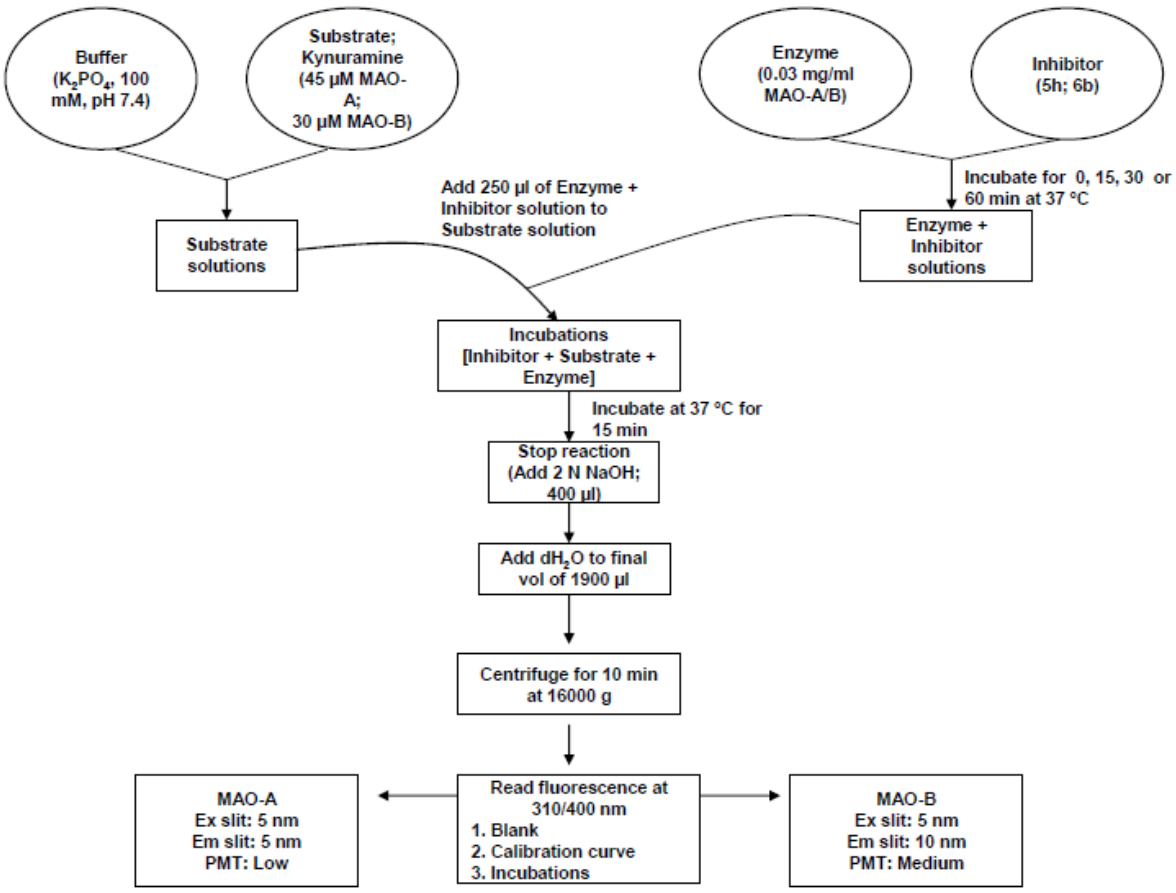

Figure 4.7 *Summary of the procedure used to determine the reversibility of MAO inhibition.*

4.2.3 Results

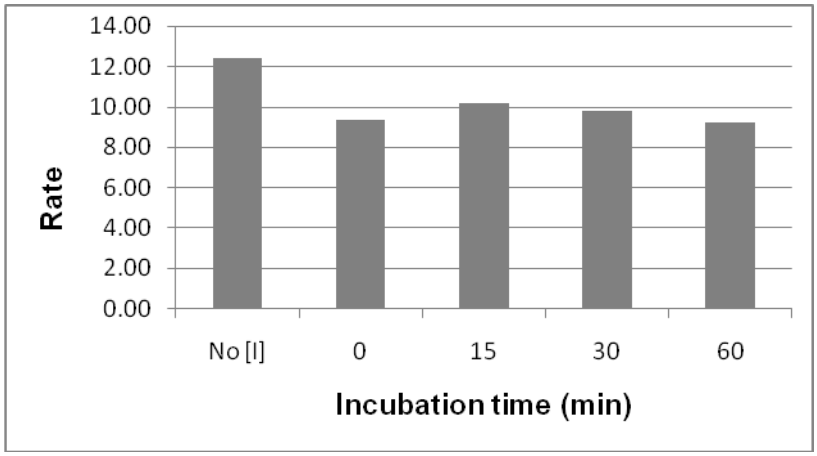

Figure 4.8 *The time-dependent inhibition of recombinant human MAO-A by **5h**.The enzymes were pre-incubated for various periods of time (0-60 min) with **5h** at a concentration of 11.56 µM. The concentration of the substrate, kynuramine, was 45 µM. The catalytic rates are expressed as nmoles 4-hydroxyquinoline formed/min/mg protein.*

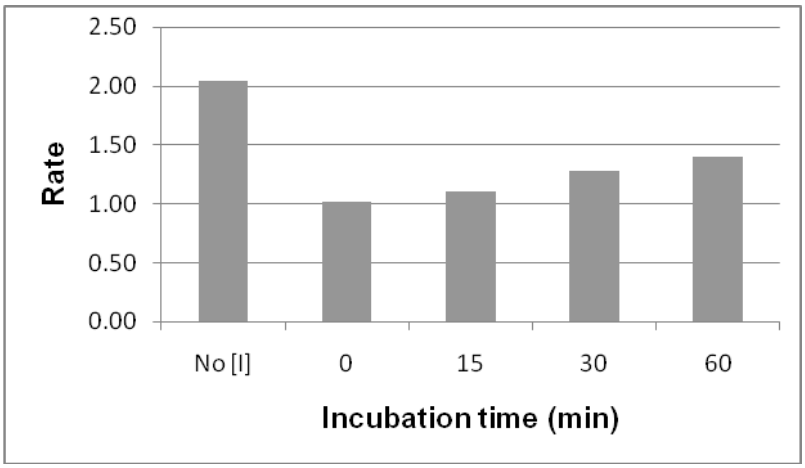

Figure 4.9 *The time-dependent inhibition of recombinant human MAO-B by **6b**.The enzymes were pre-incubated for various periods of time (0-60 min) with **6b** at a concentration of 5.94 µM. The concentration of the substrate, kynuramine, was 30 µM. The catalytic rates are expressed as nmoles 4-hydroxyquinoline formed/min/mg protein.*

- Figure 4.8 shows that there is no time-dependent reduction in the rate of MAO-A catalysed oxidation of kynuramine when compound **5h** is pre-incubated with MAO-A, for various periods of time. From this result it may be concluded that the inhibition of MAO-A is reversible, at least for 60 minutes at the inhibitor concentration (IC_{50} x2) evaluated.

- Figure 4.9 shows that there is no time-dependent reduction in the rate of MAO-B catalysed oxidation of kynuramine when compound **6b** is pre-incubated with MAO-B, for various periods of time. From this result it may be concluded that the inhibition of MAO-A is reversible, at least for 60 minutes at the inhibitor concentration (IC_{50} x2) evaluated.

4.3 MOLECULAR DOCKING STUDIES

4.3.1 Introduction

Molecular docking is a computational tool that can be applied in the development and discovery of novel drugs. It involves designing ligands for a specific receptor target by utilising structural and computational chemistry. Molecular docking is the process of fitting a ligand into the active site on an enzyme.

These days the amount of high resolution structural data available on enzymes and other proteins, makes docking studies an integral part of drug discovery (Knegtel *et al*., 1997). The interactions of the ligand in the active site of the receptor can be studied and the best possible conformations can be identified, as the computational tool assesses several different ligand poses. In combination with structure-activity relationship studies, docking studies can be used to identify critical features of a ligand for optimal activity towards an enzyme or receptor. Docking studies can also be used to study the interactions between and enzyme and a specific ligand, in order to clarify enzyme-ligand binding.

In this study, the target compound (**6b**), was computationally docked within a MAO-B model. Safinamide, the co-crystallized ligand was used as a measure of the accuracy of the docking procedure.

4.3.2 Experimental

The molecular docking studies were carried out in Windows® based Discovery Studio® (DS) 1.7. The inhibitors were drawn in DS 1.7 and prepared for docking with the 'Prepare ligand' protocol. The MAO-B (2V5Z.pdb) enzyme model, co-crystallised with safinamide, was obtained from the Brookhaven Protein Data Bank. The enzyme was prepared with the 'Clean protein' function and typed with the CHARMm force field. The backbone was fixed where after a series of three minimizations were carried out on the protein. The steepest descent minimization was first, followed by the conjugate gradient and adopted basis Newton-Raphson minimizations. During the minimizations the implicit distance-dependent solvent model was used with a dielectric constant of 4. The existing ligand was deleted from the enzyme and the backbone constraint was removed. The binding site was identified and the ligands were docked using the 'Ligandfit' protocol. *In situ* ligand minimization using the 'Smart Minimizer' algorithm was used to refine the docked ligands. Ten possible docking poses were calculated for each inhibitor.

4.3.3 Results

The 8-(methyl)aminocaffeine derivative transversed both the entrance and substrate cavities of MAO-B with the caffeinyl moiety oriented towards the FAD co-factor in the substrate cavity while the amino-side chain extended into the entrance cavity. As shown by example with inhibitor **6b**, the carbonyl oxygen at C-6 of the caffeinyl ring forms a hydrogen bond with the phenolic hydrogen of Tyr-435. The caffeinyl ring also forms a π-π interaction within the aromatic sandwich, between Tyr-435 and Tyr-398. The phenylbutyl side chain is stabilized by Van der Waals interactions in the hydrophobic entrance cavity defined by Phe-103, Trp-119, Leu-164, Leu-167, Phe-168 and Ile-316 (Novaroli *et al*., 2006).

4.4 CONCLUSION

This section demonstrated that 8-aminocaffeine and 8-(methyl)aminocaffeine derivatives are moderate to weak inhibitors of recombinant human MAO-A and MAO-B. The most potent MAO-A inhibitor, 8-{[2-(3-chlorophenyl)ethyl]amino}caffeine (**5h**), displayed an IC_{50} value of 5.78 µM. It is also a moderate MAO-B inhibitor with an IC_{50} value of 4.91 µM. **5h** displays low selectivity between the two isoforms with a SI value of 0.7. The most potent MAO-B inhibitor, 8-[methyl(4-phenylbutyl)amino]caffeine (**6b**), displayed an IC_{50} value of 2.97 µM. This compound displays selectivity towards the MAO-B isoform with a SI value of 7.8. This study demonstrates that methylation of the C8 amine of compound **5e**, to yield compound **6b**, results in enhanced inhibition towards MAO-B. Increasing the chain length of the C8

substituent also seems to enhance the MAO-B inhibition potency. This is shown by the observation that the compounds containing relatively short C8 side chains (**5e** and **5b**) are not MAO-B inhibitors. Increasing the chain length however yields structures **5c, 5d**, and **5e** which possess MAO-B inhibition properties. It is also shown that chlorine substitution on the phenyl ring of the C8 substituent enhances both the MAO-A and -B inhibition potencies of the aminocaffeine derivatives. For example, the chlorine substituted compound **5h** was found to be a more potent MAO-B inhibitor than the unsubstituted homologue, **5c**.

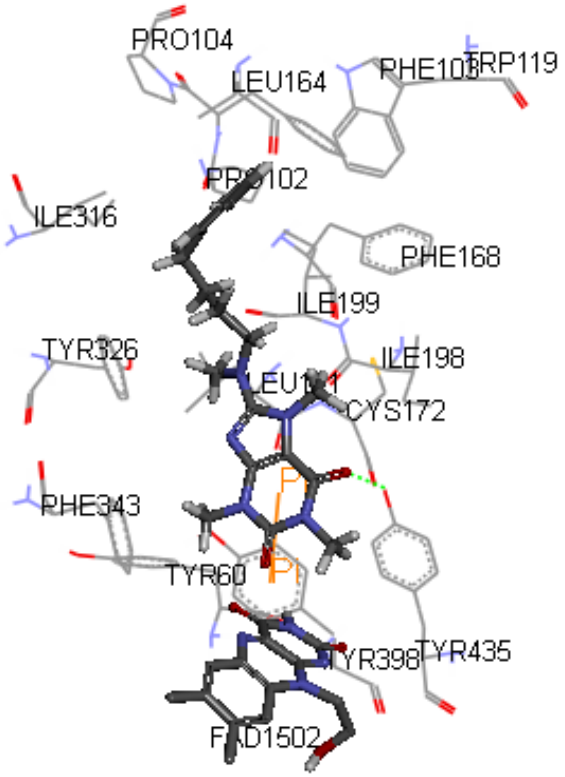

Figure 4.10 *Representation of 8-[methyl(4-phenylbutyl)amino]caffeine (**6b**) within the active site of MAO-B. Hydrogen bonds are indicated as green dashed lines and π-π interactions as orange lines.*

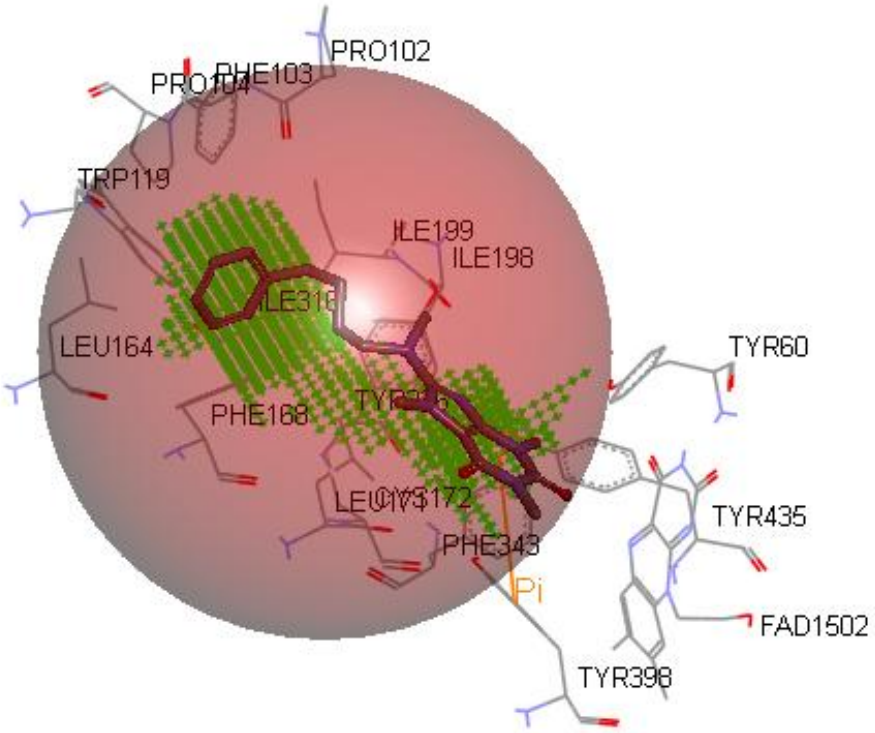

Figure 4.11 *Representation of the binding site of MAO-B indicated by the red sphere with 8-[methyl(4-phenylbutyl)amino]caffeine (**6b**) bound. The sphere encompasses all the residues involved in substrate binding.*

This study therefore proposes the following structural modifications be made to aminocaffeine derivatives in order to enhance the MAO inhibition properties:

- methylation of the C8 amine
- increasing the chain length of the C8 substituent
- chlorine substitution on the phenyl ring of the C8 substituent

A short molecular docking study indicated that compound **6b** forms various interactions with the active site of MAO-B. These interactions may be important in stabilizing the inhibitor within the active site of the enzyme, the most important interactions were:

- hydrogen bonding with the phenolic hydrogen of Tyr-435
- π-π interaction between the caffeine ring and the aromatic sandwich, Tyr-435 and Tyr-398
- The C8 side chain is stabilized by Van der Waals interactions in the hydrophobic entrance cavity.

CHAPTER 5

CONCLUSION

The MAO isozymes are important in the catabolism of neuronal dopamine and these enzymes are therefore attractive drug targets for the treatment of PD. Inhibition of particularly MAO-B may exert a neuroprotective effect by reducing the amount of toxic by-products formed during dopamine catabolism. MAO-B inhibition may therefore slow the degradation of striatal dopamine in addition to elevating the levels of this neurotransmitter in the brain.

The caffeine structure served as lead compound for this study. Although caffeine is a weak MAO-B inhibitor, previous studies have shown that C8 substitution of caffeine yields MAO-B inhibitors with improved potencies. For example, 8-benzyloxycaffeines have previously been synthesized and were found to be potent MAO-B inhibitors (Strydom *et al*., 2010). In this study the possibility that alkylamino substituents at C8 of the caffeine ring may similarly enhance the MAO inhibition potency of caffeine was explored. This study therefore investigated if alkylamino substituents possess similar biological activity compared to the benzyloxy substituent with respect to their MAO inhibition properties. For this purpose, a series of C8 substituted alkylamino and methylalkylamino caffeines were synthesized. The inhibition potencies of the resulting 8-aminocaffeines and 8-(methyl)aminocaffeines on MAO-A and -B were compared with those of previously studied 8-alkyloxycaffeine analogues. The structures of the compounds that were examined are presented in Table 5.1.

Chemistry: Eight 8-aminocaffeine derivatives were successfully synthesized by reacting 8-chlorocaffeine and the appropriate substituted amine at high temperatures. Further, two 8-(methyl)aminocaffeine derivatives were successfully synthesized by reacting the appropriate 8-aminocaffeine with methyliodide in the presence of potassium hydroxide. All the amine starting materials were commercially available. The structures of the newly synthesized inhibitors were verified by NMR and MS analysis. Both the ^{1}H NMR and ^{13}C NMR spectra corresponded with the proposed structures and the expected exact masses were also recorded for each compound. The purity of the compounds was evaluated using HPLC, which revealed a single peak for each compound, indicating a high degree of purity.

Table 5.1 *Structures of the 8-aminocaffeine and 8-(methyl)aminocaffeine derivatives synthesized in this study.*

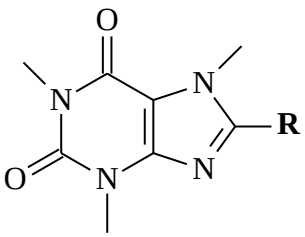

	R		R
5a	-NH-C_6H_5	**6a**	-(NCH_3)-$(CH_2)_2$-C_6H_5
5b	-NH-CH_2-C_6H_5	**6b**	-(NCH_3)-$(CH_2)_4$-C_6H_5
5c	-NH-$(CH_2)_2$-C_6H_5		
5d	-NH-$(CH_2)_3$-C_6H_5		
5e	-NH-$(CH_2)_4$-C_6H_5		
5f	-NH-C_5H_6		
5g	-NH-$(CH_2)_2$-(pyridin-2-yl)		
5h	-NH-$(CH_2)_2$-(3-ClC_6H_4)		

MAO inhibition studies: The 8-aminocaffeine and 8-(methyl)aminocaffeine derivatives were evaluated as inhibitors of recombinant human MAO-A and –B. The recombinant human MAO-A and –B enzymes used for this purpose were commercially available. The inhibition potencies of the compounds were measured by means of a spectrofluorometric method and the inhibition activities were expressed as IC_{50} values. The MAO activity was based on measuring the amount of 4-hydroxyquinoline that is formed when the substrate, kynuramine, is oxidized by the MAO enzymes. Since 4-hydroxyquinoline is a fluorescent substance its concentrations were measured spectrofluorometrically at an excitation wavelength of 310 nm and an emission wavelength of 400 nm.

IC_{50} results: It was found that 8-aminocaffeine and 8-(methyl)aminocaffeine derivatives are moderate to weak inhibitors of MAO-A and –B, but these compounds are generally more specific towards MAO-B.

- The best MAO-B inhibitor was compound **6b**, with an IC_{50} value of 2.97 µM. This compound also expressed the highest selectivity towards MAO-B with a SI value of 7.8.

The results of the inhibition studies also indicated that the following changes to the structure of the inhibitor yields better inhibition:

- Increasing the chain length of the C8 substituent: the phenylbutyl substituted derivative (**6b**) showed increased MAO-B inhibition over the phenylethyl substituted derivative (**6a**).

- Methylation of the C8 amine. This modification also seems to increase specificity towards MAO-B inhibition as the methylphenylbutyl derivative (**6b**) showed increased MAO-B inhibition and selectivity compared to the phenylbutyl derivative (**5e**).

- Halogen substitution on the phenyl ring of the C8 substituent. Chlorine substitution as shown by compound **5h** increases MAO-A and –B inhibition potencies. Chlorine substitution seems to increase inhibition potency towards both MAO-A and –B. This may be advantageous in the treatment of PD since PD patients frequently suffer from depression which may be treated with MAO-A inhibitors.

Reversibility studies: The reversibility of inhibition of both MAO-A and –B by a selected aminocaffeine derivative was evaluated. Compound **5h** was used to evaluate the reversibility of inhibition of MAO-A and **6b** was used to evaluate the reversibility of inhibition of MAO-B. The results showed that when the compounds were pre-incubated with the respective MAO-A and –B enzymes, the catalytic activities of the enzymes were not reduced as a function of time. The finding that these representative inhibitors bind reversibly to MAO-A and –B suggest that the aminocaffeine derivatives are in general reversible inhibitors.

Molecular docking: Docking studies gave insight into the binding modes of 8-aminocaffeine derivatives within the active site of MAO-B. It was found that the 8-(methyl)aminocaffeine derivative **6b** traverse both the entrance and substrate cavity of MAO-B. The caffeine moiety is oriented towards the FAD-cofactor in the substrate cavity with the amino-side chain

extending into the entrance cavity. The following interactions were noticed between the inhibitor and the MAO-B active site:

- A carbonyl oxygen of the caffeinyl ring forms a hydrogen bond with the phenolic hydrogen of Tyr-435.
- The caffeinyl ring forms π-π interactions within the aromatic sandwich, Tyr-435 and Tyr-398.
- The C8 side chain is further stabilized by hydrophobic interactions within the entrance cavity of the enzyme.

Future recommendations: This study thus reported the successful synthesis of 8-aminocaffeine and 8-(methyl)aminocaffeine derivatives. This study further showed that these compounds are moderate to weak inhibitors of MAO and proposes certain structural modifications that may increase the MAO inhibition potencies:

- Increasing the chain length of the C8 alkylamine substituent
- Methylation of the C8 amine
- Substitution of halogens (Cl, Br and F) on the phenyl ring of the C8 substituent.

This study therefore recommends that phenylbutyl substituted methylaminocaffeine derivatives containing halogens on the phenyl ring be synthesized and evaluated as MAO inhibitors. Examples of these structures are given in table 5.2

Table 5.2 *Recommended aminocaffeine derivatives for future studies.*

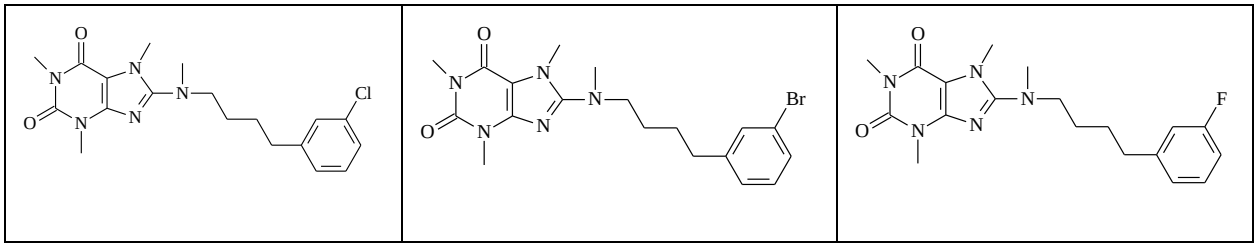

APPENDIX I

HPLC and NMR

List of HPLC chromatograms:

List of ^{1}H and ^{13}C NMR spectra:

8-(Phenylamino)caffeine (5a)

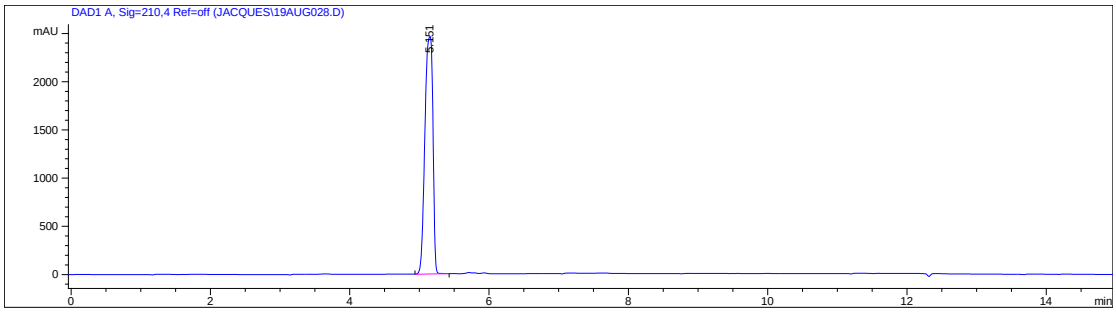

8-(Benzylamino)caffeine (5b)

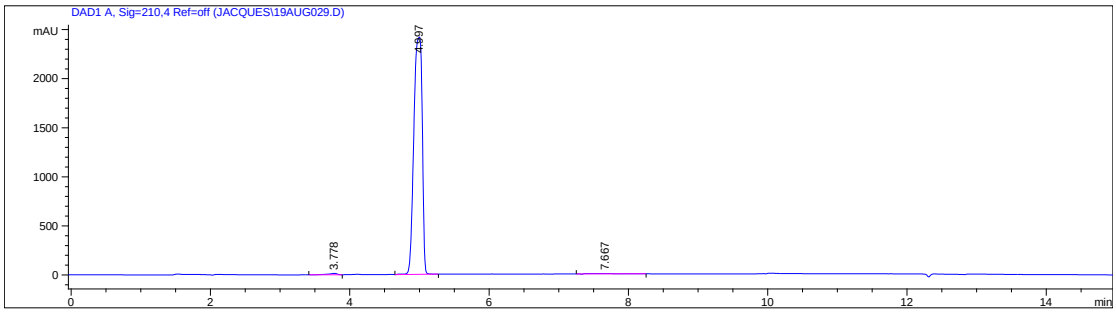

8-[(2-Phenylethyl)amino]caffeine (5c)

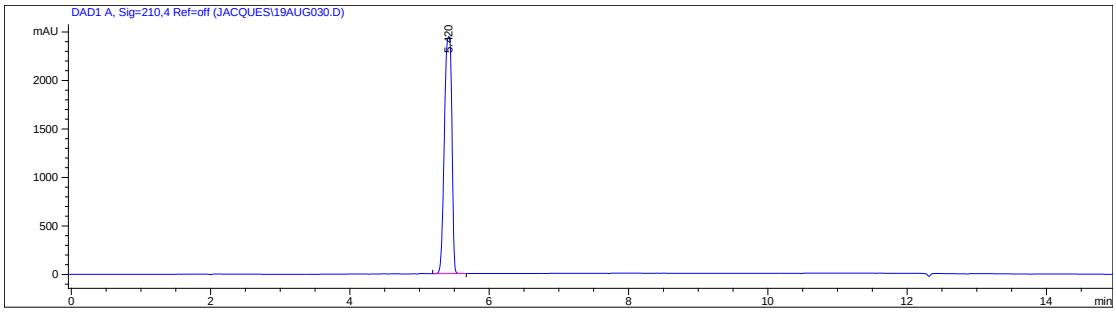

8-[(3-Phenyl-1-propyl)amino]caffeine (5d)

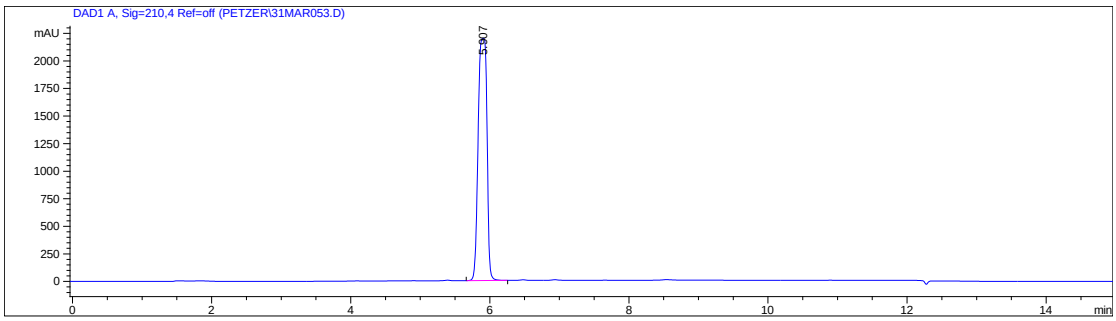

8-[(4-Phenylbutyl)amino]caffeine (5e)

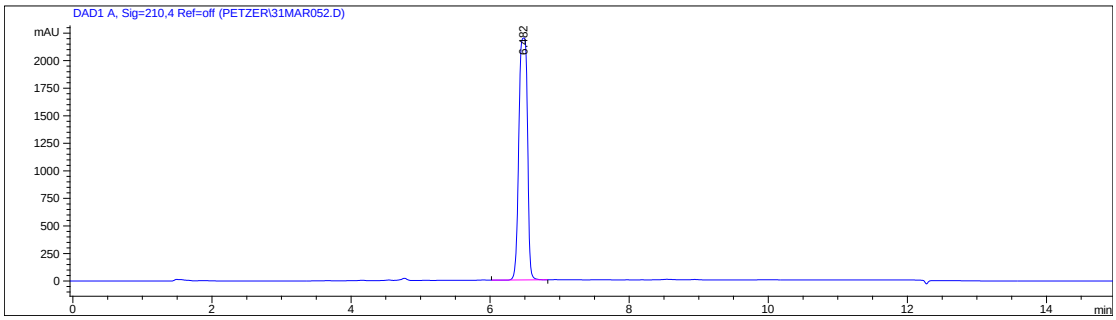

8-(Cyclopentylamino)caffeine (5f)

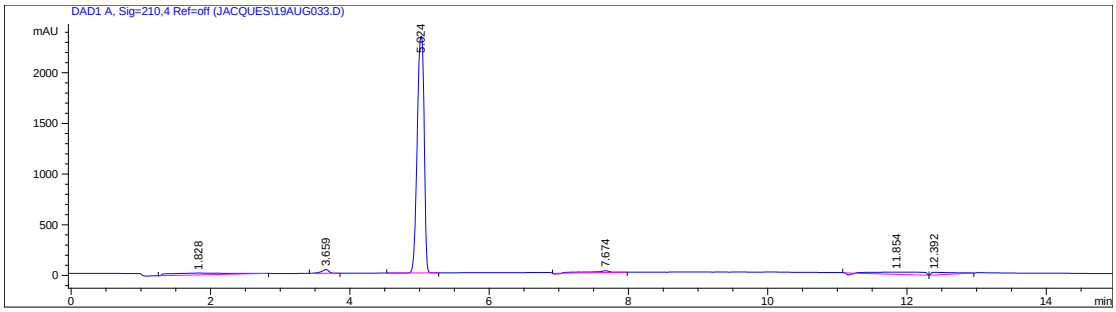

8-{[2-(2-Pyridyl)-ethyl]amino}caffeine (5g)

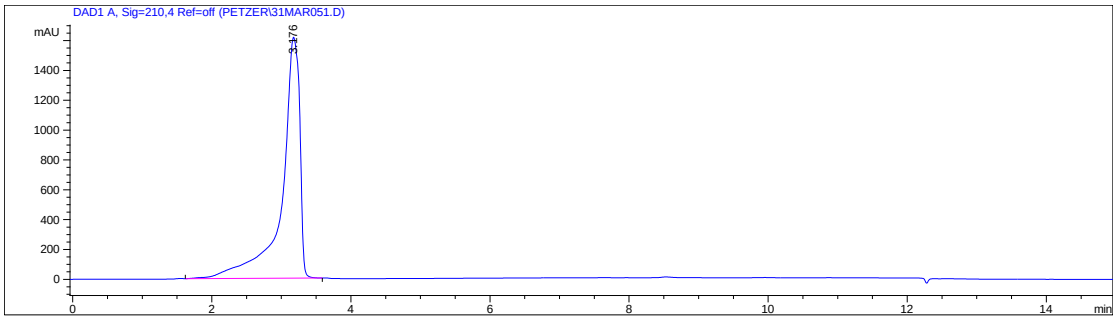

8-{[2-(3-Chlorophenyl)ethyl]amino}caffeine (5h)

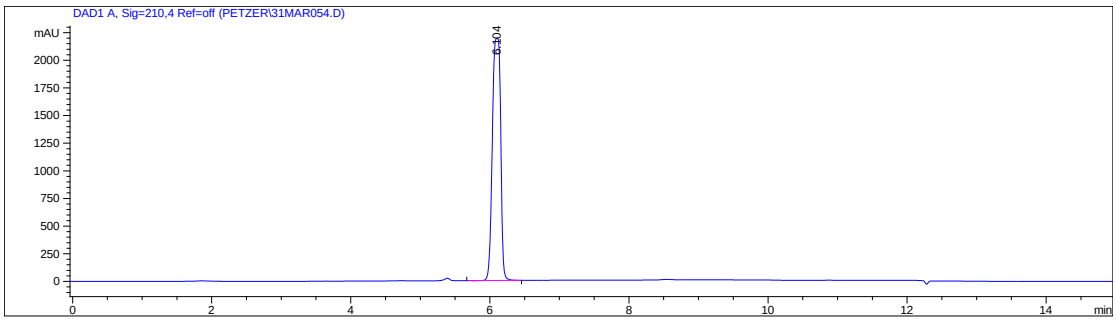

8-[Methyl(2-phenylethyl)amino]caffeine (6a)

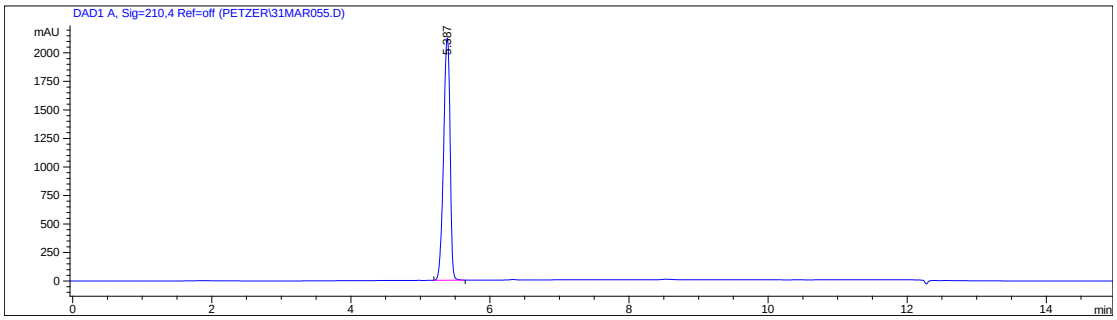

8-[Methyl(4-phenylbutyl)amino]caffeine (6b)

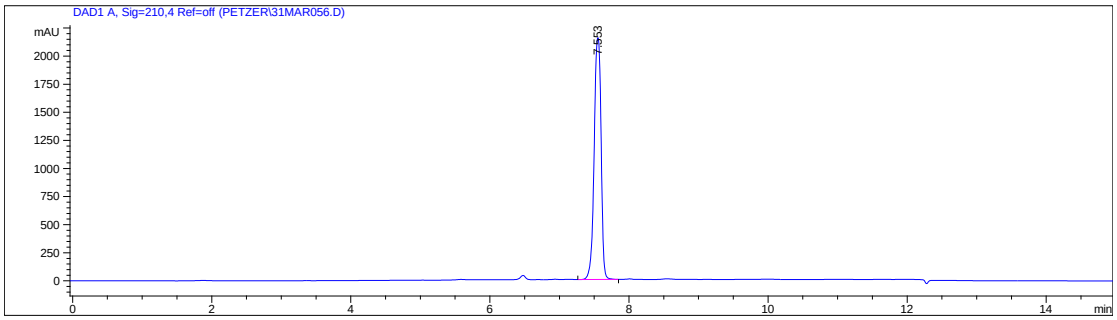

8-(Phenylamino)caffeine (5a)

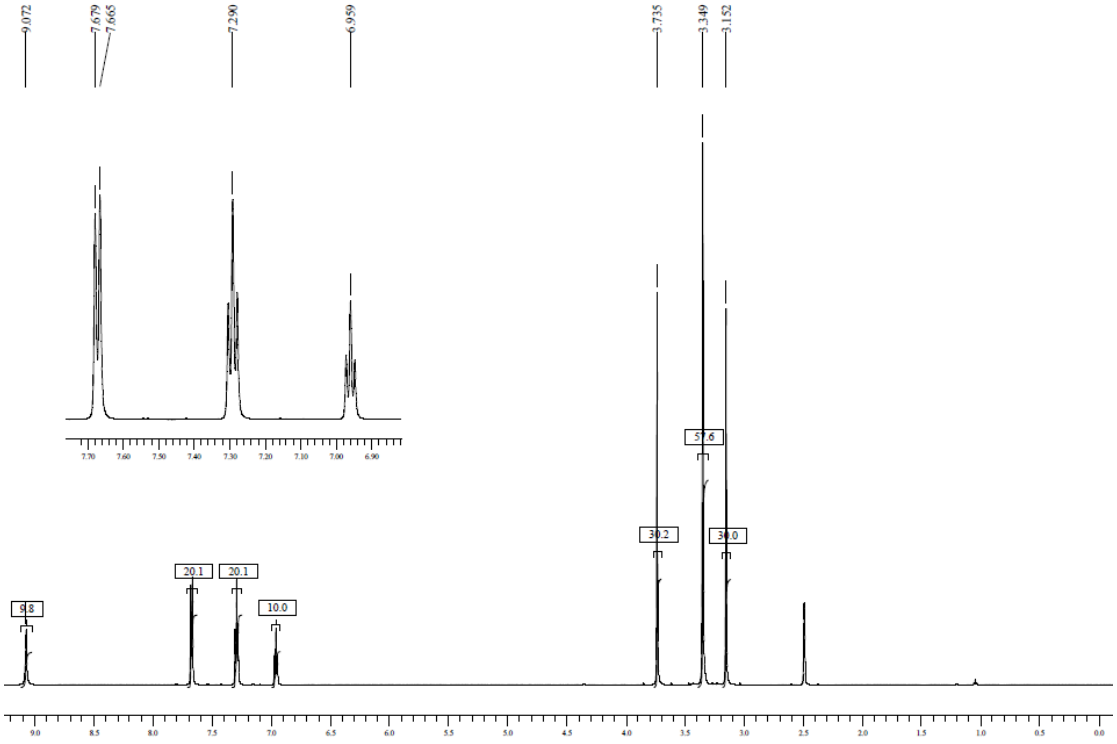

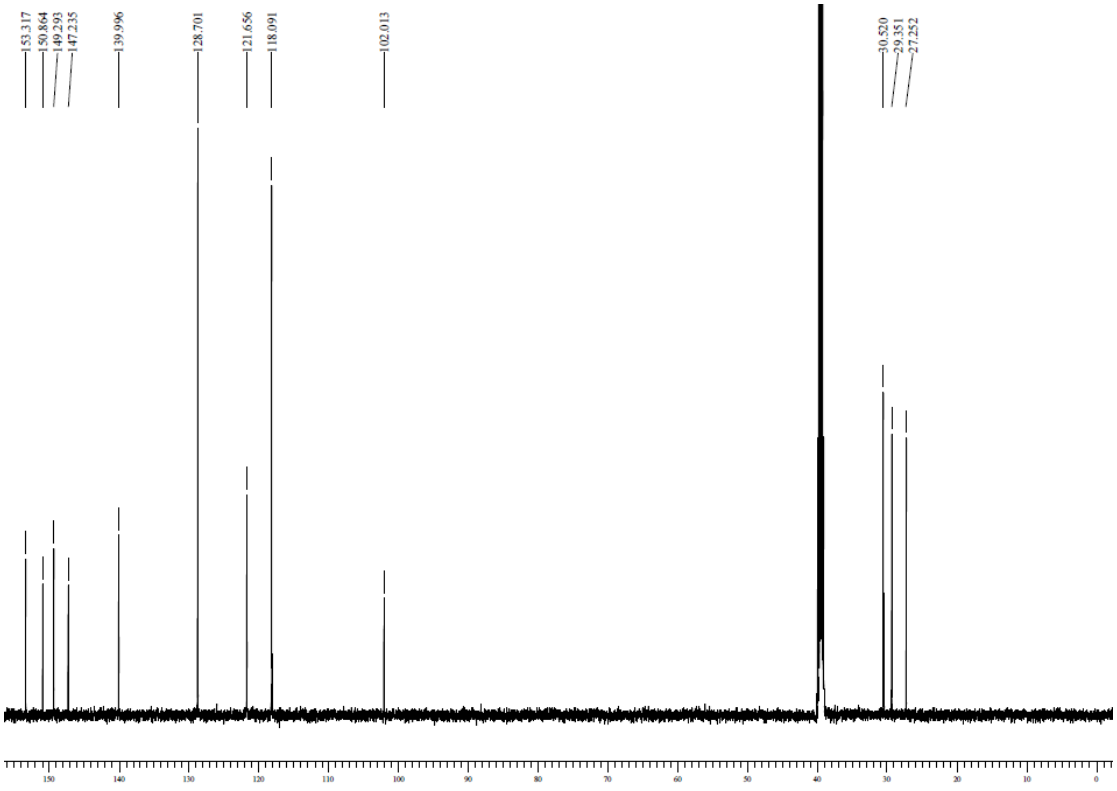

8-(Benzylamino)caffeine (5b)

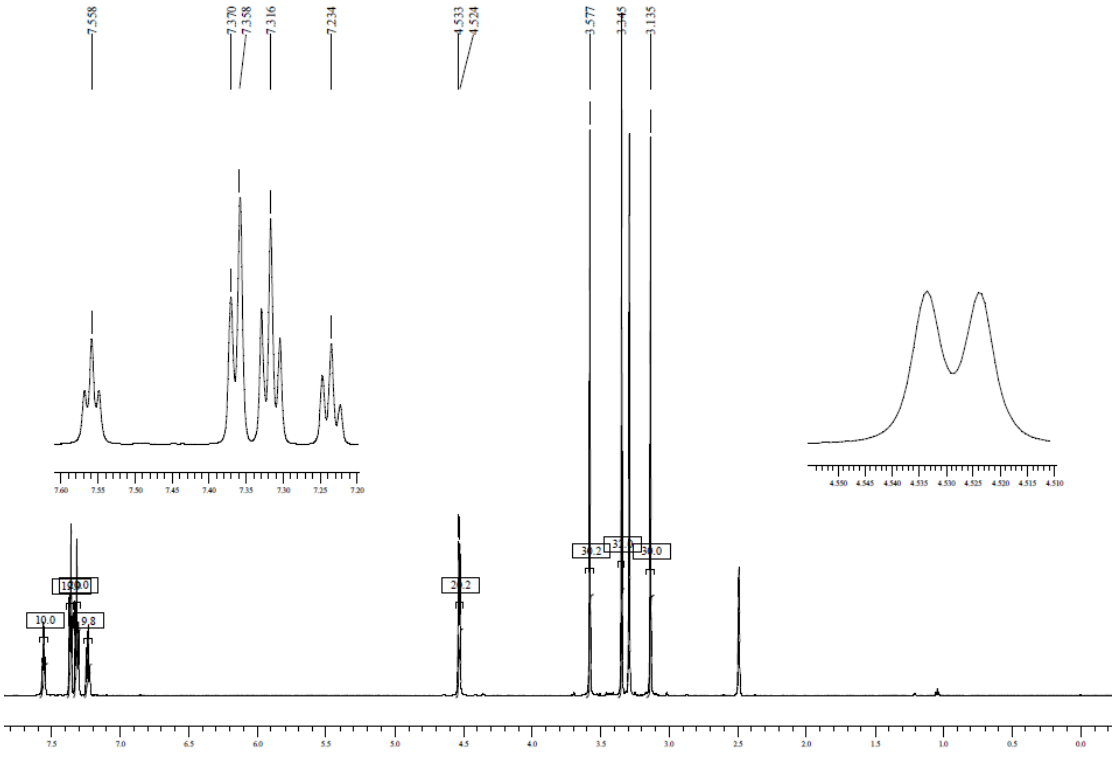

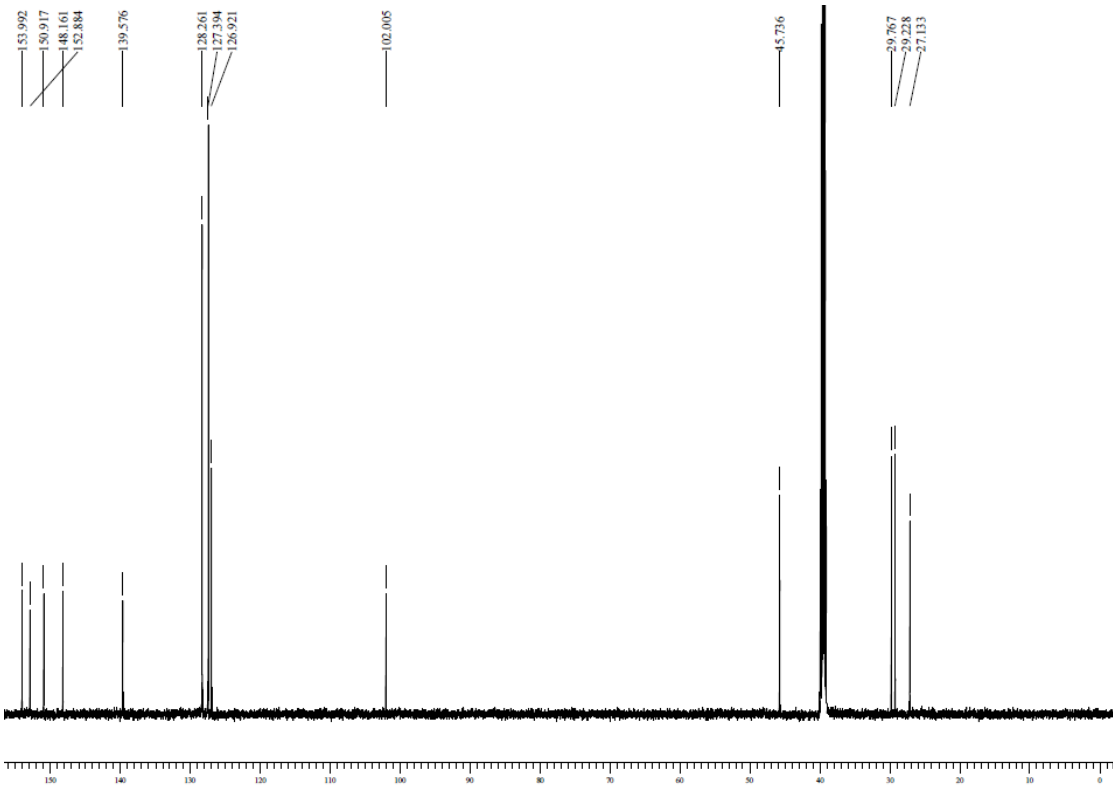

8-[(2-Phenylethyl)amino]caffeine (5c)

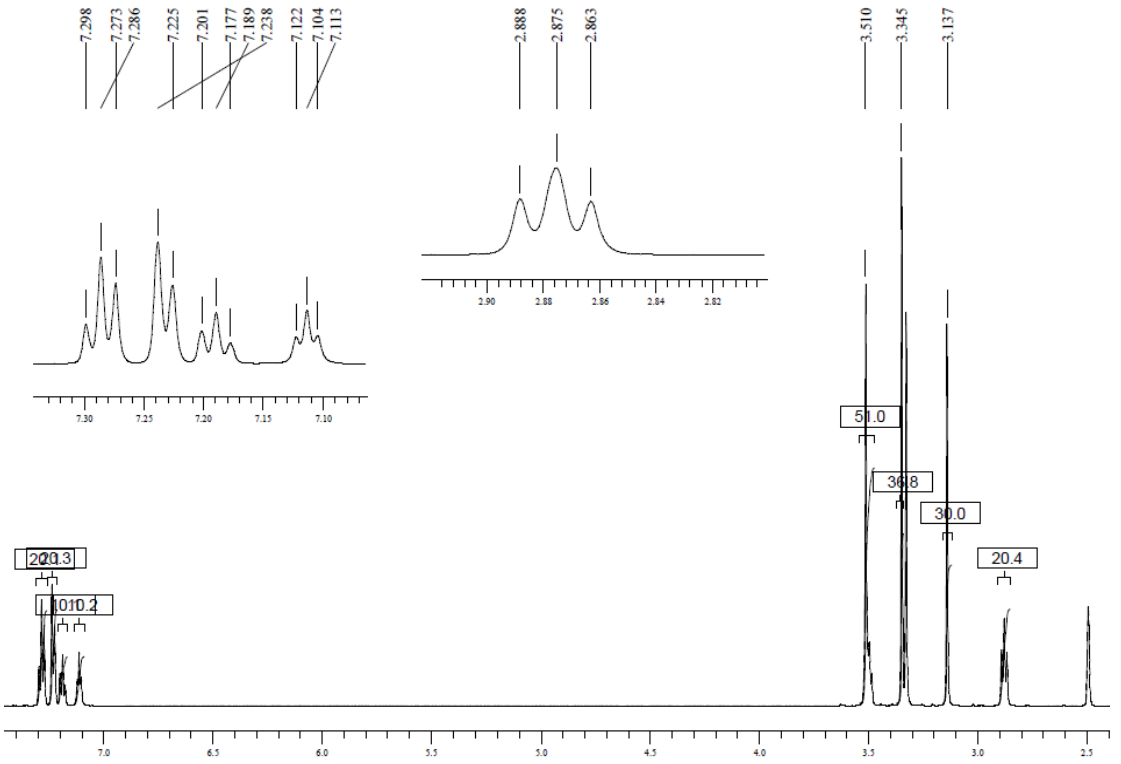

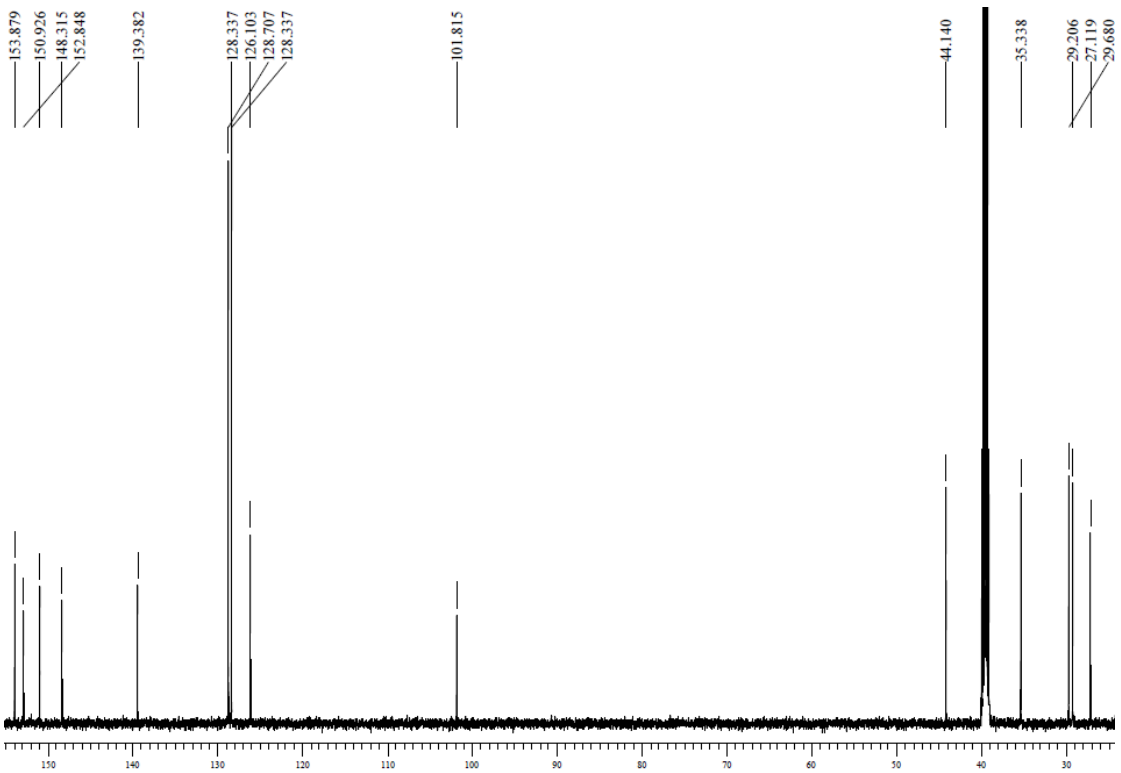

8-[(3-Phenyl-1-propyl)amino]caffeine (5d)

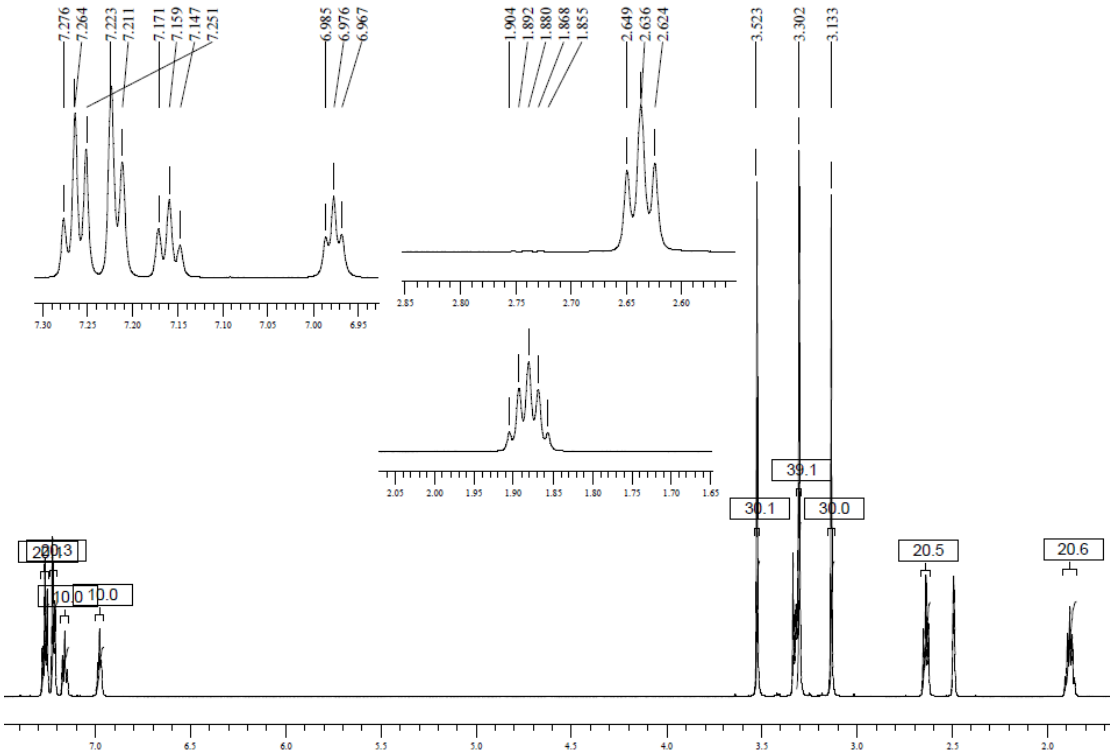

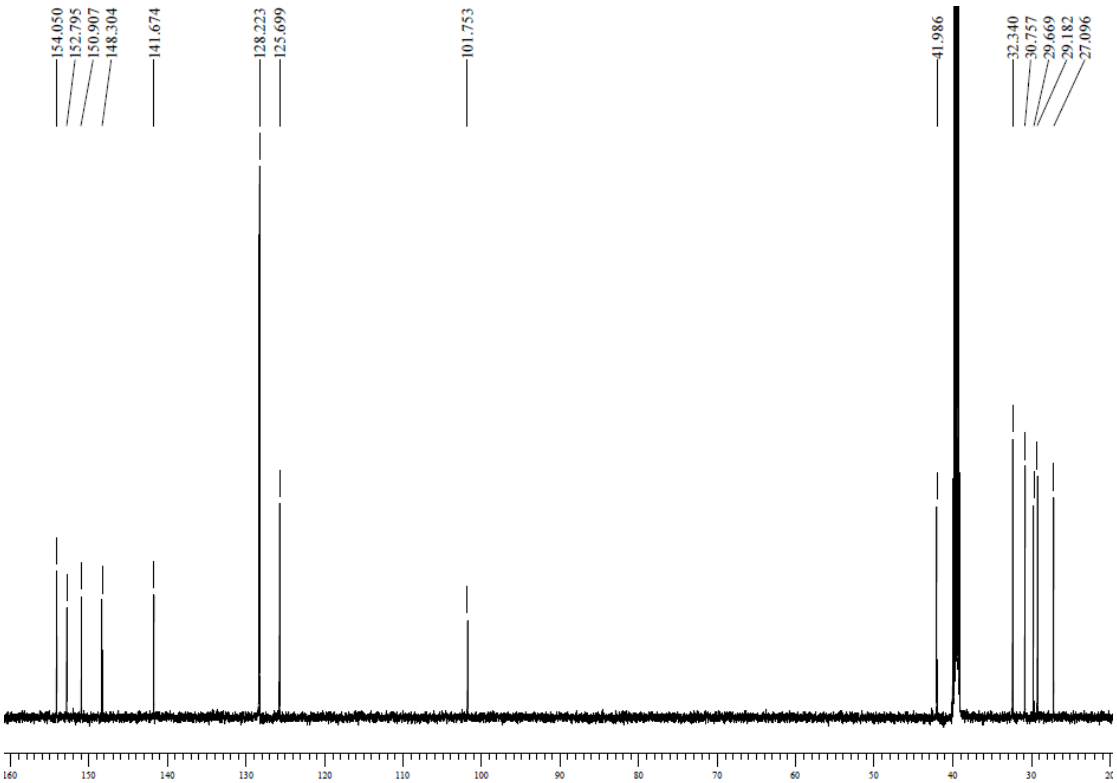

8-[(4-Phenylbutyl)amino]caffeine (5e)

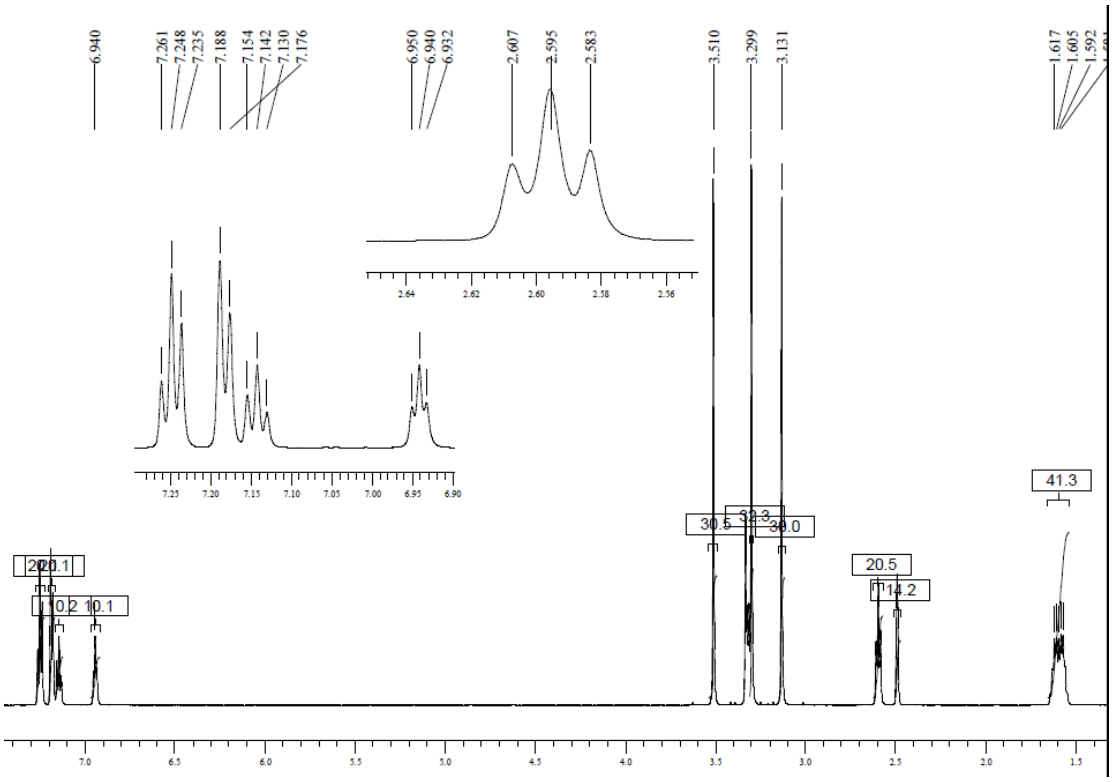

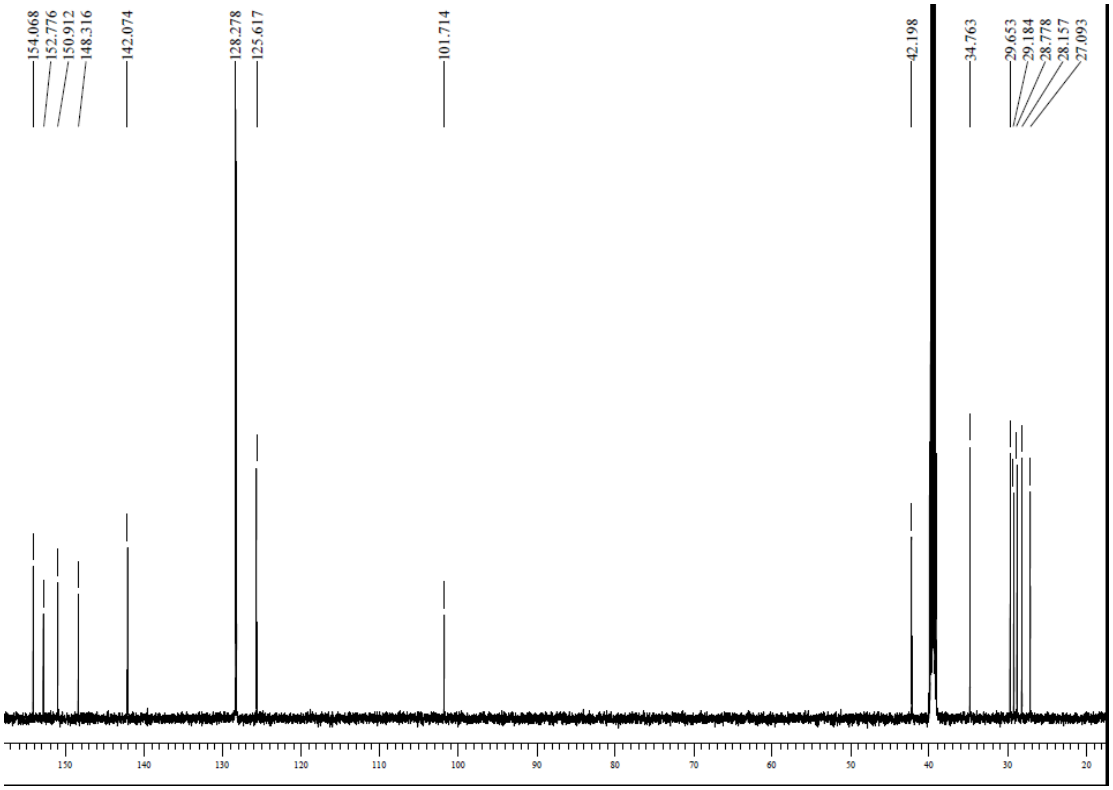

8-(Cyclopentylamino)caffeine (5f)

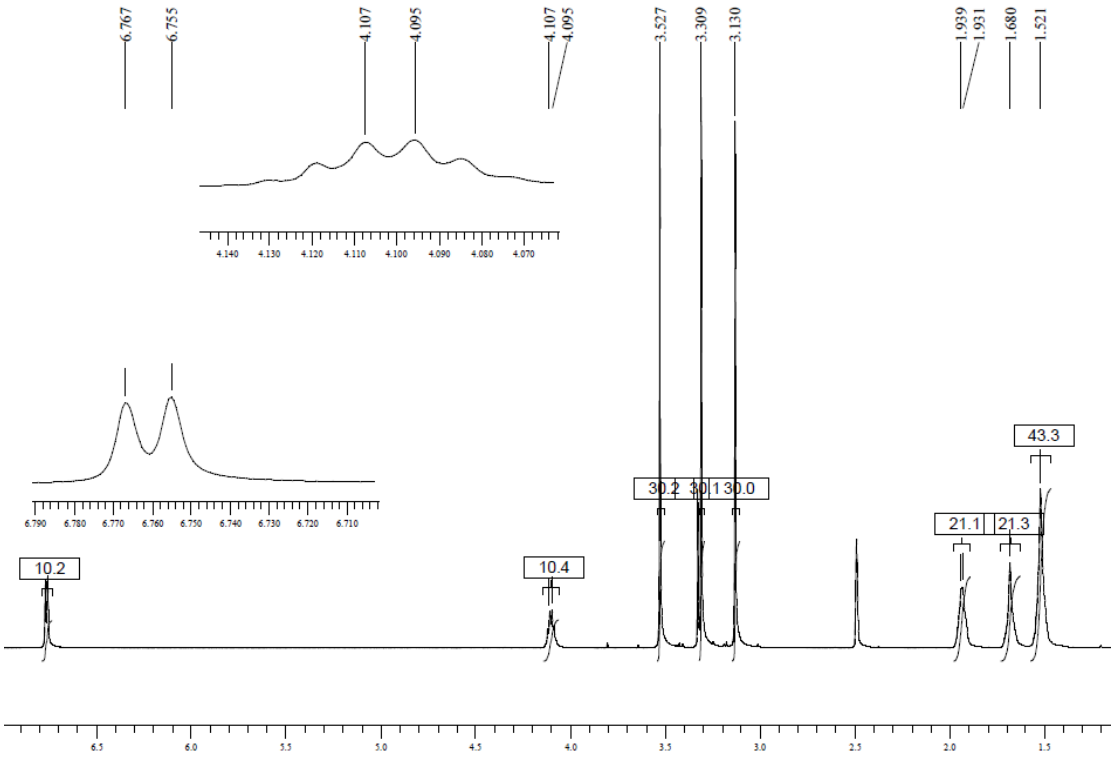

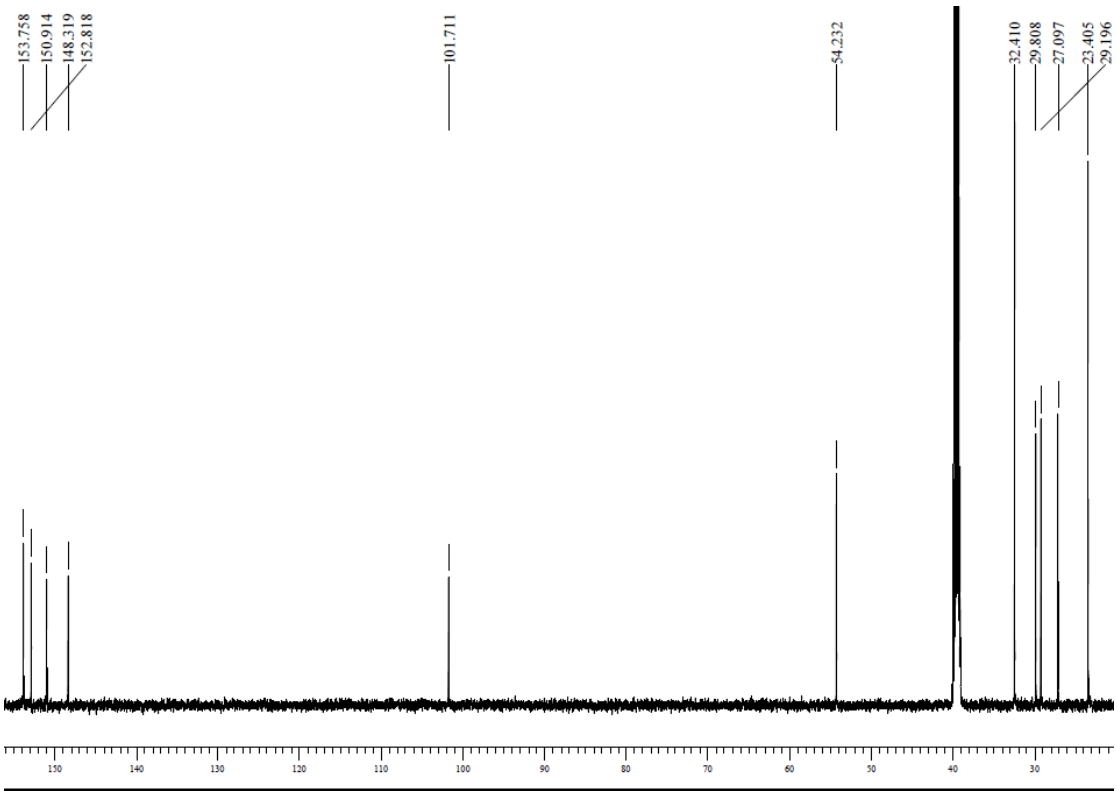

8-{[2-(2-Pyridyl)-ethyl]amino}caffeine (5g)

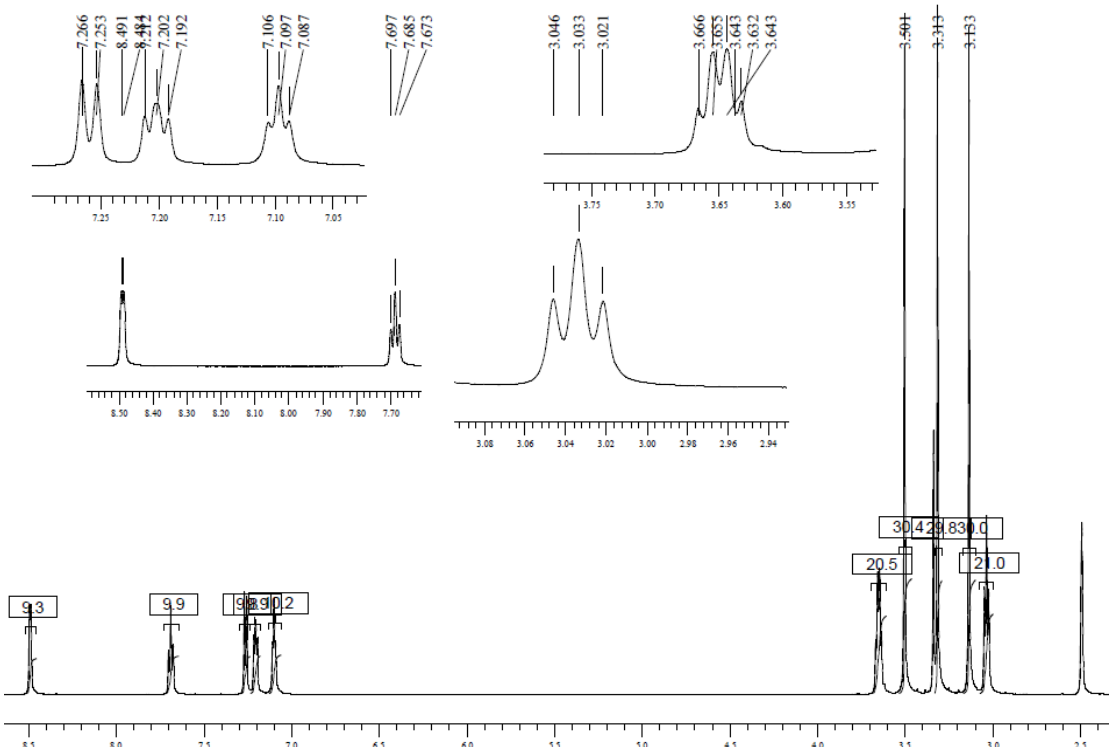

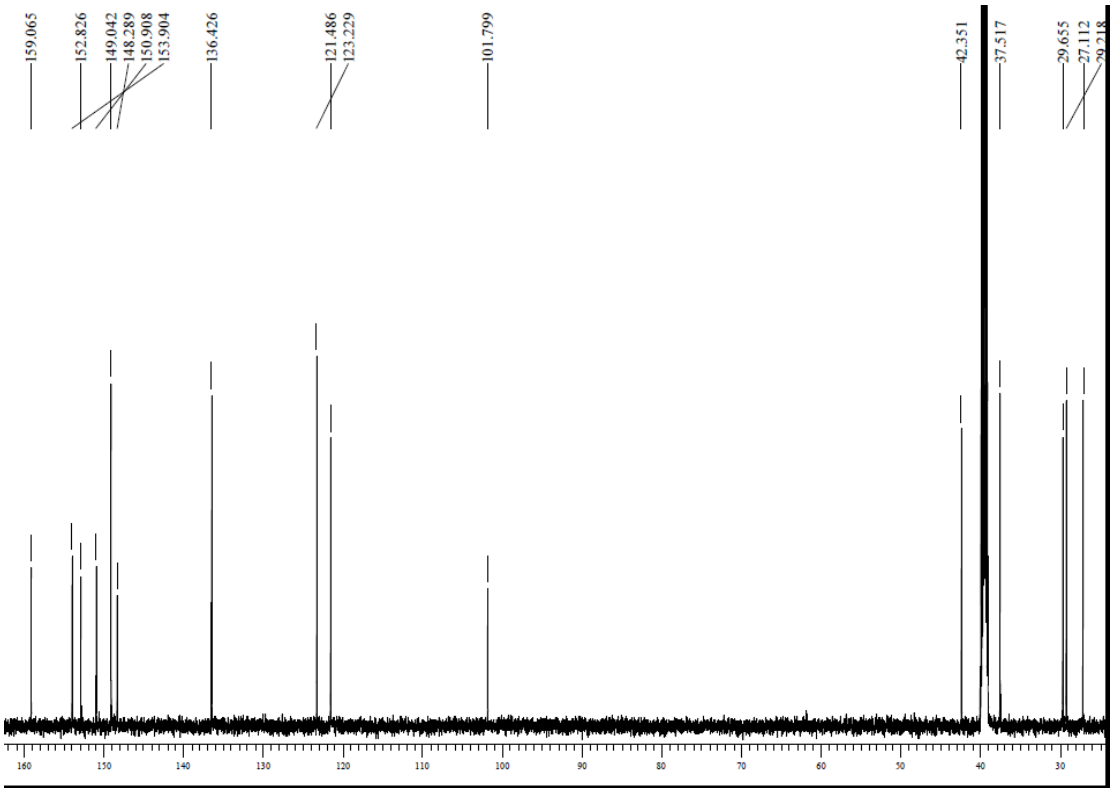

8-{[2-(3-Chlorophenyl)ethyl]amino}caffeine (5h)

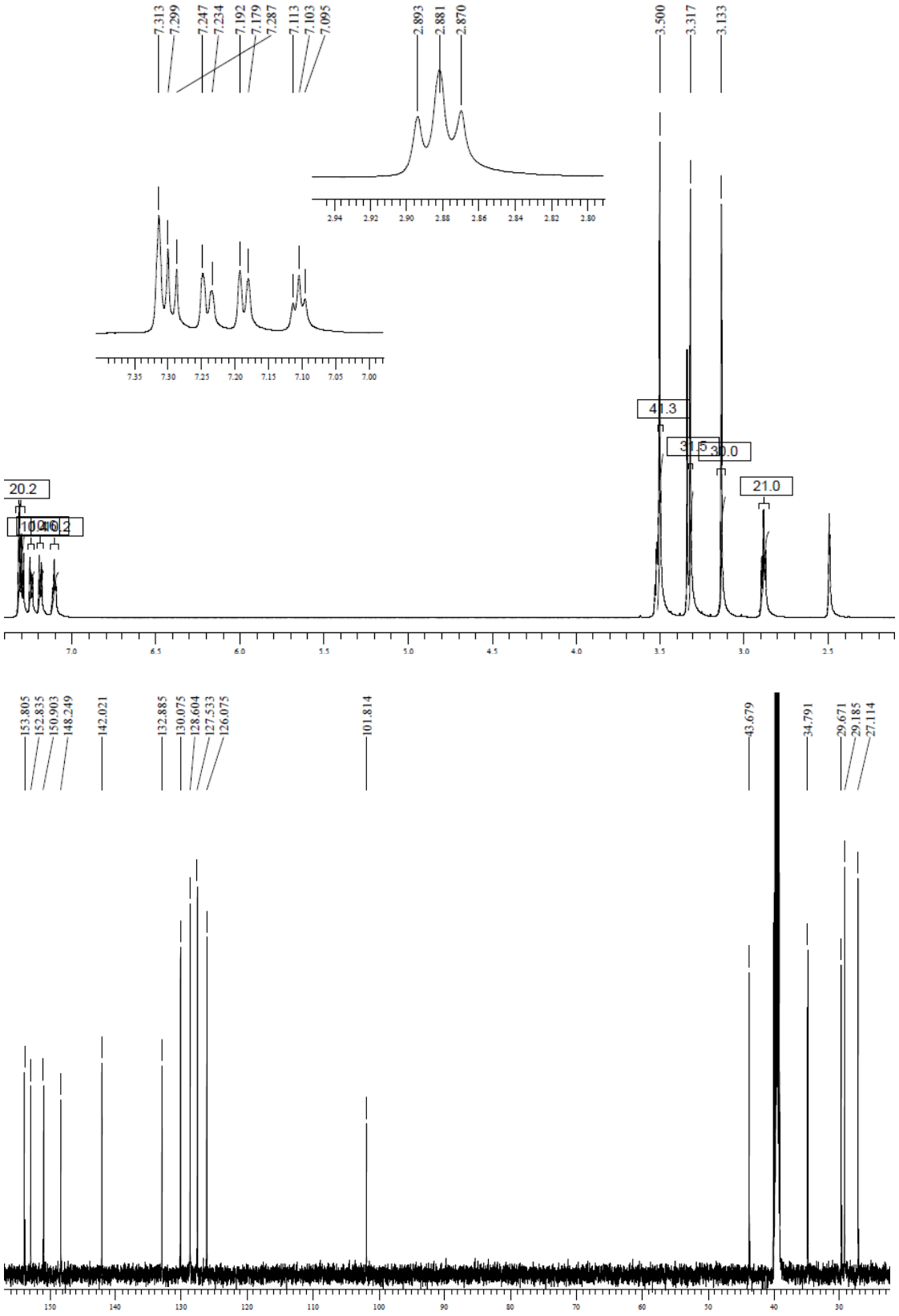

8-[Methyl(2-phenylethyl)amino]caffeine (6a)

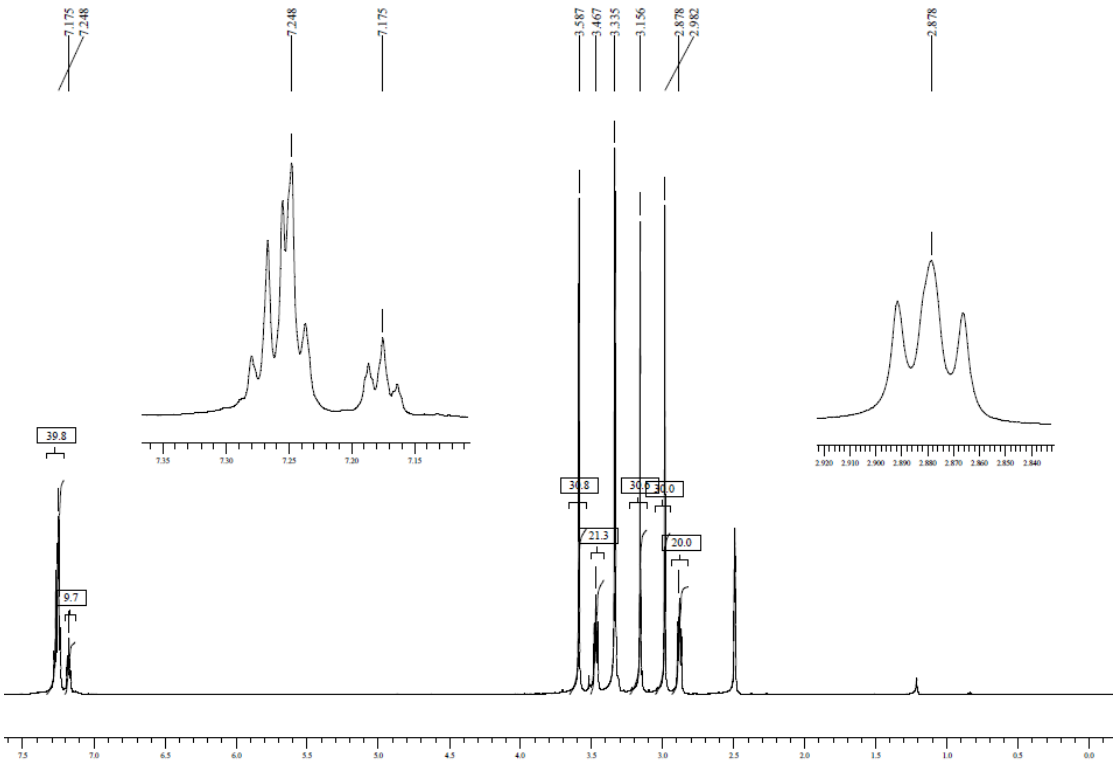

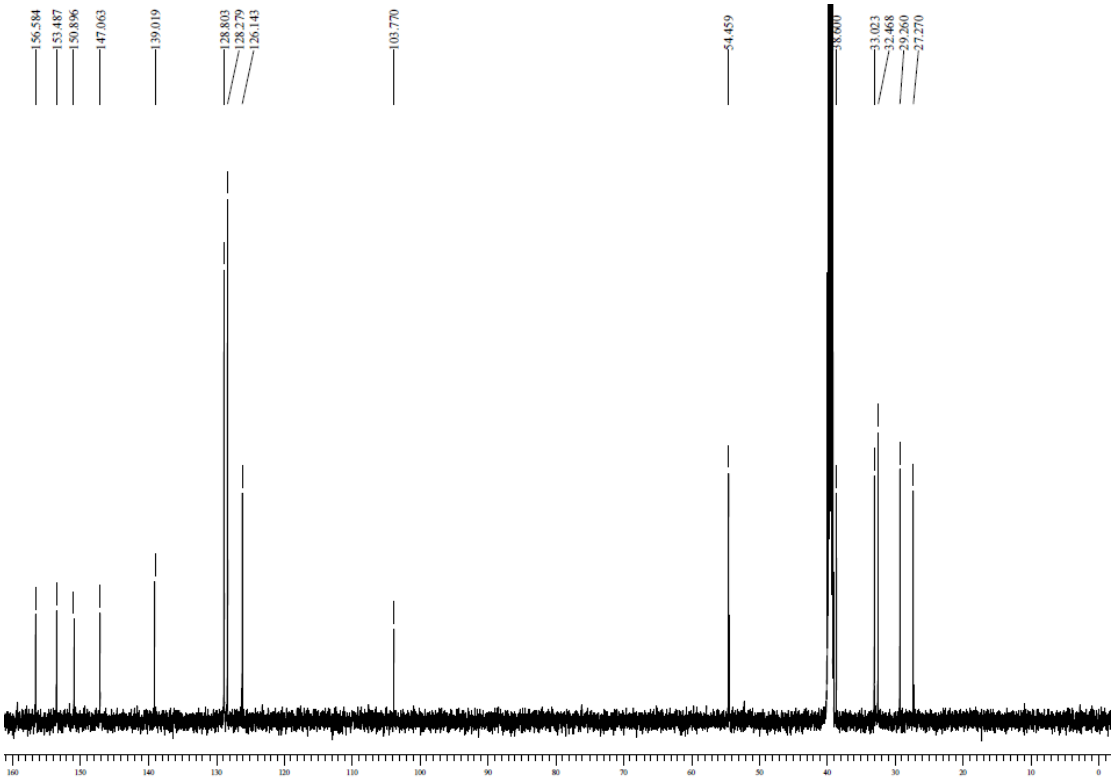

8-[Methyl(4-phenylbutyl)amino]caffeine (6b)

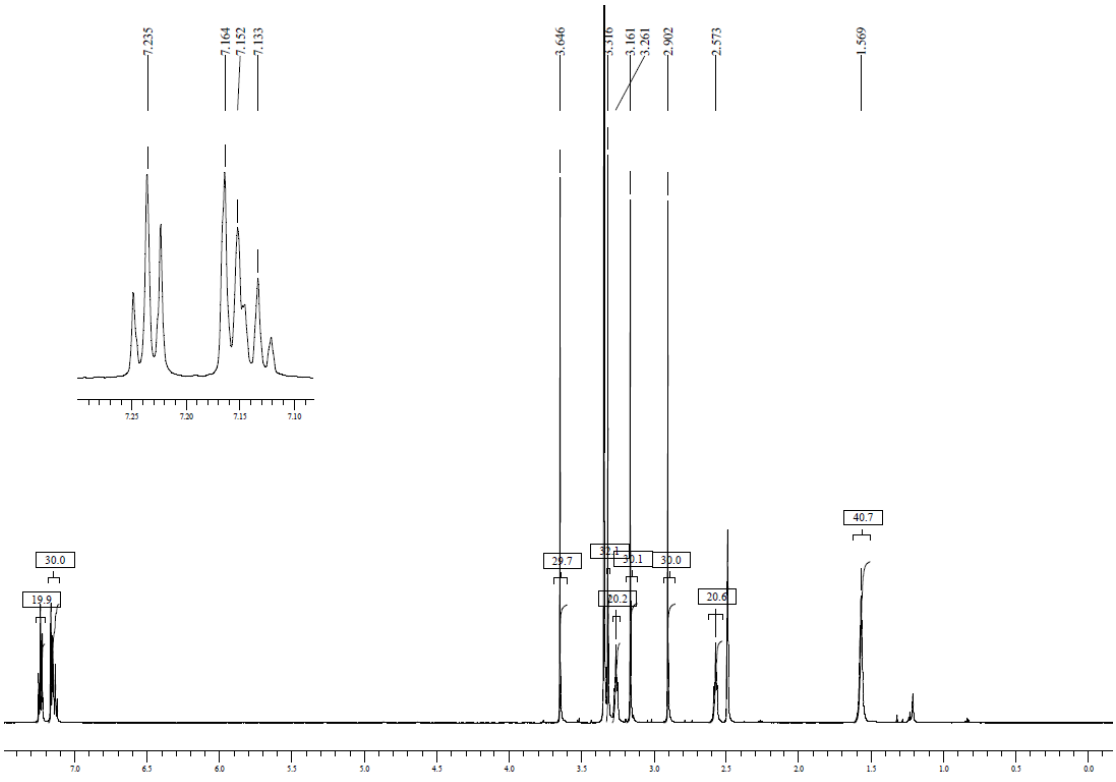

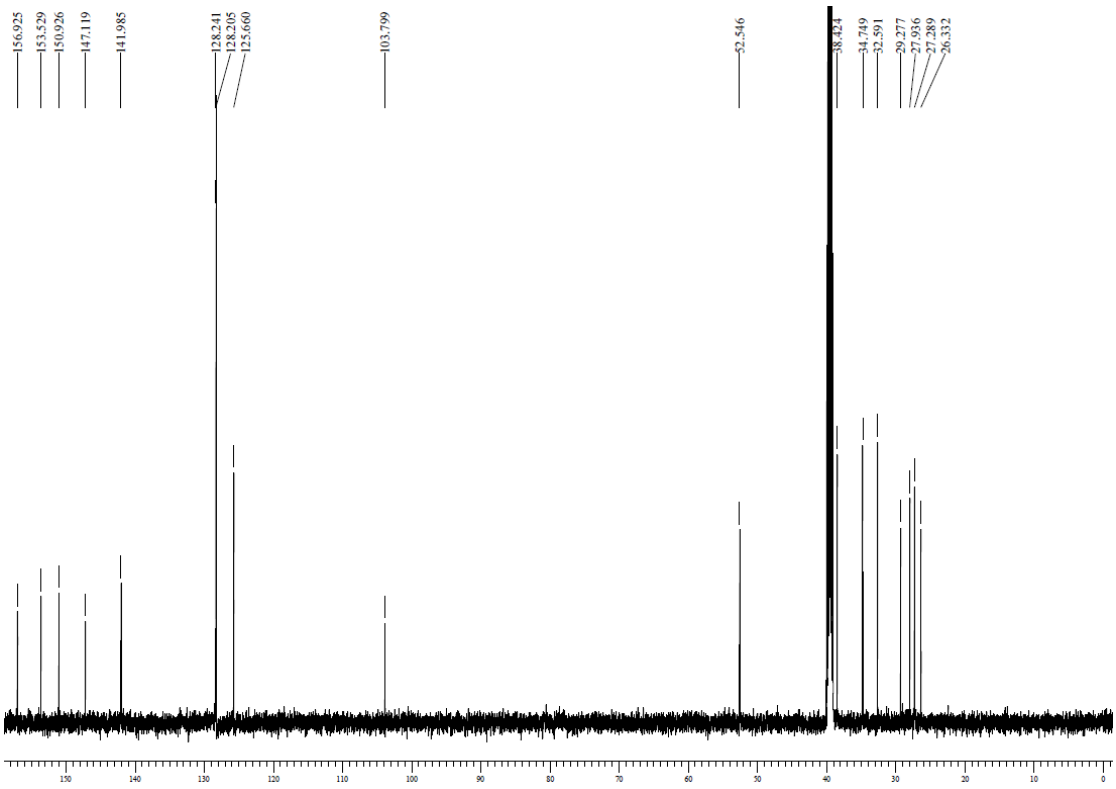

APPENDIX II

ACCEPTED ARTICLE

1 JOURNAL PUBLISHING AGREEMENT

Elsevier Ltd

1.1 Your article details

Article:	**Thio- and aminocaffeine analogues as inhibitors of human monoamine oxidase**
Corresponding author:	**Dr. Jacobus P. Petzer**
E-mail address:	**jacques.petzer@nwu.ac.za**
Journal:	**Bioorganic & Medicinal Chemistry**
Our reference	**BMC9585**
PII:	**S0968-0896(11)00845-5**
DOI:	**10.1016/j.bmc.2011.10.036**

1.2 Your Status

- I am one author signing on behalf of all co-authors of the manuscript

1.3 Data Protection & Privacy

- I do wish to receive news, promotions and special offers about products and services from Elsevier Ltd and its affiliated companies worldwide.

1.4 Assignment of publishing rights

I hereby assign toElsevier Ltdthe copyright in the manuscript identified above (government authors not electing to transfer agree to assign a non-exclusive(ADDED) licence) and any supplemental tables, illustrations or other information submitted therewith that are intended for publication as part of or as a supplement to the manuscript (the "Article") in all forms and media (whether now known or hereafter developed), throughout the world, in all languages, for the full term of copyright, effective when and if the article is accepted for publication. This transfer includes the right to provide the Article in electronic and online forms and systems. No revisions,

additional terms or addenda to this Agreement can be accepted without our express written consent. Authors at institutions that place restrictions on copyright assignments, including those that do so due to policies about local institutional repositories, are encouraged to obtain a waiver from those institutions so that the author can accept our publishing agreement.

1.5 Retention of Rights for Scholarly Purposes

I understand that I retain or am hereby granted (without the need to obtain further permission) rights to use certain versions of the Article for certain scholarly purposes, as described and defined below ("Retained Rights"), and that no rights in patents, trademarks or other intellectual property rights are transferred to the journal.

The Retained Rights include the right to use the Preprint or Accepted Author Manuscript for Personal Use, Internal Institutional Use and for ; and the Published Journal Article for Personal Use and Internal Institutional Use.

1.6 Author Representations / Ethics and Disclosure

I affirm the Author Representations noted below, and confirm that I have reviewed and complied with the relevant Instructions to Authors, the Ethics in Publishing policy, and Conflicts of Interest disclosure. For further information see the publishing ethics page at http://www.elsevier.com/publishingethics and the journal home page.

1.6.1 Author representations

- The article I have submitted to the journal for review is original, has been written by the stated authors and has not been published elsewhere.
- The article is not currently being considered for publication by any other journal and will not be submitted for such review while under review by this journal.
- The article contains no libellous or other unlawful statements and does not contain any materials that violate any personal or proprietary rights of any other person or entity.
- I have obtained written permission from copyright owners for any excerpts from copyrighted works that are included and have credited the sources in my article.
- If I am using any personal details or images of patients or research subjects, I have obtained written permission or consent from the patient (or, where applicable, the next of kin). See http://www.elsevier.com/patientphotographs for further information.

- If the article was prepared jointly with other authors, I have informed the co-author(s) of the terms of this publishing agreement and that I am signing on their behalf as their agent, and I am authorized to do so.

1.7 Funding agency and Sponsorship Options

I have also been made aware of the journal's policies with respect to funding agency requirements such as the NIH 'PublicAccess' policy, and the rapid publication 'ArticlesInPress' service. See http://www.elsevier.com/fundingbodyagreements for details.

For more information about the definitions relating to this agreement click here.

☑ **I have read and agree to the terms of the Journal Publishing Agreement.**

2nd November 2011

T-copyright-v17/2009

Thio- and aminocaffeine analogues as inhibitors of human monoamine oxidase

Hermanus P. Booysen,[a] Christina Moraal,[a] Gisella Terre'Blanche,[a] Anél Petzer,[b] Jacobus J. Bergh,[a] and Jacobus P. Petzer[a,*]

[a] *Pharmaceutical Chemistry, School of Pharmacy, North-West University, Private Bag X6001, Potchefstroom, 2520, South Africa*

[b] *Unit for Drug Research and Development, School of Pharmacy, North-West University, Private Bag X6001, Potchefstroom, 2520, South Africa*

Abstract—In a recent study it was shown that 8-benzyloxycaffeine analogues act as potent reversible inhibitors of human monoamine oxidase (MAO) A and B. Although the benzyloxy side chain appears to be particularly favorable for enhancing the MAO inhibition potency of caffeine, a variety of other C8 oxy substituents of caffeine also lead to potent MAO inhibition. In an attempt to discover additional C8 substituents of caffeine that lead to potent MAO inhibition and to explore the importance of the ether oxygen for the MAO inhibition properties of C8 oxy-substituted caffeines, a series of 8-sulfanyl- and 8-aminocaffeine analogues were synthesized and their human MAO-A and –B inhibition potencies were compared to those of the 8-oxycaffeines. The results document that the sulfanylcaffeine analogues are reversible competitive MAO-B inhibitors with potencies comparable to those of the oxycaffeines. The most potent inhibitor, 8-{[(4-bromophenyl)methyl]sulfanyl}caffeine, exhibited an IC_{50} value of 0.167 µM towards MAO-B. While the sulfanylcaffeine analogues also exhibit affinities for MAO-A, they display in general a high degree of MAO-B selectivity. The aminocaffeine analogues, in contrast, proved to be weak MAO inhibitors with a number of analogues exhibiting no binding to the MAO-A and –B isozymes. The results of this study are discussed with reference to possible binding orientations of selected caffeine analogues within the

active site cavities of MAO-A and –B. MAO-B selective sulfanylcaffeine derived inhibitors may act as lead compounds for the design of antiparkinsonian therapies.

Keywords: Monoamine oxidase; Reversible inhibition; Caffeine; Sulfanylcaffeine; Thiocaffeine; Aminocaffeine.

*Corresponding author. Tel.: +27 18 2992206; fax: +27 18 2994243;

e-mail: jacques.petzer@nwu.ac.za.

1. Introduction

The monoamine oxidases (MAO) A and B are mitochondrial bound flavin adenine dinucleotide (FAD) enzymes which catalyze the α-carbon oxidation of a variety of aminyl substrates.[1] Human MAO-A and –B consist of 529 and 520 amino acids, respectively, and the FAD is covalently bound to a cysteinyl residue in both enzymes (Cys-406 and Cys-397 in MAO-A and –B, respectively). While MAO-A and –B are products of separate genes they share approximately 70% amino acid sequence identity.[2] The X-ray crystallographic structures of MAO-A and –B indicate that the amino acid residues comprising the active sites and their relative geometries are similar with only 6 of the 16 active site amino acid residues differing between the 2 enzymes.[3,4] In spite of these similarities, MAO-A and –B have different substrate and inhibitor specificities. Most notably, MAO-A metabolizes the neurotransmitters, serotonin and norepinephrine, as well as the dietary amine, tyramine. MAO-B is well known to metabolize extraneous amines such as benzylamine and phenylethylamine. Dopamine is considered to be a substrate for both isozymes.[5]

Since MAO-A and –B are both involved in the degradation of neurotransmitter amines, inhibitors of these enzymes are employed as drugs in the treatment of several disorders.[5] For example, MAO-A inhibitors block the central oxidation of serotonin by MAO-A and are used as antidepressants. MAO-B inhibitors reduce the MAO-B catalyzed oxidative metabolism of dopamine in the brain and are used in the treatment of Parkinson's disease. Of importance is the observation that MAO-B activity and density increase in most brain

regions including the basal ganglia with age while MAO-A activity remains unchanged.[6,7] In the aged parkinsonian brain MAO-B is therefore thought to be the principal MAO isozyme responsible for dopamine catabolism. MAO-B inhibitors may conserve dopamine in the basal ganglia and offer a symptomatic benefit in the treatment of Parkinson's disease.[8–10] MAO-B inhibitors are frequently combined with levodopa therapy since inhibitors of this enzyme have been shown to enhance the elevation of dopamine levels derived from levodopa.[11] MAO-B inhibitors may permit a reduction of the dose of levodopa required for a therapeutic effect and therefore the occurrence of levodopa associated side effects.[12] MAO may also play an important role in the neurodegenerative processes associated with Parkinson's disease. The oxidation of dopamine by MAO stoichiometrically yields potentially toxic metabolic by-products.[13] For each mole of dopamine oxidized by MAO, one mole of hydrogen peroxide (which may lead to oxidative damage) and dopaldehyde (which may react with exocyclic amino groups of nucleosides and N-terminal and lysine ε-amino groups of proteins) are formed.[13] Inhibitors of MAO reduce the MAO-catalyzed metabolism of DA and as a result reduce the formation of these toxic by-products. MAO inhibitors are therefore considered as a potential treatment strategy to slow the progression of Parkinson's disease since they may exert neuroprotective effects in the brain.[13]

Based on the therapeutic value of MAO inhibitors the current study aims to discover new reversible inhibitors of the MAO enzymes, particularly the B isozyme. For this purpose caffeine (**1**) serve as lead compound (Fig. 1). Although caffeine is a weak MAO-B inhibitor (K_i = 3.6 mM), substitution at the C8 position with a variety of substituents has been shown to enhance the MAO-B inhibition potency of caffeine to a large degree.[14] In previous studies it was shown that substitution at C8 of caffeine with alkyloxy substituents (**2**) yielded particularly potent MAO-B inhibitors with a number of compounds exhibiting IC_{50} values in the nM range.[15,16] Interestingly these oxycaffeines are also MAO-A inhibitors, a property that may be attributed to the relatively large degree of rotational freedom of the C8 side chain at the carbon-oxygen ether bond. It has been suggested that structures with a relatively larger degree of conformational freedom may be better suited for binding to MAO-A than relatively rigid structures.[15] Based on these promising results the present study investigates the possibility that alkylsulfanyl and alkylamino substituents at C8 of caffeine may similarly enhance the MAO-A and –B inhibition potency of caffeine. For this purpose, a series of twelve aryl- and alkylsulfanylcaffeine analogues (**3a**–**l**) and ten aryl- and alkylaminocaffeine analogues (**4a**–**h**, **5a**–**b**) were synthesized and evaluated as potential inhibitors of recombinant human MAO-A and –B (Fig. 2 and Tables 1–3).

2. Results

2.1. Chemistry

The aryl- and alkylsulfanylcaffeine analogues (**3a**–**l**) were synthesized by reacting 8-chlorocaffeine (**6**) with an appropriate thiol reagent (**7**) in the presence of NaOH and employing a mixture of ethanol and water as reaction solvent (Scheme 1).[17] The aryl- and alkylaminocaffeine analogues (**4a**–**h**) were similarly prepared by reaction of an appropriate amine reagent (**8**) with 8-chlorocaffeine but with the exception that the addition of base and additional solvent were not required (Scheme 2).[18] Methylation of **4c** and **4e** at the C8 amine to yield methylamino caffeine analogues **5a** and **5b**, respectively, were carried out in DMSO using CH_3I as alkylating agent and KOH as base. The structures of all the target compounds were verified by ^{1}H NMR, ^{13}C NMR and mass spectrometry. The purities of the compounds were estimated by HPLC analysis.

2.2. Inhibition of MAO-A and –B

The MAO inhibition potencies of the sulfanylcaffeine (**3a**–**l**) and aminocaffeine analogues (**4a**–**h**, **5a**–**b**) were examined by employing the recombinant human MAO-A and –B enzymes as enzyme sources.[19] The mixed MAO-A/B substrate, kynuramine, was used as substrate for the inhibition studies of both MAO-A and –B. Kynuramine displays similar K_m values towards the two enzymes with values of 16.1 µM and 22.7 µM for MAO-A and –B, respectively.[15] The MAO-catalyzed oxidation of kynuramine yields 4-hydroxyquinoline, a fluorescent compound which is readily measured in basic solutions at excitation and emission wavelengths of 310 nm and 400 nm, respectively. Neither the substrate nor the test inhibitors fluoresce under these conditions, or quench the fluorescence of 4-hydroxyquinoline. The inhibition potencies of the sulfanylcaffeine and aminocaffeine analogues are expressed as the IC_{50} values which were determined from sigmoidal dose-response curves constructed in triplicate from 6 different inhibitor concentrations spanning at least 3 orders of a magnitude.

*2.2.1. MAO inhibition by sulfanylcaffeine analogues (**3a–l**)*

The MAO inhibition potencies of the sulfanylcaffeine analogues (**3a–l**) are presented in table 1. As shown by the selectivity index (SI) values, the sulfanylcaffeine analogues are selective inhibitors of MAO-B. The only exceptions are **3k** which displays slight selectivity for the MAO-A isozyme and **3l** which is essentially nonselective. 8-(Phenylsulfanyl)caffeine (**3a**) which displays slight selectivity for MAO-B, was found to be a relatively weak inhibitor of both MAO-A and –B. Extension of the C8 side chain by one methylene unit to yield the benzylsulfanyl homologue **3b** (IC_{50} = 1.86 µM) enhances the MAO-B inhibition potency 17-fold compared to **3a** (IC_{50} = 33.2 µM). A further increase in the length of the C8 side chain yields even more potent MAO-B inhibitors. For example, compounds **3c** and **3d**, the phenylethylsulfanyl and phenoxyethylsulfanyl homologues exhibited IC_{50} values of 0.223 µM and 0.332 µM, respectively. While the extension of the C8 side chain of **3a** (IC_{50} = 56.4 µM) by one methylene unit to yield **3b** (IC_{50} = 8.22 µM) also results in improved MAO-A inhibition, further increasing the length of the C8 side chain does not result in a further enhancement of inhibition activity. For example, **3c** (IC_{50} = 20.5 µM) and **3d** (IC_{50} = 15.5 µM) are weaker MAO-A inhibitors than the benzylsulfanyl homologue **3b** (IC_{50} = 8.22 µM).

Interestingly, halogen substitution of the phenyl ring of the C8 side chain is also associated with an increase in MAO-B inhibition potency. The benzylsulfanyl substituted caffeine homologues containing chlorine (**3e**; IC_{50} = 0.192 µM), bromine (**3f**; IC_{50} = 0.167 µM) and fluorine (**3g**; IC_{50} = 0.348 µM) on the benzyl phenyl ring were found to be 5–11-fold more potent than the corresponding unsubstituted homologue **3b** (IC_{50} = 1.86 µM). Methoxy substitution of the phenyl ring of 8-(benzylsulfanyl)caffeine, in contrast, is associated with a loss of both MAO-A and –B inhibition activity. Halogen substitution of 8-(benzylsulfanyl)caffeine (**3b**) also enhances MAO-A inhibition potency, although by a lesser degree compared to MAO-B. The homologues containing chlorine (**3e**; IC_{50} = 2.77 µM), bromine (**3f**; IC_{50} =2.62 µM) and fluorine (**3g**; IC_{50} = 4.80 µM) on the benzyl phenyl ring are 1.7–3-fold more potent than the corresponding unsubstituted homologue **3b** (IC_{50} = 8.22 µM).

The results document that compound **3i**, the sulfanylcaffeine analogue containing a branched alkyl side chain at C8, is also a relatively good MAO-B inhibitor with an IC_{50} value of 2.62 µM. In fact, **3i** is approximately 12-fold more potent as an MAO-B inhibitor than was

8-(phenylsulfanyl)caffeine (**3a**) which contains a C8 phenylsulfanyl side chain. This result demonstrates that a ring system in the C8 side chain is not an absolute requirement for MAO-B inhibition by sulfanylcaffeine analogues. In accordance with this view, compound **3i** also proved to be more potent as a MAO-B inhibitor than the sulfanylcaffeine analogues containing cyclohexyl (**3j**), cyclopentyl (**3k**) and napthalenyl (**3l**) C8 side chains. Interestingly the sulfanylcaffeine analogues containing cyclohexyl (**3j**), cyclopentyl (**3k**) and napthalenyl (**3l**) C8 side chains were more potent inhibitors of both MAO-A and –B than the phenyl substituted analogue **3a**. This result suggests that, with the appropriate structural modification, these moieties may be suitable for the future design of sulfanylcaffeine derived MAO inhibitors. An example of such a structural modification would be the extension of the length of the C8 side chain. Based on the observations that the naphthalenyl substituted sulfanylcaffeine analogue **3l** is 15- and 9-fold more potent as a MAO-A and –B inhibitor, respectively, than the phenyl substituted sulfanylcaffeine analogue **3a** and that **3l** is a nonselective inhibitor, the naphthalenyl moiety may be particularly suited for the design of sulfanylcaffeine derived mixed MAO-A/B inhibitors.

*2.2.2. MAO inhibition by aminocaffeine analogues (**4a**–**h**, **5a**–**b**)*

The MAO inhibition potencies of the aminocaffeine analogues **4a**–**h** are presented in tables 2 and 3. The data show that these compounds were relatively weak inhibitors of both MAO-A and –B with IC_{50} values ranging from 5.78–45.2 µM and 9.60–24.4 µM for the inhibition of MAO-A and –B, respectively. In fact, several of the compounds exhibited no binding to the MAO-A and –B isozymes. Even homologues containing extended C8 side chains such as **4d** (-NH-$(CH_2)_3$-C_6H_5) and **4e** (-NH-$(CH_2)_4$-C_6H_5) did not exhibit potent MAO inhibition. Similarly, homologue **4g** which contains a halogen on the phenyl ring of the C8 side chain was found to be a relatively weak MAO inhibitor. These results demonstrate that, in contrast to the sulfanylcaffeine analogues, extension of the length of the C8 side chain and halogen substitution do not lead to potent MAO-B inhibition by the aminocaffeine analogues. Compared to the sulfanylcaffeine analogues, the aminocaffeine analogues are therefore weak MAO-B inhibitors. For example, sulfanylcaffeine analogue **3c** (IC_{50} = 0.223 µM) is 78-fold more potent as an MAO-B inhibitor than its corresponding aminocaffeine homologue **4c** (IC_{50} = 17.6 µM).

To investigate the possibility of enhancing the MAO inhibition potencies of the aminocaffeines, selected analogues, **4c** and **4e**, were methylated at the C8 amine to yield compounds **5a** and **5b**, respectively. While methylation improved the MAO-B inhibition potency of **4e** by approximately 3-fold, MAO-A inhibition activity was slightly reduced. Methylation of **4c** did not result in a significant improvement of MAO-B inhibition potency and led to a reduction in MAO-A inhibition. Compared to the sulfanylcaffeine analogues, the aminocaffeine analogues are also weak MAO-B inhibitors. For example, sulfanylcaffeine analogue **3c** (IC_{50} = 0.223 µM) is 75-fold more potent than its methylaminocaffeine homologue **5a** (IC_{50} = 16.8 µM). It is noteworthy that the most potent MAO-B inhibitor among the aminocaffeine analogues was the C8 methylated derivative **5b** with an IC_{50} value of 2.97 µM. It can therefore be concluded that while methylation of the C8 amine of aminocaffeine analogues may result in enhanced MAO-B inhibition potency, the resulting compounds remain relatively weak inhibitors compared to the sulfanylcaffeine analogues.

2.3. Reversibility of MAO-A and –B inhibition

Based on the nature of the interactions with the MAO enzymes, inhibitors may be classified as reversible or irreversible. Irreversible inhibitors normally form covalent interactions with the enzymes while reversible inhibitors bind via intermolecular interactions. While irreversible inhibitors of MAO have been clinically used for many years, this mode of inhibition may be associated with certain shortcomings.[20] These include a slow and variable recovery of enzyme activity following withdrawal of the irreversible inhibitor.[21] The turnover rate for the biosynthesis of MAO-B in the human brain may be as much as 40 days.[22] In contrast, enzyme activity is regained relatively quickly following withdrawal of a reversible inhibitor, once the inhibitor is cleared from the tissues. Based on these observations, the reversibility of MAO-A and –B inhibition by the sulfanylcaffeine and aminocaffeine analogues was examined. For this purpose the time-dependency of the inhibition of MAO-A and –B, respectively, by sulfanylcaffeine analogue **3f** was measured. The time-dependency of the inhibition of MAO-A and –B by aminocaffiene analogues **4g** and **5b**, respectively, was also examined. While irreversible inhibitors would lead to a time-dependent reduction of enzyme activity, the degree of enzyme inhibition in the presence of a reversible MAO inhibitor remains unchanged irrespective of the time for which the inhibitor is incubated with the enzyme.[23]

The test inhibitors, at concentrations of approximately 2-fold their measured IC_{50} values for the inhibition of the respective MAO enzymes, were preincubated with recombinant human MAO-A or –B for time periods of 0, 15, 30 and 60 min. Following these preincubations the residual MAO catalytic activities were measured after the addition of the substrate, kynuramine. The results of these reversibility studies are presented in figures 3 and 4. The graphs show that when **3f** and **4g** are preincubated with MAO-A and **3f** and **5b** are preincubated with MAO-B there are no time-dependent reductions of MAO-A and –B catalytic activities. Even after a period of 60 min the test compounds do not reduce the MAO catalytic rates. These results suggest that the test caffeines are not time-dependent inhibitors of MAO-A and –B and interact reversibly, at least for the time period (0–60 min) and at the inhibitor concentrations ($2 \times IC_{50}$) evaluated.

This study also examined the possibility that **3f** may act as a competitive inhibitor of human MAO-A and –B. For this purpose, sets of Lineweaver–Burk plots were constructed for the inhibition of these enzymes by **3f**. The initial catalytic rates of MAO-A or –B were measured in the absence and presence of three different concentrations of **3f**. These measurements were carried out using four different concentrations of the substrate, kynuramine (15–90 μM). The Lineweaver–Burk plots obtained from these experiments are shown in figure 5. The graphs show that the Lineweaver–Burk plots constructed for the inhibition of MAO-A and –B are linear and intersect at the y-axis. This indicates that the inhibition of the MAO enzymes by **3f** is competitive. This result is further support that **3f** is a reversible MAO inhibitor.

2.4. Molecular modeling

The results of the MAO inhibition studies shows that among the sulfanylcaffeine analogues evaluated here, several compounds act as potent reversible inhibitors of MAO-B with IC_{50} values in the nM range. Interestingly, extension of the length of the C8 side chain leads to enhanced MAO-B inhibition potency. While the sulfanylcaffeine analogues are also MAO-A inhibitors, they display, for the most part, selectivity for the MAO-B isozyme. In contrast to the sulfanylcaffeine analogues, the aminocaffeine analogues were found to be weak MAO-B inhibitors with many analogues exhibiting no binding to either MAO-A or B. To provide additional insight, the predicted binding modes of selected analogues (**3a–c** and **4c**) in the active site cavities of MAO-A and –B were examined using molecular docking.

The docking studies were carried out using the LigandFit application of the Discovery Studio modeling software (Accelrys) according to a previously reported protocol.[23] As enzyme models, the three-dimensional structures of human MAO-A cocrystallized with harmine (PDB entry: 2Z5X)[3] and human MAO-B cocrystallized with safinamide (PDB entry: 2V5Z)[4] were selected. The enzyme models were prepared by calculating the protonation states of the ionizable residues and adding the hydrogen atoms accordingly. After the valences of the FAD cofactor and cocrystallized ligands were corrected, hydrogen atoms were added and the models were subjected to an energy minimization cascade while the protein backbone was constrained. For the purpose of the docking, only the crystal waters which are reported to be conserved and non-displaceable were retained (see Experimental).[3,4]

The best ranked docking solution for the binding of the selected analogues (**3a–c** and **4c**) to MAO-B shows one prevailing orientation for all of the inhibitors. As shown by the binding orientation of **3c**, the caffeine ring binds within the substrate cavity of MAO-B, in close proximity to the FAD cofactor (Fig. 6). This places the carbonyl oxygen at C2 of the caffeine ring 3.4 Å from the flavin N5 and the carbonyl oxygen at C6 within hydrogen bond distance to the phenolic hydrogen of Tyr-435. The caffeine ring also forms a potential π–π interaction with the aromatic ring of Tyr-398. The region defined by the flavin isoalloxazine ring, Tyr-398 and Tyr-435 is the only polar space of the MAO-B active site and is also the site where amine catalysis occurs.[24] In the MAO-B model selected for these studies, the side chain of Ile-199 is rotated into an alternative conformation to allow for the fusion of the substrate and entrance cavities.[25] This rotation of the Ile-199 side chain from the active site cavity is essential for relatively large inhibitors, such as safinamide and C8 substituted caffeine derivatives, to be able to bind to MAO-B. As a result the phenylethyl C8 side chain of **3c** is allowed to extend into the hydrophobic entrance cavity where it may be stabilized via Van der Waals interactions. As expected, the relatively shorter phenyl (**3a**) and benzyl (**3b**) C8 side chains of sulfanylcaffeine homologues **3a** and **3b** do not extend as deep into the MAO-B entrance cavity as the side chain of **3c**, and may therefore undergo interactions with the entrance cavity to a lesser extent compared to **3c** (Fig. 7). Despite the similar binding orientations of **3a** and **3b** within the MAO-B active site, **3b** was found to be a 17-fold more potent inhibitor. Since **3b** protrudes only slightly deeper (by ~1.2 Å) into the entrance cavity compared to **3a**, this result suggest that a relatively small enhancement of the space occupied by an inhibitor in the entrance cavity leads to a large increase in binding affinity.

Another possible explanation may be that the larger degree of conformational freedom afforded by the longer C8 side chain of **3b** may facilitate improved interaction with the entrance cavity. The view that interaction with the entrance cavity is essential for high affinity inhibitor binding is supported by the observation that caffeine is a weak MAO-B inhibitor.[14] Lacking a C8 side chain, caffeine is expected to bind only within the substrate cavity and is unable to interact with the entrance cavity. The lower MAO-B inhibition potencies of **3a** and **3b** compared to compound **3c** may thus be explained by weaker interaction with the entrance cavity.

Interestingly the aminocaffeine analogue **4c** adopts a similar binding mode to that described above for **3c** and as a result forms similar interactions with the MAO-B active site (Fig. 8). The only additional interaction that may occur between **4c** and MAO-B is a potential hydrogen bond between the C8 amine and the phenolic group of Tyr-326. The results of the MAO inhibition studies however documents that the aminocaffeine analogues are weak MAO-B inhibitors with **4c** being 78-fold weaker than the corresponding sulfanylcaffeine homologue **3c**. The docking studies therefore suggest that differing binding orientations cannot account for the apparent loss of MAO-B inhibition activity of the aminocaffeine analogues.

The predicted binding orientation of **3c** within the active site of MAO-A is similar to the binding orientation observed in MAO-B with the caffeine ring bound in close proximity to the FAD cofactor and the C8 side chain extending towards the entrance of the active site (Fig. 9). Interestingly, the caffeine ring is rotated by ~180 ºC compared to the binding orientation adopted in the MAO-B active site. This dissimilarity in binding orientations in the MAO-A and –B active sites has also been observed in docking studies with 8-benzyloxycaffeine analogues.[15] As a result of the flipped orientation of the caffeine ring, the C2 carbonyl oxygen is within hydrogen bond distance of the phenolic hydrogen of Tyr-444 and two active site waters. Also, the caffeine ring of **3c** binds more distant from Tyr-407 (~4.3 Å) in MAO-A than from the corresponding residue, Tyr-398 (~3.6 Å), in MAO-B. For this reason, a π–π interaction similar to that observed between the caffeine ring and Tyr-398 in MAO-B, is not observed between **3c** and the MAO-A active site. This may represent a possible reason for the finding that sulfanylcaffeine analogues are in general more potent MAO-B inhibitors than MAO-A inhibitors. Also noteworthy is the observation that, in the MAO-A active site, the C8

side chain of **3c** is bent at the CH_2-S thioether bond from the plane of the caffeine ring while in the MAO-B active site, the side chain of **3c** exhibits a modest deviation from the plane of the caffeine ring (Fig. 10). The differing binding orientations adopted by C8 substituted caffeine derivatives in MAO-A and –B may, for the most part, be attributed to steric hindrance caused by the aromatic moieties of Phe-208 in MAO-A and Tyr-326 in MAO-B. As illustrated in figure 11A, the binding orientation and position of **3c** in the MAO-B active site cannot be reproduced in MAO-A because this would result in structural overlap with the phenyl ring of Phe-208. In MAO-B, the amino acid residue that occupies the same position as Phe-208 in MAO-A is Ile-199. In MAO-B the side chain of Ile-199 may rotate out of the active site cavity to allow for the observed binding pose of **3c**.[25] Similarly, the binding orientation and position of **3c** in the MAO-A active site cannot be reproduced in MAO-B because of structural overlap with of Tyr-326 (Fig. 11B). In MAO-A, the amino acid residue that occupies the analogous position as Tyr-398 in MAO-B is Ile-335. The relatively smaller side chain of Ile-335 compared to the aromatic ring of Tyr-398, does not sterically prevent the observed binding orientation of **3c** in the MAO-A active site.[3]

3. Discussion

Based on previous reports that oxycaffeine analogues are MAO inhibitors,[15,16] the present study investigated the possibility that C8 substituted sulfanylcaffeine and aminocaffeine analogues may also act as inhibitors of human MAO-A and –B. The results demonstrated that several of the sulfanylcaffeine analogues act as potent MAO-B inhibitors and that the inhibition is reversible. For example, the bromine substituted sulfanylcaffeine analogue **3f** was the most potent MAO-B inhibitor with an IC_{50} value of 0.167 µM. The relatively high MAO-B inhibition potencies of the sulfanylcaffeine analogues may be evaluated by comparison of the IC_{50} value of **3f** (IC_{50} = 0.167 µM.) with the reversible inhibitor safinamide, which binds to MAO-B with an IC_{50} value of 0.08 µM.[4] While the sulfanylcaffeine analogues are also MAO-A inhibitors, they are for the most part selective for the MAO-B isoform. Modeling studies predict that the sulfanylcaffeine analogues adopt dissimilar binding modes in the MAO-A and –B active site cavities, respectively. Compared to the predicted orientation in MAO-B, the caffeine ring is flipped by approximately 180 º in the MAO-A active site which results in differing interactions of the caffeine ring with the polar regions of the MAO-A and –B substrate cavities. The alternative binding orientation of the caffeine ring in MAO-A may be less optimal for the formation of stabilizing polar interactions compared to the binding orientation adopted in MAO-B and may explain, at least in part, the lower binding affinities of

the sulfanylcaffeine analogues to MAO-A.[15] Interestingly, modeling studies suggest that the C8 side chain of the sulfanylcaffeine analogue **3c** is bent to a high degree from the plane of the caffeine ring at the CH_2-S thioether bond while in the MAO-B active site, the C8 side chain displays only a modest deviation from the plane of the caffeine moiety. The ability of the C8 side chain to adopt a bent orientation may be an important requirement for the inhibition of MAO-A. Rigid C8 substituted caffeine analogues such as (E)-8-(3-chlorostyryl)caffeine (CSC) (Fig. 12) are not MAO-A inhibitors while displaying high affinity binding to MAO-B.[26] The observation that CSC does not bind to MAO-A may be explained by its low degree of flexibility and inability to adopt a bent orientation similar to that observed for **3c** in the MAO-A active site.

The notion that the C8 side chains of the caffeine analogues are important structural features for MAO-A and –B inhibition is supported by the observation that caffeine is a weak MAO inhibitor.[14] Modeling shows that, in the MAO-B active site, the C8 side chains of the sulfanylcaffeine analogues may extend into the hydrophobic entrance cavity where they are stabilized by Van der Waals interactions. Since extension of the C8 chain length results in enhanced MAO-B inhibition potency it may be concluded that longer C8 side chains form more productive interactions with the MAO-B entrance cavity, which thus leads to more potent enzyme inhibition. Halogen substitution on the phenyl ring of the C8 side chain also leads to a significant enhancement of MAO-B inhibition. This result may be explained by the possibility that halogen substitution may further improve Van der Waals and dipole interactions between the MAO-B entrance cavity and the C8 side chain. While it is not clear why methoxy substitution of 8-(benzylsulfanyl)caffeine leads to a loss of both MAO-A and –B inhibition potency, this result is in accordance with the findings of a previous study which showed that MAO-B inhibition potencies of a series of benzyloxycaffeine analogues correlate with the electronegativity of substituents on the phenyl ring of the C8 side chain and that electron-withdrawing groups enhance MAO-B inhibition potency.[15] Interestingly, this study shows that C8 side chains that do not contain phenyl rings are also suitable for MAO inhibition. Examples of sulfanylcaffeine analogues containing such side chains are the 3-methylbutyl (**3i**), cyclohexyl (**3j**), cyclopentyl (**3k**) and napthalenyl (**3l**) substituted homologues.

One of the most significant findings of this study is that the aminocaffeine analogues are weak MAO inhibitors with most homologues displaying no inhibition. The predicted binding orientation and interactions of aminocaffeine analogue **4c** in the MAO-B active site is similar to the orientation of sulfanylcaffeine analogue **3c**. In fact **4c** displays an additional hydrogen bond interaction with Tyr-326. In spite of these predictions **4c** is approximately 78-fold weaker as a MAO-B inhibitor compared to **3c**. Even methylation of the C8 amines to yield tertiary amines does not produce inhibitors with similar potencies to those of the sulfanylcaffeine analogues. While the reasons for this behavior is not clear, differing ionization states of the sulfanylcaffeine and aminocaffeine analogues do not explain the difference in binding affinities to the MAO enzymes, since both the sulfanylcaffeine and aminocaffeine analogues are expected to be uncharged in the buffer used for the inhibition studies (pH 7.4). Also, it is unlikely that aminocaffeines are excluded from entering the access channel leading to the active site cavity since aminyl substrates are thought to be deprotonated prior to entering the MAO active sites.[24]

In conclusion, the sulfanylcaffeine analogues exhibit similar MAO-B inhibition potencies to those of the previously reported oxycaffeine analogues with various homologues from both series exhibiting IC_{50} values in the nM range.[15,16] The attachment of substituents at C8 of caffeine via a thioether linkage therefore enhances MAO-B inhibition activity to a similar extent compared to attachment via an oxyether. In contrast, C8 substituted aminocaffeines are not suitable for MAO inhibition. Based on the potent MAO-B inhibition properties of the sulfanylcaffeine analogues, they may be considered as lead compounds for the development of reversible MAO-B inhibitors.

4. Experimental section

4.1. Chemicals and instrumentation

Unless otherwise noted, all starting materials were obtained from Sigma-Aldrich and were used without purification. Proton (^{1}H) and carbon (^{13}C) NMR spectra were recorded on a Bruker Avance III 600 spectrometer at frequencies of 600 MHz and 150 MHz, respectively. All NMR measurements were conducted in $CDCl_3$ and DMSO-d_6 and the chemical shifts are reported in parts per million (δ) downfield from the signal of tetramethylsilane added to the deuterated solvent. Spin multiplicities are given as s (singlet), d (doublet), dd (doublet of

doublets), t (triplet), q (quartet), qn (quintet), sept (septet) or m (multiplet). High resolution mass spectra (HRMS) were obtained on a Waters Synapt G2 instrument in electrospray ionization (ESI) mode. The HRMS spectrum of **4a** was recorded on a DFS high resolution magnetic sector mass spectrometer (Thermo Electron Corporation) in atmospheric pressure chemical ionization (APCI) mode. Melting points (mp) were measured with a Stuart SMP10 melting point apparatus and are uncorrected. The purity of the synthesized compounds were determined via HPLC analyses which were conducted with an Agilent 1100 HPLC system equipped with a quaternary gradient pump and an Agilent 1100 series diode array detector (see Supplementary Material). HPLC grade acetonitrile (Merck) and Milli-Q water (Millipore) were used for the chromatography. For fluorescence spectrophotometry, a Varian Cary Eclipse fluorescence spectrophotometer was employed. Microsomes from insect cells containing recombinant human MAO-A and –B (5 mg/mL) and kynuramine.2HBr were obtained from Sigma-Aldrich.

4.2. Synthesis of C8-substituted thiocaffeine analogues (**3a–l**)

A solution of NaOH (4 mmol) in 3.5 mL water and 7 mL ethanol was cooled in an ice bath and the appropriate thiol (4 mmol) was added. The reaction mixture was stirred and 8-chlorocaffeine (4 mmol) was added in a single portion to yield a suspension. The reaction was heated under reflux for 60 min and then cooled on ice. The white precipitate was collected by filtration and washed with 30 mL ethanol. The product was recrystallized from 30 mL ethanol at room temperature and the crystals were washed with 30 mL ethanol.[17]

4.2.1. **8-(Phenylsulfanyl)caffeine (3a)**

The title compound was prepared from thiophenol in a yield of 65.1%: mp 149 °C (ethanol). ^{1}H NMR (Bruker Avance III 600, $CDCl_3$) δ 3.37 (s, 3H), 3.54 (s, 3H), 3.90 (s, 3H), 7.32 (m, 5H); ^{13}C NMR (Bruker Avance III 600, $CDCl_3$) δ 28.0, 29.9, 33.1, 109.5, 128.2, 129.6, 130.5, 130.9, 146.4, 148.0, 151.4, 154.9; ESI-HRMS *m*/*z*: calcd for $C_{14}H_{15}N_4O_2S$ (MH^+), 303.0916, found 303.0912; Purity (HPLC): 98%.

4.2.2. **8-(Benzylsulfanyl)caffeine (3b)**

The title compound was prepared from benzyl mercaptan in a yield of 59%: mp 149 °C (ethanol). ^{1}H NMR (Bruker Avance III 600, $CDCl_3$) δ 3.35 (s, 3H), 3.57 (s, 3H), 3.69 (s, 3H), 4.42 (s, 2H), 7.27 (m, 3H), 7.31 (m, 2H); ^{13}C NMR (Bruker Avance III 600, $CDCl_3$) δ 27.8, 29.7, 32.2, 37.4, 108.7, 127.9, 128.7, 128.9, 136.6, 148.3, 150.0, 151.5, 154.6; ESI-HRMS *m*/*z*: calcd for $C_{15}H_{17}O_2N_4S$, 317.1072 (MH^+), found 317.1073; Purity (HPLC): 99%.

4.2.3. **8-[(2-Phenylethyl)sulfanyl]caffeine (3c)**

The title compound was prepared from phenylethyl mercaptan in a yield of 22.9%: mp 95 °C (ethanol). ^{1}H NMR (Bruker Avance III 600, $CDCl_3$) δ 3.04 (t, 2H, J = 7.9 Hz), 3.36 (s, 3H), 3.49 (t, 2H, J – 7.9 Hz), 3.55 (s, 3H), 3.78 (s, 3H), 7.21 (m, 3H), 7.29 (m, 2H); ^{13}C NMR (Bruker Avance III 600, $CDCl_3$) δ 27.8, 29.7, 32.1, 33.8, 36.0, 108.5, 126.7, 128.5, 139.3, 148.5, 150.9, 151.5, 154.5; ESI-HRMS *m*/*z*: calcd for $C_{16}H_{19}N_4O_2S$, 331.1229 (MH^+), found 331.1229; Purity (HPLC): 99%.

4.2.4. **8-[(2-Phenoxyethyl)sulfanyl]caffeine (3d)**

The title compound was prepared from 2-phenoxyethanethiol in a yield of 43.9%: mp 114 °C (ethanol). ^{1}H NMR (Bruker Avance III 600, $CDCl_3$) δ 3.37 (s, 3H), 3.53 (s, 3H), 3.63 (t, 2H, J = 6.4 Hz), 3.83 (s, 3H), 4.30 (t, 2H, J = 6.4 Hz), 6.91 (d, 2H, J = 8.3 Hz), 6.94 (t, 1H, J = 7.2 Hz), 7.25 (m, 2H); ^{13}C NMR (Bruker Avance III 600, $CDCl_3$) δ 27.8, 29.7, 31.5, 32.2, 66.3, 108.7, 114.5, 121.3, 129.5, 148.4, 150.3, 151.5, 154.5, 158.1; ESI-HRMS *m*/*z*: calcd for $C_{16}H_{19}N_4O_3S$ (MH^+), 347.1176, found 347.1173; Purity (HPLC): 95%.

4.2.5. **8-{[(4-Chlorophenyl)methyl]sulfanyl}caffeine (3e)**

The title compound was prepared from 4-chlorobenzyl mercaptan in a yield of 85.6%: mp 169 °C (ethanol). ^{1}H NMR (Bruker Avance III 600, $CDCl_3$) δ 3.36 (s, 3H), 3.56 (s, 3H), 3.73 (s, 3H), 4.40 (s, 2H), 7.26 (m, 4H); ^{13}C NMR (Bruker Avance III 600, $CDCl_3$) δ 27.9, 29.7, 32.2, 36.4, 108.8, 128.8, 130.3, 133.8, 135.2, 148.3, 149.7, 151.5, 154.6; ESI-HRMS *m*/*z*: calcd for $C_{15}H_{16}ClN_4O_2S$ (MH^+), 351.0682, found 351.0679; Purity (HPLC): 97%.

4.2.6. **8-{[(4-Bromophenyl)methyl]sulfanyl}caffeine (3f)**

The title compound was prepared from 4-bromobenzyl mercaptan in a yield of 82.0%: mp 166 °C (ethanol). ^{1}H NMR (Bruker Avance III 600, $CDCl_3$) δ 3.35 (s, 3H), 3.55 (s, 3H), 3.72 (s, 3H), 4.38 (s, 2H), 7.21 (d, 2H, J = 8.3 Hz), 7.40 (d, 2H, J = 8.3 Hz); ^{13}C NMR (Bruker Avance III 600, $CDCl_3$) δ 27.8, 29.7, 32.2, 36.4, 108.7, 121.8, 130.6, 131.8, 135.8, 148.3, 149.6, 151.4, 154.5; ESI-HRMS *m*/*z*: calcd for $C_{15}H_{16}BrN_4O_2S$ (MH^+), 395.0177, found 395.0178; Purity (HPLC): 98%.

4.2.7. **8-{[(4-Fluorophenyl)methyl]sulfanyl}caffeine (3g)**

The title compound was prepared from 4-fluorobenzyl mercaptan in a yield of 71.6%: mp 175 °C (ethanol). ^{1}H NMR (Bruker Avance III 600, $CDCl_3$) δ 3.35 (s, 3H), 3.55 (s, 3H), 3.72 (s, 3H), 4.40 (s, 2H), 6.96 (t, 2H, J = 8.3 Hz), 7.30 (q, 2H, J = 5.3 Hz); ^{13}C NMR (Bruker Avance III 600, $CDCl_3$) δ 27.8, 29.7, 32.1, 36.4, 108.7, 115.6 (d), 130.6 (d), 132.4 (d), 148.3, 149.8, 151.4, 154.5, 161.4, 163.1; ESI-HRMS *m*/*z*: calcd for $C_{15}H_{16}FN_4O_2S$ (MH^+), 335.0976, found 335.0972; Purity (HPLC): 95%.

4.2.8. **8-{[(4-Methoxyphenyl)methyl]sulfanyl}caffeine (3h)**

The title compound was prepared from 4-methoxybenzyl mercaptan in a yield of 90.5%: mp 159 °C (ethanol). ^{1}H NMR (Bruker Avance III 600, $CDCl_3$) δ 3.36 (s, 3H), 3.58 (s, 3H), 3.71 (s, 3H), 3.76 (s, 3H), 4.39 (s, 2H), 6.80 (d, 2H, J = 8.7 Hz), 7.24 (d, 2H, J = 8.7 Hz); ^{13}C NMR (Bruker Avance III 600, $CDCl_3$) δ 27.8, 29.7, 32.1, 37.0, 55.3, 108.6, 114.1, 128.4, 130.2, 148.4, 150.2, 151.5, 154.6, 159.2; ESI-HRMS *m*/*z*: calcd for $C_{16}H_{19}N_4O_3S$ (MH^+), 347.1176, found 347.1171; Purity (HPLC): 94%.

4.2.9. **8-[(3-Methylbutyl)sulfanyl]caffeine (3i)**

The title compound was prepared from 3-methyl-1-butanethiol in a yield of 35.3%: mp 79 °C (ethanol). ^{1}H NMR (Bruker Avance III 600, $CDCl_3$) δ 0.91 (d, 6H, J = 6.8 Hz), 1.59 (q, 2H, J = 7.9 Hz), 1.69 (sept, 1H, J = 6.8 Hz), 3.23 (t, 2H, J = 7.5 Hz), 3.34 (s, 3H), 3.51 (s, 3H), 3.79 (s, 3H); ^{13}C NMR (Bruker Avance III 600, $CDCl_3$) δ 22.1, 27.4, 27.8, 29.6, 30.8, 32.1, 38.5,

108.4, 148.4, 151.3, 151.5, 154.5; ESI-HRMS *m*/*z*: calcd for $C_{13}H_{21}N_4O_2S$ (MH^+), 297.1385, found 297.1382; Purity (HPLC): 97%.

4.2.10. **8-(Cyclohexylsulfanyl)caffeine (3j)**

The title compound was prepared from cyclohexanethiol in a yield of 37.2%: mp 133 °C (ethanol). ^{1}H NMR (Bruker Avance III 600, $CDCl_3$) δ 1.28 (m, 1H), 1.38 (m, 2H), 1.48 (m, 2H), 1.58 (m, 1H), 1.74 (m, 2H), 2.03 (m, 2H), 3.34 (s, 3H), 3.52 (s, 3H), 3.71 (m, 1H), 3.82 (s, 3H); ^{13}C NMR (Bruker Avance III 600, $CDCl_3$) δ 25.4, 25.8, 27.8, 29.7, 32.3, 33.4, 47.2, 108.4, 148.4, 150.3, 151.5, 154.6; ESI-HRMS *m*/*z*: calcd for $C_{14}H_{21}N_4O_2S$ (MH^+), 309.1385, found 309.1385; Purity (HPLC): 99%.

4.2.11. **8-(Cyclopentylsulfanyl)caffeine (3k)**

The title compound was prepared from cyclopentanethiol in a yield of 60.9%: mp 135 °C (ethanol). ^{1}H NMR (Bruker Avance III 600, $CDCl_3$) δ 1.63 (m, 4H), 1.76 (m, 2H), 2.15 (m, 2H), 3.34 (s, 3H), 3.51 (s, 3H), 3.80 (s, 3H), 3.99 (qn, 1H); ^{13}C NMR (Bruker Avance III 600, $CDCl_3$) δ 24.6, 27.8, 29.7, 32.2, 33.8, 46.4, 108.2, 148.5, 151.3, 151.5, 154.6; ESI-HRMS *m*/*z*: calcd for $C_{13}H_{19}N_4O_2S$ (MH^+), 295.1229, found 295.1233; Purity (HPLC): 95%.

4.2.12. **8-(Naphthalen-2-ylsulfanyl)caffeine (3l)**

The title compound was prepared from 2-naphthalenethiol in a yield of 87.7%: mp 175 °C (ethanol). ^{1}H NMR (Bruker Avance III 600, $CDCl_3$) δ 3.37 (s, 3H), 3.53 (s, 3H), 3.91 (s, 3H), 7.35 (dd, 1H, J = 1.9, 8.3 Hz), 7.48 (m, 2H), 7.73 (m, 1H), 7.78 (m, 2H), 7.84 (s, 1H); ^{13}C NMR (Bruker Avance III 600, $CDCl_3$) δ 27.9, 29.8, 33.1, 109.5, 126.9, 127.0, 127.4, 127.5, 127.8, 127.9, 129.4, 129.7, 132.6, 133.6, 146.4, 148.0, 151.4, 154.9; ESI-HRMS *m*/*z*: calcd for $C_{18}H_{17}N_4O_2S$ (MH^+), 353.1072, found 353.1074; Purity (HPLC): 94%.

4.3. Synthesis of C8-substituted aminocaffeine analogues (4a–h)

A mixture of 8-chlorocaffeine (2 mmol) and the appropriate amine (10 mmol) was heated under reflux (175–180 ºC) for 3 hours. The reaction was cooled to room temperature and treated with 50 mL acetic acid (5%). The resulting suspension was stirred for 15 min at room temperature and the precipitate was collected by filtration. The product was dried at 60 ºC and recrystallized twice from ethanol (30 mL) at 0 ºC.[18]

4.3.1. **8-(Phenylamino)caffeine (4a)**

The title compound was prepared from aniline and 8-chlorocaffeine in a yield of 24.2%: mp 164–265 °C (ethanol). ^{1}H NMR (Bruker Avance III 600, DMSO-d_6) δ 3.15 (s, 3H), 3.35 (s, 3H), 3.74 (s, 3H), 6.96 (t, 1H, J = 7.5 Hz), 7.29 (t, 2H, J = 7.5 Hz), 7.67 (d, 2H, J = 8.3 Hz), 9.07 (s, 1H); ^{13}H NMR (Bruker Avance III 600, DMSO-d_6) δ 27.3, 29.4, 30.5, 102.0, 118.1, 121.7, 128.7, 140.0, 147.2, 149.3, 150.9, 153.3; APCI-HRMS *m*/*z*: calcd for $C_{14}H_{15}N_5O_2$ (M^+), 285.1226, found 285.1230; Purity (HPLC): 98%.

4.3.2. **8-(Benzylamino)caffeine (4b)**

The title compound was prepared from benzylamine and 8-chlorocaffeine in a yield of 74.0%: mp 230 °C (ethanol). ^{1}H NMR (Bruker Avance III 600, DMSO-d_6) δ 3.14 (s, 3H), 3.35 (s, 3H), 3.58 (s, 3H), 4.53 (d, 2H, J = 5.6 Hz), 7.23 (t, 1H, J = 7.5 Hz), 7.32 (t, 2H, J = 7.5 Hz), 7.36 (d, 2H, J = 7.5 Hz), 7.56 (t, 1H, J = 5.6 Hz); ^{13}H NMR (Bruker Avance III 600, DMSO-d_6) δ 27.1, 29.2, 29.8, 45.7, 102.0, 126.9, 127.4, 128.3, 139.6, 148.2, 150.9, 152.9, 154.0; ESI-HRMS *m*/*z*: calcd for $C_{15}H_{18}N_5O_2$ (MH^+), 300.1460, found 300.1459; Purity (HPLC): 99%.

4.3.3. **8-[(2-Phenylethyl)amino]caffeine (4c)**

The title compound was prepared from 2-phenylethylamine and 8-chlorocaffeine in a yield of 68.3%: mp 221 °C (ethanol). ^{1}H NMR (Bruker Avance III 600, DMSO-d_6) δ 2.88 (t, 2H, J = 7.2 Hz), 3.14 (s, 3H), 3.32 (s, 3H), 3.49 (m, 2H), 3.51 (s, 3H), 7.11 (t, 1H, J = 5.3 Hz), 7.19 (t, 1H, J = 7.2 Hz), 7.22 (d, 2H, J = 7.5 Hz), 7.29 (t, 2H, J = 7.5 Hz); ^{13}H NMR (Bruker Avance III 600, DMSO-d_6) δ 27.1, 29.2, 29.7, 35.3, 44.1, 101.8, 126.1, 128.3, 128.7, 139.4, 148.3,

150.9, 152.9, 153.9; ESI-HRMS *m*/*z*: calcd for $C_{16}H_{20}N_5O_2$ (MH^+), 314.1617, found 314.1621; Purity (HPLC): 99%.

4.3.4. **8-[(3-Phenylpropyl)amino]caffeine (4d)**

The title compound was prepared from 3-phenylpropylamine and 8-chlorocaffeine in a yield of 76.8%: mp 204–205 °C (ethanol). ^{1}H NMR (Bruker Avance III 600, DMSO-d_6) δ 1.88 (qn, 2H, 7.5 Hz), 2.64 (t, 2H, J = 7.5 Hz), 3.13 (s, 3H), 3.30 (s, 3H), 3. 32 (m, 2H), 3.52 (s, 3H), 6.98 (t, 1H, J = 5.3 Hz), 7.16 (t, 1H, J = 7.2 Hz), 7.22 (d, 2H, J = 7.5 Hz), 7.26 (t, 2H, J = 7.5 Hz); ^{13}H NMR (Bruker Avance III 600, DMSO-d_6) δ 27.1, 29.2, 29.7, 30.8, 32.3, 42.0, 101.8, 125.7, 128.2, 128.3, 141.7, 148.3, 150.9, 152.8, 154.1; ESI-HRMS *m*/*z*: calcd for $C_{17}H_{22}N_5O_2$ (MH^+), 328.1773, found 328.1774; Purity (HPLC): 99%.

4.3.5. **8-[(4-Phenylbutyl)amino]caffeine (4e)**

The title compound was prepared from 4-phenylbutylamine and 8-chlorocaffeine in a yield of 63.0%: mp 179–180 °C (ethanol). ^{1}H NMR (Bruker Avance III 600, DMSO-d_6) δ 1.59 (m, 4H), 2.60 (t, 2H, J = 7.2 Hz), 3.13 (s, 3H), 3.30 (s, 3H), 3.32 (m, 2H), 3.51 (s, 3H), 6.94 (t, 1H, J = 5.6 Hz), 7.14 (t, 1H, J = 7.2 Hz), 7.18 (d, 2H, J = 7.2 Hz), 7.25 (t, 2H, J = 7.2 Hz); ^{13}C NMR (Bruker Avance III 600, DMSO-d_6) δ 27.1, 28.2, 28.8, 29.2, 29.7, 34.8, 42.2, 101.7, 125.6, 128.2, 128.3, 142.1, 148.3, 150.9, 152.8, 154.1; ESI-HRMS *m*/*z*: calcd for $C_{18}H_{24}N_5O_2$ (MH^+), 342.1930, found 342.1929; Purity (HPLC): 99%.

4.3.6. **8-{[2-(Pyridin-2-yl)ethyl]amino}caffeine (4f)**

The title compound was prepared from 2-(2-pyridyl)ethylamine and 8-chlorocaffeine in a yield of 20.4%: mp 196–197 °C (ethanol). ^{1}H NMR (Bruker Avance III 600, DMSO-d_6) δ 3.03 (t, 2H, J = 7.2 Hz), 3.13 (s, 3H), 3.31 (s, 3H), 3.50 (s, 3H), 3.65 (q, 2H, 6.7 Hz), 7.10 (t, 1H, J = 5.6 Hz), 7.20 (t, 1H, J = 5.6 Hz), 7.26 (d, 1H, J = 7.5 Hz), 7.69 (t, 1H, J = 7.5 Hz), 8.49 (d, 1H, J = 4.1 Hz); ^{13}C NMR (Bruker Avance III 600, DMSO-d_6) δ 27.1, 29.2, 29.7, 37.5, 42.4, 101.8, 121.5, 123.2, 136.4, 148.3, 149.0, 150.9, 152.8, 153.9, 159.1; ESI-HRMS *m*/*z*: calcd for $C_{15}H_{19}N_6O_2$ (MH^+), 315.1569, found 315.1570; Purity (HPLC): 98%.

4.3.7. **8-{[2-(3-Chlorophenyl)ethyl]amino}caffeine (4g)**

The title compound was prepared from 2-(3-chlorophenyl)ethanamine and 8-chlorocaffeine in a yield of 48.5%: mp 111–113 °C (ethanol). ^{1}H NMR (Bruker Avance III 600, DMSO-d_6) δ 2.88 (t, 2H, J = 7.2 Hz), 3.13 (s, 3H), 3.32 (s, 3H), 3.50 (s, 3H), 3.52 (m, 2H), 7.10 (t, 1H, J = 5.6 Hz), 7.18 (d, 1H, J = 7.5 Hz), 7.24 (d, 1H, J = 8.3 Hz), 7.29 (d, 1H, J = 7.5 Hz), 7.31 (s, 1H); ^{13}C NMR (Bruker Avance III 600, DMSO-d_6) δ 27.1, 29.2, 29.7, 34.8, 43.7, 101.8, 126.1, 127.5, 128.6, 130.1, 132.9, 142.0, 148.3, 150.9, 152.8, 153.8; ESI-HRMS *m*/*z*: calcd for $C_{16}H_{19}N_5O_2Cl$ (MH^+), 348.1227, found 348.1225; Purity (HPLC): 98%.

4.3.8. **8-(Cyclopentylamino)caffeine (4h)**

The title compound was prepared from cyclopentylamine and 8-chlorocaffeine in a yield of 38.6%: mp 217–218 °C (ethanol). ^{1}H NMR (Bruker Avance III 600, DMSO-d_6) δ 1.52 (m, 4H), 1.68 (m, 2H), 1,93 (m, 2H), 3.13 (s, 3H), 3.31 (s, 3H), 3.53 (s, 3H), 4.10 (m, 1H), 6.76 (d, 1H, J = 7.2 Hz); ^{13}H NMR (Bruker Avance III 600, DMSO-d_6) δ 23.4, 27.1, 29.2, 29.8, 32.4, 54.2, 101.7, 148.3, 150.9, 152.8, 153.8; ESI-HRMS *m*/*z*: calcd for $C_{13}H_{20}N_5O_2$ (MH^+), 278.1617, found 278.1612; Purity (HPLC): 96%.

4.4. Methylation of the C8-substituted aminocaffeine analogues (5a–b)

Potassium hydroxide (0.05 g) was powderized and suspended in 5 mL DMSO. The resulting mixture was stirred for 30 min at room temperature and the aminocaffeine analogue (3 mmol) dissolved in DMSO (5 mL) was added. The reaction was heated to 40 ºC (in order for the aminocaffeine analogue to remain in solution) and iodomethane (0.8 mmol) was added. Stirring of the reaction was continued and another portion of iodomethane (0.8 mmol) was added every 20 min until silica gel TLC (petroleum ether/ ethyl acetate 30:70) indicated completion of the reaction. The pH of the reaction was also continually measured, and when acidic (pH paper), another portion of potassium hydroxide (0.05 g) was added. Upon completion, the reaction was cooled to room temperature and water (250 mL) was added. The resulting solution was incubated for several days at 4 ºC and the formed crystals were collected by filtration.

4.4.1. **8-[Methyl(2-phenylethyl)amino]caffeine (5a)**

The title compound was prepared from 8-[(2-phenylethyl)amino]caffeine (**4c**) and iodomethane in a yield of 57.7%: mp 103 °C (ethanol). ^{1}H NMR (Bruker Avance III 600, DMSO-d_6) δ 2.88 (t, 2H, J = 7.5 Hz), 2.98 (s, 3H), 3.16 (s, 3H), 3.33 (s, 3H), 3.47 (t, 2H, J = 7.5 Hz), 3.59 (s, 3H), 7.18 (m, 1H), 7.25 (m, 4H); ^{13}C NMR (Bruker Avance III 600, DMSO-d_6) δ 27.3, 29.3, 32.5, 33.0, 38.6, 54.5, 103.8, 126.1, 128.3, 128.8, 139.0, 147.1, 150.9, 153.5, 156.6; ESI-HRMS *m*/*z*: calcd for $C_{17}H_{22}N_5O_2$ (MH^+), 328.1774, found 328.1734; Purity (HPLC): 99%.

4.4.2. **8-[Methyl(4-phenylbutyl)amino]caffeine (5b)**

The title compound was prepared from 8-[(4-phenylbutyl)amino]caffeine (**4e**) and iodomethane in a yield of 49.9%: mp 114 °C (ethanol). ^{1}H NMR (Bruker Avance III 600, DMSO-d_6) δ 1.57 (m, 4H), 2.57 (t, 2H, J = 7.15 Hz), 2.90 (s, 3H), 3.16 (s, 3H), 3.26 (t, 2H, J = 7.15 Hz), 3.32 (s, 3H), 3.65 (s, 3H), 7.15 (m, 3H), 7.24 (t, 2H, J = 7.91 Hz); ^{13}C NMR (Bruker Avance III 600, DMSO-d_6) δ 26.3, 27.3, 27.9, 29.3, 32.6, 34.7, 38.4, 52.5, 103.8, 125.7, 128.2, 128.2, 142.0, 147.1, 150.9, 153.5, 156.9; ESI-HRMS *m*/*z*: calcd for $C_{19}H_{26}N_5O_2$ (MH^+), 356.2087, found 356.2088; Purity (HPLC): 98%.

4.5. IC_{50} determinations for the inhibition of human MAO

Microsomal preparations form insect cells containing recombinant human MAO-A and –B (5 mg/mL) served as enzyme sources and all enzymatic reactions were conducted in potassium phosphate buffer (100 mM, pH 7.4, made isotonic with KCl) to a final volume of 500 µL.[19] The reactions contained the MAO-A/B mixed substrate, kynuramine, at concentrations of 45 µM and 30 µM for the incubations with MAO-A and –B, respectively, various concentrations of the test inhibitor (0–100 µM) and the MAO enzymes (0.0075 mg/mL). The enzyme activities employed for the IC_{50} value determinations were 24–28 nmoles 4-hydroxyquinoline formed/min/mg protein for MAO-A and 6–8 nmoles 4-hydroxyquinoline formed/min/mg protein for MAO-B. Stock solutions of the test inhibitors were prepared in DMSO and added to the reactions to yield a final concentration of 4% (v/v) DMSO. The enzyme reactions were incubated at 37 °C for 20 minutes and then terminated with the addition of 400 µL NaOH (2 N) and 1000 µL distilled water. After centrifugation at

16,000 *g* for 10 min, the fluorescence of the MAO generated 4-hydroxyquinoline in the supernatant fractions were measured (λ_{ex} = 310 nm, λ_{em} = 400 nm). To determine the concentrations of 4-hydroxyquinoline, a linear calibration curve was constructed from solutions of 4-hydroxyquinoline (0.047–1.50 µM) in potassium phosphate buffer. The calibration standards were prepared to a volume of 500 µL and contained 4% DMSO, 400 µL NaOH (2 N) and 1000 µL distilled water. The initial rate of MAO catalysis was plotted versus the logarithm of the inhibitor concentration to obtain a sigmoidal dose–response curve. Each curve was constructed from 6 different inhibitor concentrations spanning at least 3 orders of a magnitude. These data were fitted to the one site competition model incorporated into the GraphPad Prism software and the IC_{50} values were determined in triplicate and are expressed as mean ± standard deviation (SD).

4.6. Time-dependent inhibition studies

The reversibility of MAO inhibition was examined by determining the time-dependence of inhibition of three selected inhibitors, **3f**, **4g** and **5b**. The selected inhibitors were preincubated in potassium phosphate buffer (100 mM, pH 7.4, made isotonic with KCl) with MAO-A and –B (0.015–0.03 mg/mL) for periods of 0, 15, 30, 60 min at 37 ºC. The concentrations of the inhibitors used were two-fold their measured IC_{50} values for the inhibition of the respective MAO enzymes and were: 5.22 µM (**3f**) and 11.56 µM (**4g**) for the studies with MAO-A, and 0.32 µM (**3f**) and 5.94 µM (**5b**) for the studies with MAO-B. To compensate for a potential time-dependent loss of enzyme activity, the enzyme preincubations were firstly incubated at 37 ºC and the inhibitors were subsequently added at different time points. These time points were selected as to ensure that all enzyme preparations were preheated at 37 ºC for exactly 60 min, irrespective of the time period (0–60 min) for which the enzyme preparations were preincubated in the presence of the test inhibitor. These reactions were diluted 2-fold by the addition of kynuramine at concentrations of 45 µM and 30 µM for the incubations with MAO-A and –B, respectively, and the resulting reactions (500 µL final volume) were incubated at 37 °C for a further 15 minutes. The final enzyme concentration in these reactions was 0.0075–0.015 mg/mL and the concentrations of the selected inhibitors were approximately equal to their IC_{50} values for the inhibition of the respective isozymes. The reactions were terminated with the addition of 400 µL NaOH (2 N) and 1000 µL distilled water and the rates of MAO catalyzed generation of 4-hydroxyquinoline were measured and calculated as described above. All measurements were carried out in triplicate and are expressed as mean ± SD.[23]

4.7. Construction of Lineweaver-Burk plots

A set consisting of four Lineweaver–Burk plots were constructed for the inhibition of MAO-A and –B by the selected inhibitor **3f**. One plot was constructed in the absence of inhibitor while three plots were constructed in the presence of three different concentrations of **3f** each. These concentrations were 1.31–5.22 µM and 0.04–0.16 µM for the inhibition studies with MAO-A and –B, respectively. Four different kynuramine concentrations (15–90 µM) were employed for each plot and the concentrations of recombinant human MAO-A and –B used were 0.015 mg/mL. The initial MAO catalytic rates were measured as described above. Linear regression analysis was performed using GraphPad Prism.[23]

4.8. Molecular modeling studies

The modeling studies were carried out with the Windows based Discovery Studio 1.7 molecular modeling software (Accelrys).[23,27] For this purpose the crystallographic structures of MAO-A co-crystallized with harmine (PDB code: 2Z5X)[3] and MAO-B co-crystallized with safinamide (PDB code: 2V5Z)[4] were obtained from the Brookhaven Protein Data Bank (www.rcsb.org/pdb). The protonation states of the ionizable amino acids residues were calculated at pH 7.4 and hydrogen atoms were added to the receptor models. The valences of the FAD cofactors (oxidized state) and co-crystallized ligands were corrected and hydrogen atoms were added according to the appropriate protonation states at pH 7.4. The structures were typed automatically with the Momany and Rone CHARMm forcefield, the backbone of the protein was constrained and the structures were subjected to a three step energy minimization. The first step was a steepest descent minimization which was followed by conjugate gradient minimization. For both protocols the termination criteria was set to a maximum of 2500 steps or a minimum value of 0.1 for the root mean square of the energy gradient. The final step was an adopted basis Newton-Rapheson minimization and the termination criteria was set to a maximum of 5000 steps or a minimum value for the root mean square of the energy gradient of 0.01. For these minimization steps the implicit generalized Born solvation model with simple switching was employed with the dielectric constant set to 4. For both the MAO-A and –B models, the crystal water molecules were removed with the exception of 3 active site waters in each model. The X-ray crystallographic structures of MAO-B shows that three active site water molecules (HOH 1155, 1170 and 1351; A-chain) are conserved, all located in the vicinity of the FAD cofactor.[4] In the MAO-A model, the crystal waters HOH 710, 718 and 739 which occupies the analogous positions in

the MAO-A active site compared to those cited above for MAO-B, were retained. The co-crystallized ligands and the backbone constraints were subsequently removed from the models and the binding sites were identified by a flood-filling algorithm. The structures of **3a–c** and **4c** were constructed within Discovery Studio, their hydrogen atoms were added according to the appropriate protonation states at pH 7.4. The geometries of the ligands were briefly optimized in Discovery Studio using a fast Dreiding-like forcefield (1000 iterations) and the atom potential types and partial charges were assigned with the Momany and Rone CHARMm forcefield. Docking of the ligands was carried out with the LigandFit application of Discovery Studio and the docking solutions were refined using the Smart Minimizer algorithm. The parameters for the docking runs were set to their default values, ten possible binding solutions were computed for each docked ligand and the best-ranked binding conformation of each ligand was determined according to the DockScore values. The illustrations were prepared in PyMOL.[28] It is interesting to note that among the 10 best ranked binding orientations, there were orientations which exhibited a reversed binding mode with the caffeine ring directed towards the entrance of the MAO-A and –B active sites while the C8 sulfanyl and amino side chains project towards the FAD cofactor. Based on the low DockScore values these orientations were however deemed unlikely.

Acknowledgements

The NMR spectra were recorded by André Joubert of the SASOL Centre for Chemistry, North-West University while the MS spectra were recorded by the Mass Spectrometry Service, University of the Witwatersrand and the Mass Spectrometry Unit, Stellenbosch University. This work was supported by grants from the National Research Foundation and the Medical Research Council, South Africa.

References

1. Binda, C.; Newton-Vinson, P.; Hubálek, F.; Edmondson, D. E.; Mattevi, A. *Nat. Struct. Biol.* **2002**, *9*, 22.
2. Shih, J. C.; Chen, K.; Ridd, M. J.; *Annu. Rev. Neurosci*. **1999**, *22*, 197.
3. Son, S. –Y.; Ma, J.; Kondou, Y.; Yoshimura, M.; Yamashita, E.; Tsukihara, T. *Proc. Natl. Acad. Sci. U.S.A*. **2008**, *105*, 5739.

4. Binda, C.; Wang, J.; Pisani, L.; Caccia, C.; Carotti, A.; Salvati, P.; Edmondson, D. E.; Mattevi, A. *J. Med. Chem*. **2007**, *50*, 5848.

5. Youdim, M. B. H.; Edmondson, D.; Tipton, K. F. *Nat. Rev. Neurosci*. **2006**, *7*, 295.

6. Nicotra, A.; Pierucci, F.; Parvez, H.; Senatori, O. *Neurotoxicology*. **2004**, *25*, 155.

7. Fowler, J. S.; Volkow, N. D.; Wang, G. J.; Logan, J.; Pappas, N.; Shea, C.; MacGregor, R. *Neurobiol. Aging*. **1997**, *18*, 431.

8. Youdim, M. B. H.; Collins, G. G. S.; Sandler, M.; Bevan-Jones, A. B.; Pare, C. M.; Nicholson, W. J. *Nature*. **1972**, *236*, 225.

9. Collins, G. G. S.; Sandler, M.; Williams, E. D.; Youdim, M. B. H. *Nature*. **1970,** *225*, 817.

10. Di Monte, D. A.; DeLanney, L. E.; Irwin, I.; Royland, J. E.; Chan, P.; Jakowec, M. W.; Langston, J. W. *Brain. Res*. **1996**, *738*, 53.

11. Finberg, J. P.; Wang, J.; Bankiewich, K.; Harvey-White, J; Kopin, I. J.; Goldstein, D. S. *J. Neural Transm. Suppl*. **1998**, *52*, 279.

12. Fernandez, H. H.; Chen, J. J. *Pharmacotherapy*. **2007**, *27*, 174S.

13. Youdim, M. B. H.; Bakhle, Y. S. *Br. J. Pharmacol*. **2006**, *147*, S287.

14. Van der Walt, E. M.; Milczek, E. M.; Malan, S. F.; Edmondson, D. E.; Castagnoli, N., Jr.; Bergh, J. J.; Petzer, J. P. *Bioorg. Med. Chem. Lett*. **2009**, *19*, 2509.

15. Strydom, B.; Malan, S. F.; Castagnoli, N.; Bergh, J. J.; Petzer, J. P. *Bioorg. Med. Chem*. **2010**, *18*, 1018.

16. Strydom, B.; Bergh, J. J.; Petzer, J. P. *Eur. J. Med. Chem*. **2011**, *46*, 3474.

17. Long, L. M. *J. Am. Chem. Soc*. **1947**, *69*, 2939.

18. Cramer, L. *Chem. Ber*. **1894**, *27*, 3089.

19. Novaroli, L.; Reist, M.; Favre, E.; Carotti, A.; Catto, M.; Carrupt, P. A. *Bioorg. Med. Chem*. **2005**, *13*, 6212.

20. Prins, L. H. A.; Petzer, J. P.; Malan, S. F. *Eur. J. Med. Chem*. **2010**, *45*, 4458.

21. Tipton, K.F.; Boyce, S.; O'Sullivan, J.; Davey, G. P.; Healy, J. *Curr. Med. Chem*. **2004**, *11*, 1965.

22. Fowler, J. S.; Volkow, N. D.; Logan, J.; Wang, G.; MacGregor, R. R.; Schlyer, D.; Wolf, A. P.; Pappas, N.; Alexoff, D.; Shea, C.; Dorflinger, E.; Kruchowy, L.; Yoo, K.; Fazzini, E.; Patlak, C. *Synaps*. **1994**, *18*, 86.

23. Manley-King, C. I.; Bergh, J. J.; Petzer, J. P. *Bioorg. Med. Chem*. **2011**, *19*, 261.

24. Binda, C.; Mattevi, A.; Edmondson, D. E.; *J. Biol. Chem*. **2002**, *277*, 23973.

25. Hubálek, F.; Binda, C.; Khalil, A.; Li, M.; Mattevi, A.; Castagnoli, N., Jr.; Edmondson, D. E. *J. Biol. Chem.* **2005**, *280*, 15761.

26. Vlok, N.; Malan, S. F.; Castagnoli, N., Jr.; Bergh, J. J.; Petzer, J. P. *Bioorg. Med. Chem.* **2006**, *14*, 3512.

27. Accelrys Discovery Studio 1.7, Accelrys Software Inc., San Diego, CA, USA. 2006, http://www.accelrys.com.

28. DeLano, W. L. The PyMOL Molecular Graphics System. DeLano Scientific, San Carlos, USA, 2002.

Table 1.The IC_{50} values for the inhibition of recombinant human MAO-A and –B by compounds **3a–l**

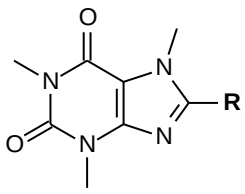

		IC_{50} (μM)[a]		
	R	MAO-A	MAO-B	SI[b]
3a	-S-C_6H_5	56.4 ± 12.9	33.2 ± 3.41	1.7
3b	-S-CH_2-C_6H_5	8.22 ± 1.13	1.86 ± 0.034	4.4
3c	-S-$(CH_2)_2$-C_6H_5	20.5 ± 4.49	0.223 ± 0.010	91.9
3d	-S-$(CH_2)_2$-O-C_6H_5	15.5 ± 2.17	0.332 ± 0.033	46.7
3e	-S-CH_2-(4-Cl-C_6H_4)	2.77 ± 0.570	0.192 ± 0.025	14.4
3f	-S-CH_2-(4-Br-C_6H_4)	2.62 ± 0.104	0.167 ± 0.020	15.7
3g	-S-CH_2-(4-F-C_6H_4)	4.80 ± 0.584	0.348 ± 0.036	13.8
3h	-S-CH_2-(4-CH_3O-C_6H_4)	–[c]	–[c]	–
3i	-S-$(CH_2)_2$-$CH(CH_3)_2$	15.2 ± 4.09	2.62 ± 0.546	5.8
3j	-S-C_6H_{11}	24.4 ± 8.76	13.1 ± 3.49	1.9
3k	-S-C_5H_9	9.40 ± 0.572	20.9 ± 3.11	0.4
3l	-S-2-Naphthalenyl	3.60 ± 0.291	3.60 ± 1.10	1.0

[a] All values are expressed as the mean ± SD of triplicate determinations.

[b] The selectivity index is the selectivity for the MAO-B isoform and is given as the ratio of IC_{50}(MAO-A)/IC_{50}(MAO-B).

[c]No inhibition observed at a maximum concentration of 100 μM of the test inhibitor.

Table 2.The IC_{50} values for the inhibition of recombinant human MAO-A and –B by compounds **4a**–**h**

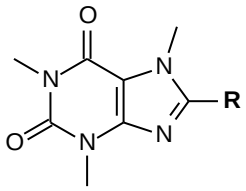

		IC_{50} (μM)[a]		
	R	MAO-A	MAO-B	SI[b]
4a	-NH-C_6H_5	–[c]	–[c]	–
4b	-NH-CH_2-C_6H_5	–[c]	–[c]	–
4c	-NH-$(CH_2)_2$-C_6H_5	45.2 ± 9.19	17.6 ± 2.48	2.6
4d	-NH-$(CH_2)_3$-C_6H_5	–[c]	–[c]	–
4e	-NH-$(CH_2)_4$-C_6H_5	30.9 ± 6.74	9.60 ± 0.759	3.2
4f	-NH-$(CH_2)_2$-(pyridin-2-yl)	–[c]	19.4 ± 5.07	–
4g	-NH-$(CH_2)_2$-(3-ClC_6H_4)	5.78 ± 0.411	24.4 ± 18.0	0.2
4h	-NH-C_5H_9	–[c]	–[c]	–

[a] All values are expressed as the mean ± SD of triplicate determinations.

[b] The selectivity index is the selectivity for the MAO-B isoform and is given as the ratio of IC_{50}(MAO-A)/IC_{50}(MAO-B).

[c]No inhibition observed at a maximum concentration of 100 μM of the test inhibitor.

Table 3.The IC_{50} values for the inhibition of recombinant human MAO-A and –B by compounds **5a–b**

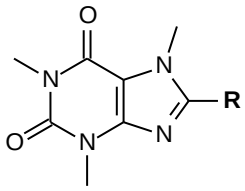

		IC_{50} (μM)[a]		
	R	MAO-A	MAO-B	SI[b]
5a	-(NCH_3)-$(CH_2)_2$-C_6H_5	107 ± 9.85	16.8 ± 6.83	6.4
5b	-(NCH_3)-$(CH_2)_4$-C_6H_5	37.7 ± 6.40	2.97 ± 0.536	12.7

[a] All values are expressed as the mean ± SD of triplicate determinations.

[b] The selectivity index is the selectivity for the MAO-B isoform and is given as the ratio of IC_{50}(MAO-A)/IC_{50}(MAO-B).

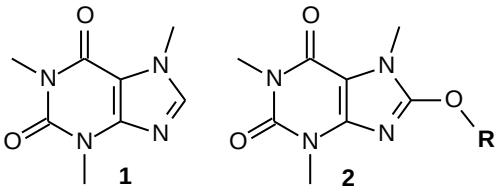

Figure 1. The structures of caffeine (**1**) and oxycaffeine analogues (**2**).

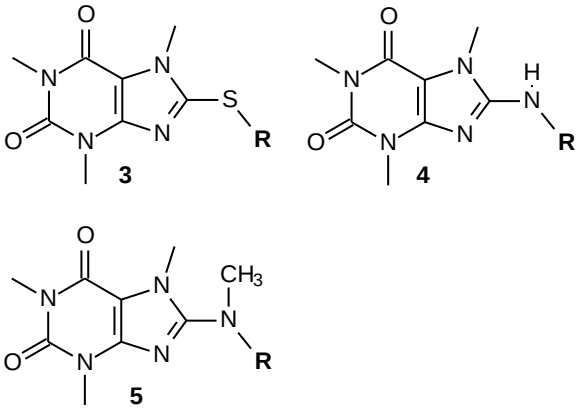

Figure 2. The structures of sulfanylcaffeine analogues (**3**), aminocaffeine analogues (**4**) and methylaminocaffeine analogues (**5**).

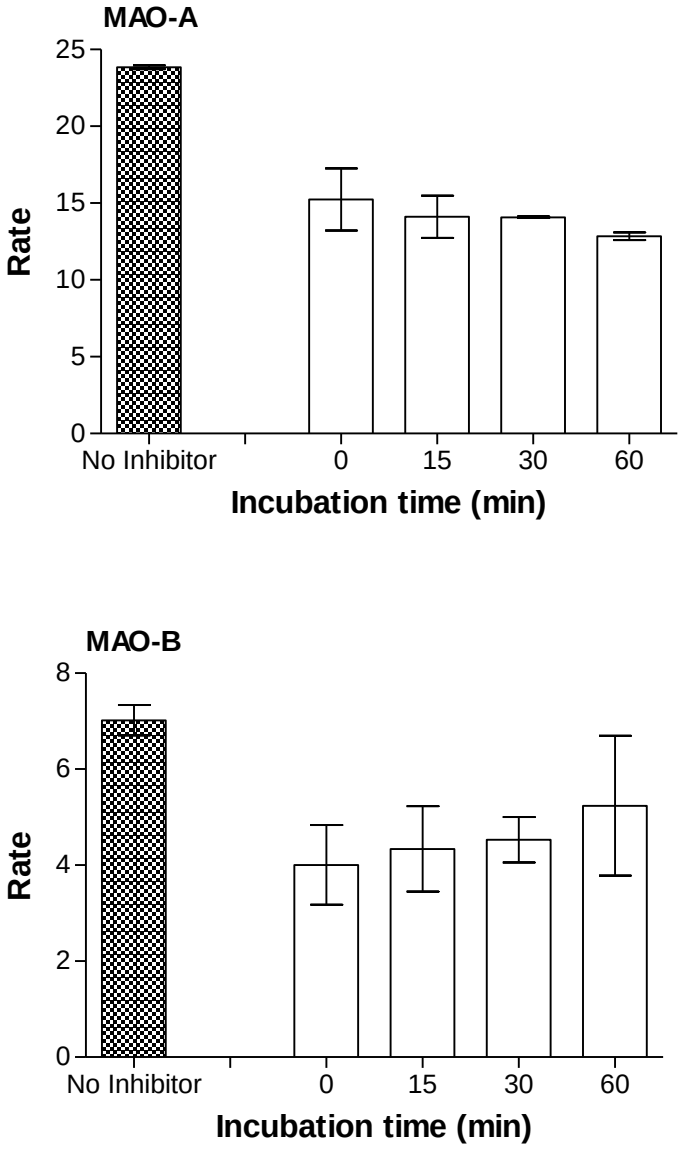

Figure 3. Time-dependent inhibition of recombinant human MAO-A and –B by **3f**. The enzymes were preincubated for various periods of time (0–60 min) with **3f** at concentrations of 5.22 µM and 0.32 µM for MAO-A and –B, respectively. The concentrations of the enzyme substrate, kynuramine, were 45 and 30 µM for the studies with MAO-A and MAO-B, respectively, and the enzyme concentrations were 0.015 mg/mL. The catalytic rates are expressed as nmoles 4-hydroxyquinoline formed/min/mg protein.

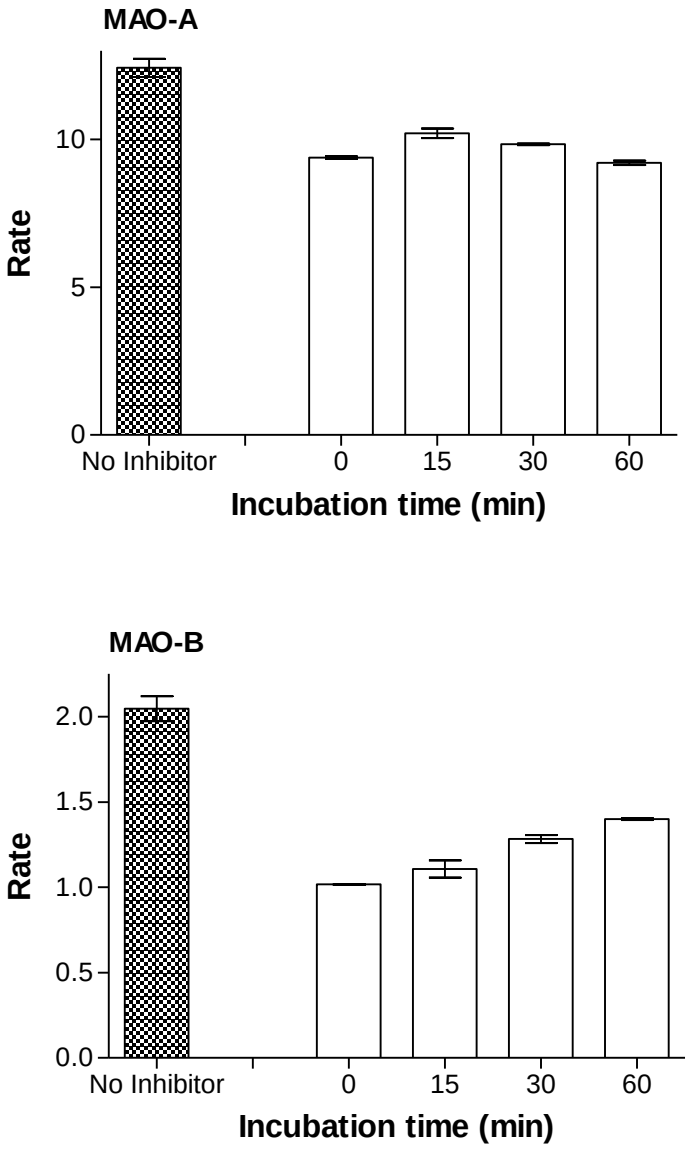

Figure 4. Time-dependent inhibition of recombinant human MAO-A and –B by **4g** and **5b**, respectively. The enzymes were preincubated for various periods of time (0–60 min) with **4g** (MAO-A) and **5b** (MAO-B) at concentrations of 11.56 µM and 5.94 µM, respectively. The concentrations of the enzyme substrate, kynuramine, were 45 and 30 µM for the studies with MAO-A and MAO-B, respectively, and the enzyme concentrations were 0.0075 mg/mL. The catalytic rates are expressed as nmoles 4-hydroxyquinoline formed/min/mg protein.

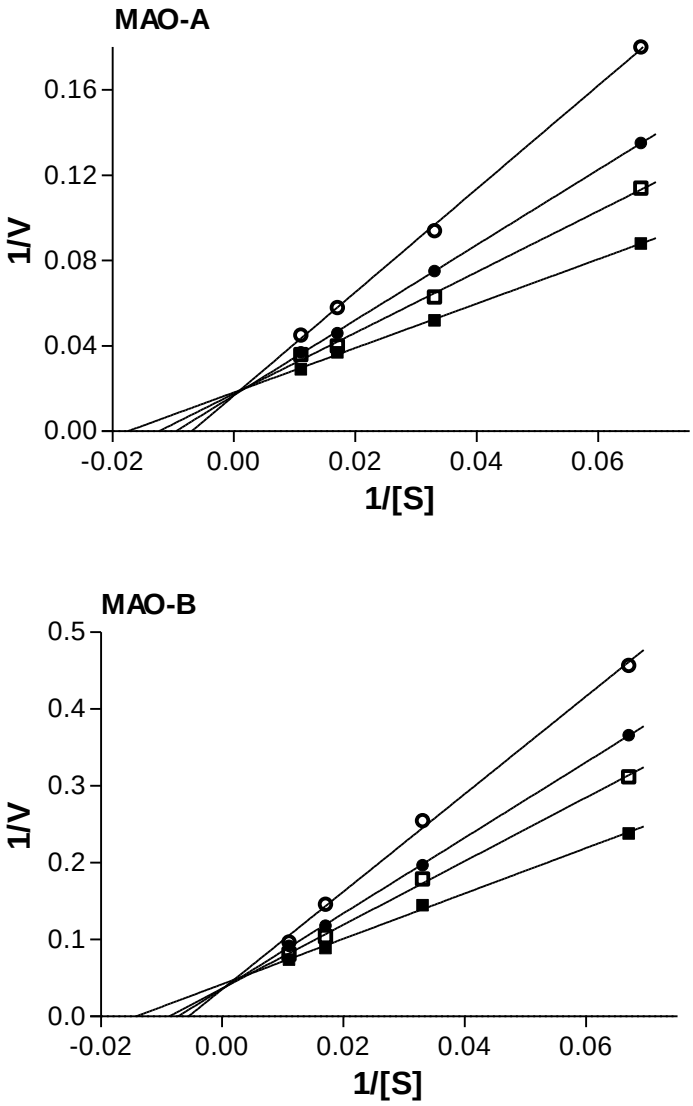

Figure 5. Lineweaver-Burk plots of the recombinant human MAO-A and –B catalyzed oxidation of kynuramine in the absence (filled squares) and presence of various concentrations of **3f**. For the studies with MAO-A the concentrations of **3f** were: 1.31 µM (open squares), 2.61 µM (filled circles), 5.22 µM (open circles). For the studies with MAO-B the concentrations of **3f** were: 0.04 µM (open squares), 0.08 µM (filled circles), 0.16 µM (open circles).The rates (V) are expressed as nmol product formed/min/mg protein.

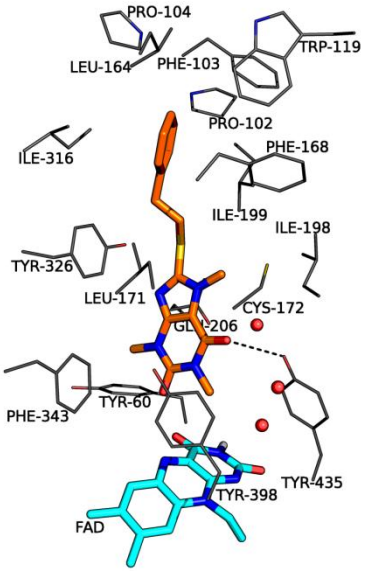

Figure 6. The predicted binding orientation of **3c** (orange) in the MAO-B active site.

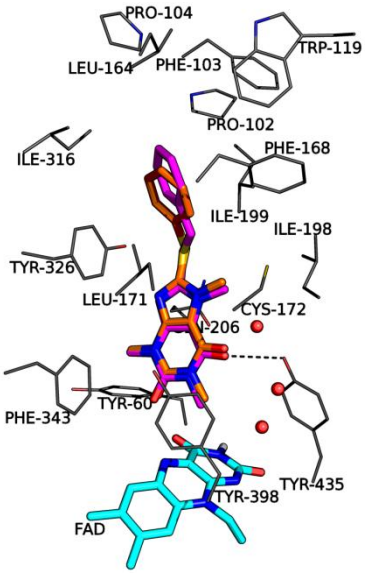

Figure 7. The predicted binding orientations of **3a** (orange) and **3b** (magenta) in the MAO-B active site.

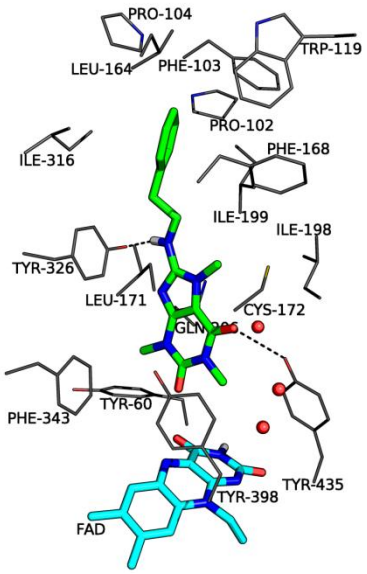

Figure 8. The predicted binding orientation of **4c** (green) in the MAO-B active site.

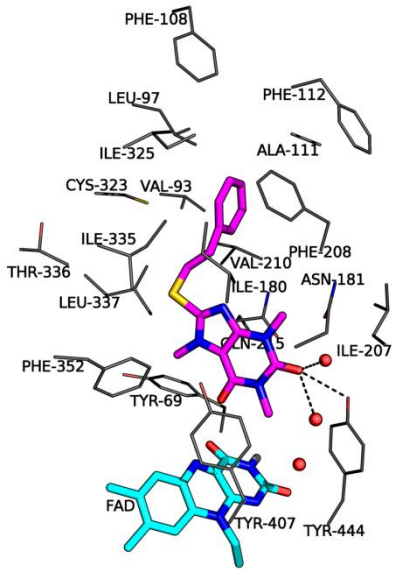

Figure 9. The predicted binding orientation of **3c** (magenta) in the MAO-A active site.

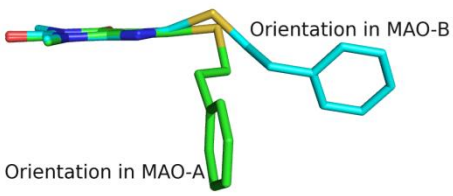

Figure 10. The predicted binding orientations of **3c** within the active sites of MAO-A (green) and MAO-B (cyan) with the caffeine moieties of the respective orientations overlaid.

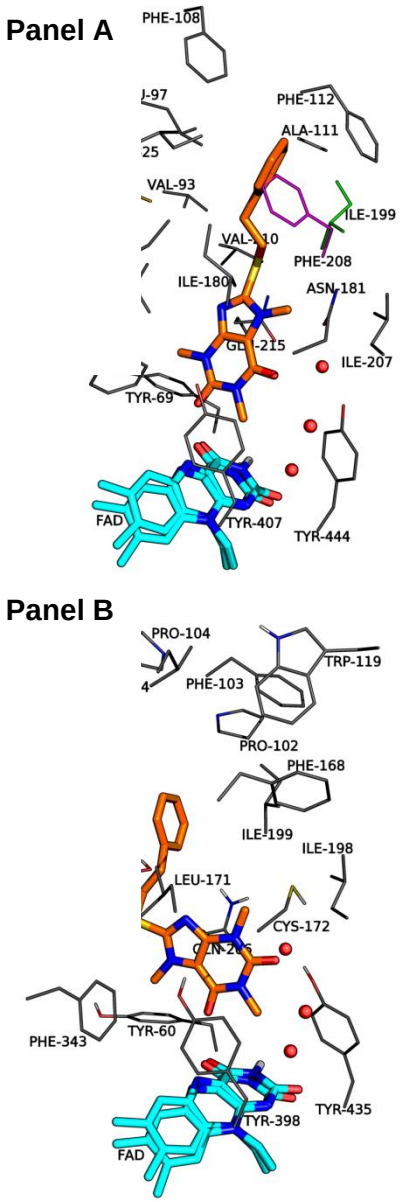

Figure 11. Illustrations of the overlaid active sites of human MAO-A and –B. Panel A: The predicted binding orientation of **3c** as docked within the active site of MAO-B is shown in the MAO-A active site. The active site residues of MAO-A are displayed in gray with Phe-208 in magenta while residue Ile-199 in MAO-B is displayed in green. Panel B: The predicted binding orientation of **3c** as docked within the active site of MAO-A is shown in the MAO-B active site. The active site residues of MAO-B are displayed in gray with Tyr-326 in magenta while residue Ile-325 in MAO-A is displayed in green.

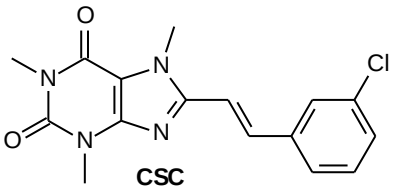

Figure 12. The structure of (E)-8-(3-chlorostyryl)caffeine (CSC).

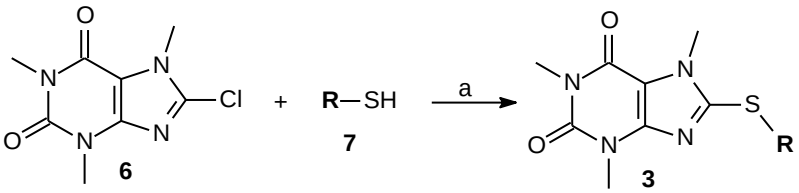

Scheme 1. Synthetic pathway to sulfanylcaffeine analogues (**3**). Reagents and conditions: (a) NaOH, H_2O/ethanol, reflux.

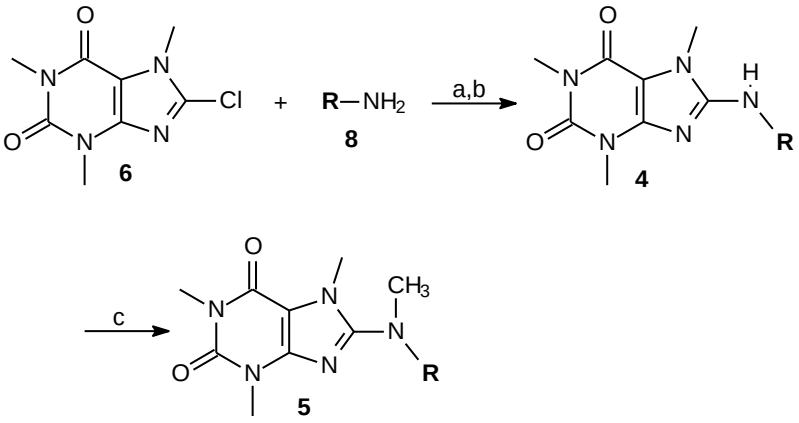

Scheme 2. Synthetic pathway to aminocaffeine analogues (**4** and **5**). Reagents and conditions: (a) reflux; (b) acetic acid; (c) KOH, DMSO, CH_3I.

REFERENCES

Ascherio, A., Zhang, S.M., Hernan, M.A., Kawachi, I., Colditz, G.A., Speizer, F.E., Willet, W.C. 2001. To sip or not to sip: The potential health risks and benefits of coffee drinking. *Annals of neurology.* 50: 56 – 53.

Avilla-Zarraga, J.G. & Martinez, R. 2001. Efficient methylation of carboxylic acids with potassium hydroxide/methyl sulfoxide and iodomethane. *Synthetic Communications.* 31: 2177 – 2183.

Bara-Jimenez, W., Sherzai, A., Dimitrova, T., Favit, A., Bibbiani, F., Gillespie, M., Morris, M.J., Mouradian, M.M., Chase, T.N. 2003 Adenosine A_{2A} receptor antagonist treatment of Parkinson's disease. *Neurology*. 61: 293 – 296.

Betarbet, R., Sherer, T.B., MacKenzie, G., Garcia-Osuna, M., Panov, A.V., Greenamyre, J.T. 2000. Chronic systematic pesticide exposure reproduces features of Parkinson's disease. *Nature Neuroscience*. 3: 1301 – 1306.

Bové, J., Prou, D., Perier, C., Przedborski, S. 2005. Toxin-induced models of Parkinson's disease. *Journal of the American society for experimental neurotherapeutics.* 2: 484 – 494.

Brooks, D.J. 2000. Dopamine agonists: their role in the treatment of Parkinson's disease. *Journal of neurology, neurosurgery and psychiatry.* 68: 685 – 689.

Brunner, H.G., Nelen, M., Breakefield, X.O., Ropers, H.H., van Oost, B.A. 1993. Abnormal behavior associated with a point mutation in the structural gene for monoamine oxidase A. *Science.* 262: 578 – 580.

Chen, J., Steyn, S., Staal, R., Petzer, J.P., Xu, K., Van der Schyf, C.J., Castagnoli, K., Sonsalla, P.K., Castagnoli, N., Schwarzschild, M.A. 2002. 8-(3-Chlorostyryl)caffeine may attenuate MPTP neurotoxicity through dual actions of monoamine oxidase inhibition and A_{2A} receptor antagonism. *Journal of biological chemistry*. 277: 36040 – 36044.

Chen, J.J. & Swope, D.M. 2007. Pharmacotherapy for Parkinson's disease. *Pharmacotherapy.* 27(12 Pt 2): 161S – 173S.

Chen, J-F., Xu, K., Petzer, J.P., Staal, R., Xu, Y.H., Beilstein, M., Sonsalla, P.K., Castagnolli, K., Castagnolli, N., Schwarzschild, M.A. 2001. Neuroprotection by caffeine and A(2A) adenosine receptor inactivation in a model of Parkinson's disease. *Journal of neuroscience.* 21: RC143.

Cheng, Y., & Prusoff, W.H. 1973. Relationship between the inhibition constant and the concentration of inhibitor which causes 50 percent inhibition of an enzymatic reaction. *Biochemical pharmacology.* 22: 3099 – 3108.

Cicchetti, F., Bronwell, A.L., Williams, K., Chen, Y.I., Livni, E., Isacson, O. 2002. Neuroinflammation of the nigrostriatal pathway during progressive 6-OHDA dopamine degeneration in rats monitored by immunohistochemistry and PET imaging. *European journal of neuroscience.* 15: 991 – 998.

Conway, K.A., Harper, J.D., Lansbury, P.T. 1998. Accelerated in vitro fibril formation by a mutant α-synuclein linked to early-onset Parkinson disease. *Nature Medicine.* 4: 1318 – 1320.

Cramer, L. 1894. Ueber einige derivate des caffeine. *Chemische Berichte.* 27: 3089 – 3091.

Dauer, W. & Prezdborski, S. 2003. Parkinson's disease: Mechanisms and Models. *Neuron*. 39: 889 – 909.

Dall'Inga, O.P., Porciuncula, L.O., Souza, D.O., Cuhna, R.A., Lara, D.R. 2003. Neuroprotection by caffeine and adenosine A_{2A} receptor blockade of β-amyloid toxicity. *British journal of pharmacology.* 138: 1207 – 1209.

Dawson, T.M. & Dawson, V.L. 2002. Neuroprotective and neurorestorative strategies for Parkinson's disease. *Nature Neuroscience*. 5 (Suppl): 1058 – 1061.

Decamp, E. & Schneider, J.S. 2004. Attention and executive function deficits in chronic low-dose MPTP-treated non-human primates. *European journal of neuroscience*. 20: 1371 – 1378.

Deng, H., Le, W., Huang, M., Xie, W., Pan, T., Jankovic, J. 2007. Genetic analysis of LRRK2 P755L variant in caucasian patients with Parkinson's disease. *Neuroscience letters.* 419: 104 – 107.

Dingemanse, J., Wood, N., Jorga, K., Kettler, R. 1997. Pharmacokinetics and pharmacodynamics of single and multiple doses of the MAO-B inhibitor lazabemide in healthy subjects. *British journal of clinical pharmacology.* 43: 41 – 47.

Dobson, C.M. 2003. Protein folding and misfolding. *Nature.* 426: 884 – 890.

Du, Y., Ma, Z., Lin, S., Dodel, R.C., Gao, F., Bales, R.K., Trairhou, L.C., Chernet, E., Perry, K.W., Nelson, D.L.G., Luekce, S., Phebus, L.A., Bymaster, F.P., Paul S.M. 2001. Minocycline prevents nigrostriatal dopaminergic neurodegeneration in the MPTP model of Parkinson's disease. *Proceedings of the natural academy of sciences.* 98: 14669 – 14674.

Edmondson, D.E., Mattevi, A., Binda, C., Li., M., Hubalek, F. 2004. Structure and mechanism of monoamine oxidase. *Current medicinal chemistry.* 11: 1983 – 1993.

Fearnley, J.M., Lees, A.J. 1991. Ageing and Parkinson's disease: substantia nigra regional selectivity. *Brain.* 114: 2283 – 2301.

Fernandez, H.H. & Chen, J.J. 2007. Monoamine oxidase-B inhibition in the treatment of Parkinson's disease. *Pharmacotherapy.* 27(12 Pt 2): 174S – 185S.

Fischer, E. & Reese, L. 1883. Ueber caffeine, xanthin and guanine. *Liebigs Annalen der Chemie.* 221: 336 – 344.

Fiskum, G., Starkov, A., Polster, B.M., Chinopoulos, C. 2003. Mitochondrial mechanisms of neural cell death and neuroprotective interventions in Parkinson's disease. *Annals of the New York academy of sciences.* 991: 1 – 9.

Fowler, J.S., Logan , J., Wang, J., Volkow, N.D., Telang, F., Zhu, W., Franceschi, D., Pappas, N., Ferrieri, R., Shea, C., Garza, V., Xu, Y., Schyler, D., Gatley, S.J., Ding, Y-S., Alexoff, D., Warner, D., Netusil, N., Carter, P., Jayne, M., King, P., Vaska, P. 2003. Low monoamine oxidase B in peripheral organs in smokers. *Proceedings of the natural academy of sciences.* 100: 11600 – 11605.

Frucht, S., Rogers, J.D., Greene, P.E., Fahn, S., Gordon, M.F. 2000. Falling asleep at the wheel: Motor vehicle mishaps in people taking pramipexole and ropinirole. *Neurology.* 54: 274 – 279.

Gibb, W.R.G., Lees, A.J. 1988. The relevance of the Lewy Body to the pathogenesis of idiopathic Parkinson's disease. *Journal of neurology, neurosurgery and psychiatry.* 51: 745 – 752.

Greenamyre, J.T., Sherer, T.B., Betarbet, R., Panov, A.V. 2001. Complex I and Parkinson's disease. *IUBMB Life.* 52: 135 – 141.

Haefely, W., Burkard, W.P., Cesura, A.M., Kettler, R., Lorez, H.P., Martin, J.R., Richards, J.G., Scherschlicht, R., Da Prada, M. 1992. Biochemistry and pharmacology of moclobemide, a prototype RIMA. *Psychopharmacology (Berlin).* 106 (Suppl): S6 – S14.

Herkenham, M., Little, M.D., Bonkiewicz, K., Yang, S.C., Markey, S.P., Johannessen, J.N. 1991. Selective retention of MPP^+ within the monoaminergic systems of the primate brain following MPTP administration: an *in vivo* autoradiographic study. *Neuroscience*. 40: 133 – 158.

Holt, A., Sharman, D.F., Baker, G.B., Palcic, M.M. 1997 A continuous spectrophotometric assay for monoamine oxidase and related enzymes in tissue homogenates. *Analytical Biochemistry.* 244: 384 – 392.

Hubalek, F., Binda, C., Kjalil, A., Li, M., Mattevi, A., Castagnoli, N., Edmondson, D.E. 2005. Demonstration of isoleucine 199 as a structural determinant for the selective inhibition of human monoamine oxidase B by specific reversible inhibitors. *Journal of biological chemistry.* 280: 15761 – 15766.

Hubalek, F., Binda, C., Li, M., Mattevi, A., Edmondson, D.E. 2003. Polystyrene microbridges used in sitting-drop crystallization release 1,4-diphenyl-2-butene, a novel inhibitor of human MAO B. *Acta crystallographica section D.* D59: 1874 – 1876.

Kalaria, R.N., Harik, S.I. 1987. Blood-brain barrier monoamine oxidase: enzyme characterisation in cerebral microvessels and other tissues from six mammalian species including human. *Journal of neurochemistry*. 49: 856 – 864.

Kearney, E.B., Salach, J.I., Walker, W.H., Seng, R.L., Kenney, W., Zeszotek, E., Singer, T.P. 1971. The covalently-bound flavin of hepatic monoamine oxidase. Isolation and sequence of a flavin peptide and evidence for binding at the 8alpha position. *European journal of biochemistry.* 24: 321 – 327.

Kitamura, Y., Kakimura, J., Taniguch, T. 1998. Protective effect of talipexole on MPTP-treated planarian, a unique parkinsonian worm model. *Japanese journal of pharmacology*. 78: 28 – 29.

Knegtel, R.M.A., Kuntz, I.D., Oshiro, C.M. 1997. Molecular docking to ensembles of protein structures. *Journal of Molecular Biology.* 266: 424 – 440.

Kopito, R.R. 2000. Aggresomes, inclusion bodies and protein aggregation. *Trends in cell biology.* 10 : 524 – 530.

Kostic, V., Przedborski, S., Flaster, E., Sternic, N. 1991. Early development of levodopa-induced dyskinesias and response fluctuations in young-onset Parkinson's disease. *Neurology.* 41: 202 – 205.

Krueger, M.J. & Singer, T.P. 1993. An examination of the reliability of the radiochemical assay for monoamine oxidases A and B. *Analytical Biochemistry*. 214: 116 – 123.

Lamensdorf, I., Eisenhofer, G., Harvey-White, J., Nechustan, A., Kirk, K., Kopin, I.J. 2000. 3,4-dihydroxy-phenylacetalaldehyde potentiates the toxic effects of metabolic stress in PC 12 cells. *Brain research.* 861: 191 – 201.

Langston, J.W., Ballard, P., Tetrud, J.W., Irwin, I. 1983. Chronic Parkinsonism in humans due to a product of meperidine-analog synthesis. *Science*. 219: 979 – 980.

Lees, A.J., Hardy, J., Revesz, T. 2009. Parkinson's disease. *Lancet*. 373: 2055 – 2066.

Lesage, S., Durr, A., Tazir, M., Lohmann, E., Leutenegger, A.L., Janin, S., Pollak, P., Brice, A. B. 2006. French Parkinson's Disease Genetics study group, LRRK2 G2019S as a cause of Parkinson's disease in North African Arabs. *New England journal of medicine*. 354: 422 – 423.

LeWitt, P.A. & Taylor, D.C. 2008. Protection against Parkinson's disease progression: Clinical experience. *Neurotherapeutics.* 5: 210 – 225.

Lipton, S.A., Gu, Z., Nakamura, T. 2007. Inflammatory mediators leading to protein misfolding and uncompetitive/fast off-rate drug therapy for neurodegenerative disorders. *International review of neurobiology.* 82: 1 – 27.

Lwin, A., Orvisky, E., Goker-Alpan, O., LaMarca, M.E., Sidransky, E. 2004. Glucocerebrosidase mutations in subjects with parkinsonism. *Molecular genetics and metabolism.* 81: 70 – 73.

Mandel, S., Weinreb, O., Amit, T., Youdim, M.B. 2005. Mechanism of neuroprotective action of the anti-Parkinson drug rasagiline and its derivatives. *Brain Research. Brain Research Reviews.* 48: 379 – 387.

Manning-Bog, A.B., McCormack, A.L., Li, J., Uversky, V.N., Fink, A.L., Di Monte, D.A. 2002. The herbicide paraquat causes up-regulation and aggregation of alpha-synuclein in mice: paraquat and α-synuclein. *Journal of biological chemistry*. 277: 1641 - 1644.

Marsden, C.D. 1983. Neuromelanin and Parkinson's disease. *Journal of neural transmission. Supplementum.* 19: 121 – 141.

Marzo, A., Dal Bo, L., Monti, N.C., Crivelli, F., Ismaili, S., Caccia, C., Cattaneo, C., Fariello, R.G. 2004. Pharmacokinetics and pharmacodynamics of safinamide, a neuroprotectant with anti-parkinsonian and anti-convulsant activity. *Pharmacological research.* 50: 77 – 85.

Matsumoto, T., Suzuki, O., Futura, T., Asai, M., Kurokawa, Y., Nimura, Y., Katsumata, Y., Takahashi, I. 1985. A sensitive fluorometric assay for serum monoamine oxidase with kynuramine as substrate. *Clinical Biochemistry*. 18: 126 – 129.

Mayasaki, J.M., Martin, W., Suchowersky, O., Weiner, W.J., Lang, A.E. 2002. Practice parameter: Initiation of treatment for Parkinson's disease: An evidence-based review. *Neurology*. 58: 11 – 17.

McCormack, A.L. & Di Monte, D.A. 2003. Effects of l-dopa and other amino acids against paraquat-induced nigrostriatal degeneration. *Journal of neurochemistry.* 85: 82 – 86.

McCormack, A.L., Thiruchelvam, M., Manning-Bog, A.B., Thiffault, C., Langston, J.W., Cory-Slechta, D.A., Di Monte, D.A. 2002. Environmental risk factors and Parkinson's disease: Selective degeneration of nigral dopaminergic neurons caused by the herbicide paraquat. *Neurobiology of disease.* 10: 119 – 127.

McGeer, P.L., Itagaki, S., Tago, H., McGeer, E.G. 1987. Reactive microglia in patients with senile dementia of the Alzheimer type are positive for the histocompatability glycoprotein HLA-DR. *Neuroscience letters*. 79: 195 – 200.

Mizuno, Y., Ohta, S., Tanaka, M., Jakamiya, S., Suzuki, K., Sato, T., Oya, H., Ozawa, T., Kagawa, Y. 1989. Deficiencies in complex I subunits of the respiratory chain in Parkinson's disease. *Biochemical and biophysical research communications*. 163: 1450 – 1455.

Nagatsu, T. 2004. Progress in Monoamine Oxidase (MAO) research in relation to genetic engineering. *NeuroToxicology*. 25: 11-20.

Nicklas, W.J., Yougster, S.K., Kindt, M.V., Heikkila, R.E. 1987. MPTP, MPP^+ and mitochondrial function. *Life sciences*. 40: 721 – 729.

Nicotra, A. & Parvez, S.H. 1999. Methods for assaying monoamine oxidase A and B activities: recent developments. *Biogenic Amines*. 15: 307 – 320.

Novaroli, L., Reist, M., Favre, E., Carotti, A., Catto, M., Carrupt, P.A. 2005. Human recombinant monoamine oxidase B as a reliable and efficient enzyme source for inhibitor screening. *Bioorganic & Medicinal Chemistry.* 13: 6212 – 6217.

O'Brien, E., Kiely, K., Tipton, K. 1978. A discontinuous luminometric assay for monoamine oxidase using an ammonia-selective electrode. *Analytical Biochemistry*. 86: 287 – 297.

Oreland, L. 2004. Platelet monoamine oxidase, personality and alcoholism: The rise, fall and resurrection. *Neurotoxicology.* 25: 79 – 89.

Palmer, T. & Bonner, P.L. 2007. *Enzymes: Biochemistry, biotechnology, clinical chemistry.* 2nd ed. Horwood publishing limited, UK. P. 107 – 112.

Polymeropoulos, M.H. & Layedan, C. 1997. Mutation in the alpha-synuclein gene identified in families with Parkinson's disease. *Science.* 276: 2045 – 2048.

Przedborski, S. 2005. Pathogenesis and nigral cell death in Parkinson's disease. *Parkinsonism and related disorders.* 11: S3 – S7.

Riederer, P., Lachenmayer, L., Laux, G. 2004. Clinical applications of MAO-Inhibitors. *Current Medicinal Chemistry*. 11: 2033 – 2043.

Ross, G.W., Abbott, R.D., Petrovitch, H., Morens, D.M., Grandinetti, A., Tung, K.H., Tanner, C.M., Masaki, K.H., Blanchette, P.L., Curb, J.D., Popper, J.S., White, L. 2000. Association of coffee and caffeine intake with the risk of Parkinson's disease. *Journal of the American medical association.* 283: 2674 – 2679.

Sagi, Y., Drigues, N., Youdim, M.B.H. 2005. The neurochemical and behavioral effects of the novel cholinesterase-monoamine oxidase inhibitor, ladostigil, in response to L-dopa and L-tryptophan, in rats. *British journal of pharmacology.* 146: 553 – 560.

Saudou, F., Finkbeiner, S., Devys, D., Greenberg, M.E. 1998. Huntingtin acts in the nucleus to induce apoptosis but death does not correlate with the formation of intranuclear inclusion. *Cell.* 95: 55 – 66.

Schultz, C.W., Oakes, D., Kieburtz, K., Beal, M.F., Haas, R., Chir, M.B., Plumb, S., Juncos, J.L., Nutt, J., Shoulson, I., Carter, J., Kompoliti, K., Perlmutter, J.S., Reich, S., Stern, M.,

Watts, R.L., Kurlon, R., Molho, E., Harrison, M., Lew, M. and the Parkinson Study Group. 2002. Effects of Coenzyme Q_{10} in early Parkinson disease: Evidence of slowing of the functional decline. *Archives of Neurology*. 59: 1541 – 1550.

Sherer, T.B., Betarbet, A., Stout, A.K., Lund, S., Baptista, M., Panov, A.V., Cookson, M.R., Greenamyre, J.T. 2002. An *in vitro* model of Parkinson's disease: Linking mitochondrial impairment to altered α-synuclein metabolism and oxidative stress. *Journal of neuroscience.* 22: 7006 – 7015.

Shih, J.C., Chen, K., Ridd, M.J. 1999. Monoamine oxidase: From genes to behaviour. *Annual Review of Neuroscience.* 22: 197-217.

Shimura, H., Hattori, N., Kubo, S-I., Mizuno, Y., Askawara, S., Minoshima, S., Shimizu, N., Iwai, K., Chiba, T., Tanaka, K., Suzuki, T. 2000. Familial Parkinson disease gene product, parkin, is a ubiquitin-protein ligase. *Nature Genetics*. 25: 302-305.

Singer, T.P., Ramsay, R.R., McKeown, K., Trevor, A., Casatgnoli, N.E. 1988. Mechanism of the neurotoxicity of 1-methyl-4-phenylpyridinium (MPP^+), the toxic bioactivation product of 1-methyl-4-phenyl-1,2,3,6-tetrahydropyridine (MPTP). *Toxicology.* 49: 17 – 23.

Son, S., Ma, J., Kondou, Y., Yoshimura. M., Yamashita, E., Tsukihara, T. 2008. Structure of human monoamine oxidase A at 2.2-Å resolution: The control of opening the entrance for substrates/inhibitors. *Proceedings of the National Academy of Sciences*. 105: 5739 – 5744.

Strydom, B., Malan, S.F., Castagnoli Jr. N., Bergh, J.J., Petzer, J.P. 2010. Inhibition of monoamine oxidase by 8-benzyloxycaffeine analogues. *Bioorganic & Medicinal Chemistry.* 18: 1018 – 1028.

Tanner, C.M. 1992. Epidemiology of Parkinson's disease. *Neurologic clinics.* 10: 317 – 329.

Tayebi, N., Walker, J., Stubblefield, B., Orvisky, E., LaMarca, M.E., Wong, K., Rosenbaum, H., Schiffmann, R., Bembi, B., Sidransky, E. 2003. Gaucher disease with parkinsonian manifestations: does glucocerebrosidase deficiency contribute to a vulnerability to parkinsonism? *Molecular genetics and metabolism.* 79: 104 – 109.

Tipton, K.F. & Singer, T.P. 1993. The radiochemical assay for monoamine oxidase activity. Problems and pitfalls. *Biochemical Pharmacology*. 46: 1311 – 1316.

Trojanowski, J.Q., Goedert, M., Iwatsubo, T., Lee, V.M. 1998. Fatal attractions: abnormal protein aggregation and neuron death in Parkinson disease and Lewy body dementia. *Cell death and differentiation*. 5: 832 – 837.

Ungerstedt, U. & Arbuthnott, G. 1970. Quantitative recording of rotational behavior in rats after 6-hydroxydopamine lesions of the nigro-striatal dopmaine system. *Brain research*. 24: 485 – 493.

Van den Eeden, S.K., Tanner, C.M., Bernstein, A.L., Fross, R.D., Leimpeter, A., Bloch, D.A., Nelson, L.M. 2003. Incidence of Parkinson's disease: Variation by age, gender, race/ethnicity. *American journal of epidemiology.* 157: 1015 – 1022.

Vlok, N., Malan, S.F., Castagnoli Jr., N., Bergh, J.J., Petzer, J.P. 2006. Inhibition of monoamine oxidase B by analogues of the adenosine A_{2A} receptor antagonist (E)-8-(3-chlorostryryl)caffeine (CSC). *Bioorganic & Medicinal Chemistry.* 14:3512 – 3521.

Wooten, G.F., Currie, L.J., Bovbjerg, V.E., Lee, J.K., Patrie, J. 2004. Are men at greater risk for Parkinson's disease than women? *Journal of neurology, neurosurgery and psychiatry.* 75: 637 – 639.

Wu, D., Teismann, P., Tieu, K., Vila, M., Jackson-Lewis, V., Ischiropoulos, H., Przedborski, S. 2003. NADPH oxidase mediates oxidative stress in the 1-methyl-4-phenyl-1,2,3,6-tetrahydropyridine model of Parkinson's disease. *Proceeding of the national academy of sciences.* 100: 6145 – 6150.

Yamada, T., McGeer, P.L., McGeer, E.G. 1992. Lewy bodies in Parkinson's disease are recognized by antibodies of complement proteins. *Acta neuropathologica*. 84: 100 – 104.

Youdim, M.B.H., Bakhle, Y.S. 2006. Monoamine oxidase: isoforms and inhibitors in Parkinson's disease and depressive illness. *British journal of pharmacology.* 147: S287 – S296.

Youdim, M.B.H., Edmondson, D., Tipton, K.F. 2006. The therapeutic potential of monoamine oxidase inhibitors. *Nature reviews: Neuroscience.* 7: 295 – 309.

Youdim, M.B. & Green, A.R. 1975. Biogenic monoamine metabolism and functional activity in iron-deficient rats: behavioural correlates. *Ciba foundation symposium*. 51: 201 – 225.

Zhou, J.J.P., Zhong, B., Silverman, R.B. 1996. Direct continuous fluorometric assay for monoamine oxidase B. *Analytical Biochemistry*. 234: 9 – 12.

Zimprich, A., Biskup, S., Leitner, P., Lichtner, P., Farrer, M., Lincoln, S., Kachergus, J., Hulihan, M., Uitti, R.J., Calne, D.B. *et al*. 2004. Mutations in LRRK2 causes autosomal-dominant parkinsonism with pleomorphic pathology. *Neuron.* 44: 601 – 607.